

UNIVERSIDAD AUTÓNOMA DE MADRID
Facultad de Ciencias
Departamento de Física Teórica

Gaussian Many-Body States: Tachyonic Quenches and Conformal Blocks

Memoria de Tesis Doctoral realizada por

Sebastián Montes Valencia

y presentada ante el Departamento de Física Teórica
de la Universidad Autónoma de Madrid
para la obtención del Título de Doctor en Física Teórica.

Tesis Doctoral dirigida por

Germán Sierra Rodero,

Instituto de Física Teórica (IFT), UAM-CSIC, Madrid,

y

Javier Rodríguez Laguna,

Departamento de Física Fundamental, Universidad Nacional de Educación a Distancia
(UNED), Madrid.



Instituto de
Física
Teórica
UAM-CSIC

Madrid, 28 de febrero de 2018

a mi familia, mis amigos y mis amigas.

“La realidad –todo lo que somos, todo lo que nos envuelve, nos sostiene y, simultáneamente, nos devora y alimenta– es más rica y cambiante, más viva, que los sistemas que pretenden contenerla. A cambio de reducir la rica y casi ofensiva espontaneidad de la naturaleza a la rigidez de nuestras ideas, la mutilamos de una parte de sí, la más fascinante: su naturalidad. El hombre, al enfrentarse con la realidad, la sojuzga, la mutila y la somete a un orden que no es el de la naturaleza –si es que ésta posee, acaso, equivalente a lo que llamamos orden– sino el del pensamiento. Y así, no es la realidad lo que realmente conocemos, sino esa parte de la realidad que podemos reducir a lenguaje y conceptos. Lo que llamamos conocimiento es el saber que tenemos sobre cualquier cosa para dominarla y sujetarla.”

Octavio Paz, *Poesía de soledad y poesía de comunión*.

“Numbers it is. All music when you come to think. Two multiplied by two divided by half is twice one. Vibrations: chords those are. One plus two plus six is seven. Do anything you like with figures juggling. Always find out this equal to that, symmetry under a cemetery wall. [...] Musemathematics. And you think you’re listening to the ethereal. But suppose you said it like: Martha, seven times nine minus x is thirtyfive thousand. Fall quite flat. It’s on account of the sounds it is.”

James Joyce, *Ulysses*.

Abstract

This thesis is divided into two independent parts:

- Part I is based on Reference [1]. We present a characterization of a bosonic field theory driven by a free (Gaussian) tachyonic Hamiltonian. This regime is motivated using a theory describing two coupled bosonic fields. Relevant physical quantities such as simple correlators, entanglement entropies, and the mutual information of disconnected subregions are computed. We show that the causal structure resembles a critical (massless) quench. Because of the inherent instability of the driving Hamiltonian, an exponential growth ends up dominating the dynamics in a very characteristic way. This is related to the fact that the low-frequency modes do not equilibrate, but rather become exponentially occupied. Some applications and extensions to other physical systems are outlined.
- Part II is based in References [2, 3]. We present a characterization of the many-body lattice wave functions obtained from the conformal blocks (CBs) of the Ising conformal field theory (CFT). The formalism is interpreted as a matrix product state using continuous ancillary degrees of freedom. We provide analytic and numerical evidence that the resulting states can be written as BCS states. We give a complete proof that the translationally invariant 1D configurations have a BCS form and we find suitable parent Hamiltonians. We find interesting relations to the Kramers-Wannier (KW) duality and the Temperley-Lieb-Jones algebra. In particular, we prove that the ground state of the finite-size critical Ising transverse field (ITF) Hamiltonian can be obtained exactly with this construction. Finally, we study 2D configurations using an operator product expansion (OPE) approximation. We associate these states to the weak pairing phase of the $p + ip$ superconductor via the scaling of the pairing function and the entanglement spectrum.

Resumen

Esta tesis se divide en dos partes independientes:

- La parte I se basa en la referencia [1]. En ella presentamos una caracterización de una teoría de campos bosónica que evoluciona con un hamiltoniano libre (gausiano) taquiónico. Este régimen se motiva a través de una teoría de dos bosones acoplados. Calculamos cantidades físicas relevantes como los correladores, las entropías de entrelazamiento y la información mutua entre regiones desconectadas. Mostramos que la estructura causal se parece a la de un “quench” crítico (sin masa). Dada la inestabilidad inherente del hamiltoniano que dicta la dinámica, esta termina dominada por un crecimiento exponencial característico en las funciones de correlación. Esto se puede relacionar con el hecho que los modos de baja frecuencia no equilibran, sino que se van ocupando de forma exponencial. Para terminar, discutimos algunas aplicaciones y extensiones a otros sistemas físicos.
- La parte II se basa en las referencias [2, 3]. En ella presentamos una caracterización de las funciones de onda colectivas obtenidas a partir de los bloques conformes de la teoría de campos conformes del modelo de Ising. Este formalismo se interpreta como un “matrix product state” con grados de libertad auxiliares de dimensión infinita. Presentamos evidencia analítica y numérica de que los estados resultantes se pueden reescribir como estados BCS. Damos una prueba completa de que las configuraciones 1D con invarianza traslacional tienen forma BCS y obtenemos los hamiltonianos correspondientes. Encontramos también relaciones interesantes con la dualidad Kramers-Wannier y el álgebra de Temperley-Lieb-Jones. En particular, probamos que el estado fundamental de la cadena de Ising con campo transversal crítico puede obtenerse de forma exacta usando este formalismo. Finalmente, estudiamos una configuración 2D usando una aproximación derivada de la expansión del producto de operadores. Logramos asociar estos estados a la fase en apareamiento débil de los superconductores $p + ip$ usando el espectro y la entropía de entrelazamiento.

Acknowledgements

I would like to thank:

- Germán Sierra and Javi Rodríguez for their equanimity and guidance.
- Hong-Hao Tu for his hospitality.
- Guifré Vidal for his generosity and inspiring mentoring during the first part of my doctoral life.
- Alonso Botero and Andrés Reyes for their sincere academic friendship.
- Belén Paredes for giving me the opportunity of coming to Madrid.
- All the IFT staff for their help and their patience with my bureaucratic problems.
- Anette Knebe for her bureaucratic expertise.

This work is supported by the Spanish Research Agency (Agencia Estatal de Investigación) through the grant IFT Centro de Excelencia Severo Ochoa SEV-2016-0597, by the FPI-Severo Ochoa Ph.D. fellowship No. SVP-2013-067869, and funded by Grant No. FIS2015-69167-C2-1-P from the Spanish government, and QUITEMAD+ S2013/ICE-2801 from the Madrid regional.

Contents

Introduction	13
I Tachyonic Quenches	15
1 Quantum Quenches: a Primer	17
1.1 Motivation	17
1.2 Quantum Quenches and Equilibration	18
1.3 Eigenstate Thermalization Hypothesis and Generalized Gibbs Ensembles	20
1.4 Lieb-Robinson Bounds and Entanglement Growth	21
2 Quantum Quenches for Bosonic Systems	23
2.1 A Simple Harmonic Oscillator	23
2.1.1 Thermal State as Initial State	24
2.2 Model Hamiltonian: the Harmonic Chain	25
2.2.1 Some Basic Results for Higher Dimensions	26
2.3 Lieb-Robinson Bound for Harmonic Systems	26
2.4 Correlators After a Quantum Quench	27
2.4.1 Massless Quenches	29
2.5 Equilibration After a Massive Bosonic Quench	30
2.5.1 Generalized Gibbs Ensemble	30
2.5.2 Effective Temperature	31
2.6 Evolution of the Entanglement Entropy	32
3 Tachyonic Quenches in a Bosonic Field Theory	35
3.1 Introduction	35
3.2 Coupled bosonic QFT	36
3.3 Quenching the Frequency of a Simple Harmonic Oscillator	37
3.4 Tachyonic Quench for the Harmonic Chain	38
3.5 Causal Structure After a Tachyonic Quench	39
3.6 Entanglement and Mutual Information Growth After the Quench	41
3.7 Possible Connections to Physical Systems	43
3.8 Discussion	44
II Conformal Blocks	47
4 Conformal Blocks as Wave Functions	49
4.1 Introduction	49

4.2	A Very Brief Primer on 2D Conformal Field Theory	50
4.3	The Simplest Conformal Blocks	51
4.4	Chiral Vertex Operators and Conformal Blocks	54
4.5	Lattice Wave Functions from Conformal Blocks	56
4.6	Abelian Case Study: the Haldane-Shastry Chain	58
4.7	Wave Functions for Fractional Quantum Hall Physics	59
5	Some Aspects of the Ising Model	63
5.1	Classical 2D Ising Model	63
5.2	Ising Transverse Field Spin Chain	65
5.2.1	A Primer on BCS States	66
5.3	KW Duality for the Ising Transverse Field Spin Chain	67
5.4	Majorana Fermions and the (Chiral) Ising CFT	69
5.5	Conformal Blocks of the Ising CFT	70
6	Ising Conformal Blocks as Spin Wave Functions	75
6.1	Introduction	75
6.2	Lattice States from the Ising Vertex Operators	76
6.3	First-Order Analysis: OPE Approximation	77
6.4	1D Wave Functions	79
6.4.1	Determinant Form for the 1D Wave Function	81
6.4.2	BCS State for 1D Wave Functions	83
6.5	Fixed Point Ground States of the ITF Model from CBs	85
6.6	Braiding and Kramers-Wannier Duality	86
6.7	The Temperley-Lieb-Jones Algebra	87
6.8	Parent Hamiltonians for 1D	89
6.8.1	Forcing the ITF Hamiltonian	91
6.8.2	Some Algebraic Properties of the Hamiltonian Family	92
6.9	Excited States	93
6.10	2D Wave Functions	94
6.10.1	Fourier Transform of 2D Pairing Function	98
6.11	BCS Structure Beyond OPE: General Observations	99
6.12	Moving Beyond the Ising CFT	99
6.13	Conclusions and Discussion	101
III	Appendices and General Conclusions	103
A	Appendices	105
A.1	A Useful Relation	105
A.2	Finding a Parent Hamiltonian	106
A.3	Bogoliubov Transformation from a BCS Pairing Matrix	107
A.4	Towards a Generalized Wick Theorem	108
	Bibliography	115

Introduction

The present thesis is divided into two independent parts:

I. **Part I** is based on the article:

[1] S. Montes, G. Sierra and J. Rodríguez-Laguna, *Tachyonic quench in a free bosonic field theory*, Journal of Statistical Mechanics: Theory and Experiment **2018** (2018) 023102.

Its content is divided into three chapters. The first two correspond to an introduction and a presentation of the basic technology already introduced in the literature. The third chapter summarizes our original results.

- Chapter 1 presents a short introduction to the field of quantum quenches. Some important concepts (equilibration, the eigenstate thermalization hypothesis, generalized Gibbs ensembles, Lieb-Robinson bounds) are motivated and summarized.
- Chapter 2 presents a survey of results regarding quantum quenches in free bosonic systems. We use the harmonic chain as the UV regularized Hamiltonian to study the many-body physics of these systems. The corresponding equilibration properties are studied by means of a generalized Gibbs ensemble (GGE). The evolution of physical quantities such as correlators and the entanglement entropy are studied.
- Chapter 3 presents a characterization of a bosonic field theory driven by a free (Gaussian) tachyonic Hamiltonian. This regime is motivated by means of a theory describing two coupled bosonic fields. Relevant physical quantities such as simple correlators, entanglement entropies, and the mutual information of disconnected subregions are computed and discussed. We show that the causal structure resembles a critical (massless) quench. Because of the inherent instability of the driving Hamiltonian, exponential growth end up dominating the dynamics in a very characteristic way. This is related to the fact that the low-frequency modes do not equilibrate, but rather become exponentially occupied. Some applications and extensions to other physical systems are outlined.

II. **Part II** is based on the articles:

[2] S. Montes, J. Rodríguez-Laguna, H.-H. Tu and G. Sierra, *Many-body lattice wave functions from conformal blocks*, Physical Review B **95** (2017) 085146.

[3] S. Montes, J. Rodríguez-Laguna and G. Sierra, *BCS wave function, matrix product states, and the Ising conformal field theory*, Physical Review B **96** (2017) 195152.

Once again, this part is divided into three chapters. Our original results are summarized in Chapter 6. However, it should be noted that the general construction presented in Section 4.5 was originally introduced in Ref. [2].

- Chapter 4 starts with a motivation for the use of conformal blocks (CBs) in 2D conformal field theory (CFT). The notion of chiral vertex operators (CVOs) is introduced in order to have a general framework to manipulate CBs. This technology is exploited to construct many-body lattice wave functions using CBs. The general construction is illustrated using the Haldane-Shastry spin chain. We end with a summary of results regarding the use of CBs in fractional quantum Hall (FQH) systems.
- Chapter 5 summarizes several results regarding the 2D Ising model. The exact solution is obtained via the Ising transverse field (ITF) spin chain. The Kramers-Wannier (KW) duality and its implications are discussed. We also present a summary of the main features of the Ising CFT and how to compute all of its CBs using bosonization.
- Chapter 6 presents a characterization of the many-body lattice wave functions obtained from the CBs of the Ising CFT, in particular using the spin field operator σ . The formalism is interpreted as a matrix product state (MPS) using continuous ancillary degrees of freedom. We provide analytic and numerical evidence that the resulting states can be written as Gaussian states, more concretely, as BCS states. Remarkably, we give a complete proof that the translationally invariant 1D configurations have a BCS form and we find suitable parent Hamiltonians. In particular, we prove that the ground state of the finite-size critical ITF Hamiltonian can be obtained exactly from the CBs of the Ising CFT. Finally, we study 2D configurations using an operator product expansion (OPE) approximation. We associate these states to the weak pairing phase of the $p + ip$ superconductor via the scaling of the pairing function and the entanglement spectrum.

The title of this thesis highlights a remarkable, though unexpected connection between these two projects. On one hand, the ground state of a free bosonic system is a Gaussian many-body state. Given that we assume that the driving Hamiltonian is quadratic, these systems are always described by Gaussian states. On the other hand, we present evidence that the many-body lattice wave functions constructed using CBs of the Ising spin field operator σ have a BCS structure. This is a highly non-trivial result, pointing at the rich, unexplored inner structure of these mathematical objects. Given that BCS states are Gaussian by construction, both topics become vaguely, but excitingly related.

Part I

Tachyonic Quenches

Quantum Quenches: a Primer

1.1. Motivation

The development of statistical mechanics is one of the major achievements of theoretical physics. After the pioneering work of Boltzmann, Maxwell and Gibbs, it was possible to deduce general macroscopic laws from the dynamics of microscopic constituents. This became a powerful framework that sets the stage for most of the modern understanding of every day phenomena. However, despite some of these astounding successes being already canonized in modern textbooks, there are several questions in statistical mechanics that still elude clean, simple answers.

One of the main open problems in this area is the emergence of equilibrium states (described by statistical ensembles) from time-reversal symmetric microscopic interactions [4]. This relates to some fundamental concepts, such as the validity of the second law of thermodynamics and the notion of temperature. The first important result in this direction was obtained by Boltzmann in 1872 (the so-called *H-theorem*) [5], however it was far from being the final answer. (See [6] for a short historical review.) Things became even more nuanced after the development of quantum mechanics: already in 1929, John von Neumann attempted bridging the gap between unitary dynamics (as prescribed by Schrödinger's equation) and stationary ensembles [7].

In order to tackle this question, the study of closed quantum systems out of equilibrium has become a central concern in contemporary physics. Even though the main ideas can be traced back to the origins of quantum theory, this field has experienced a strong resurgence in the past few decades. This is due to the development of both experimental and theoretical tools that have delivered new insights into the core foundations of statistical mechanics. (For comprehensive reviews, see [8, 9, 10, 11, 12].)

First and foremost, new experimental techniques allow for a very precise control of quantum systems with many degrees of freedom. The most paradigmatic may be the achievement of Bose-Einstein condensation (BEC) and Fermi degeneracy in cold, dilute gases [13, 14]. Following these steps, the study of coherent matter waves has become a well-established setting for the study of interacting many-body systems. These experiments require ultracold temperatures (at around 10^{-8}K) and usually feature optical traps composed of standing electromagnetic waves to constrain the geometry and topology of the system [15]. Remarkably, these setups can realize artificial systems that are very closely related to well-known theoretical models [16, 17, 18, 19, 20, 21, 22]. Relevant to

this thesis, the non-equilibrium dynamics of these systems can also be studied with very high precision [23, 24, 25, 26, 27, 28, 29].

In parallel, we have also developed a better theoretical understanding of quantum mechanics. John Bell’s questioning of established facts about the quantum world urged physicists to take the formalism more seriously [30, 31]. The groundbreaking experiments performed by Aspect in 1982 [32, 33] convinced the community that wave functions were more than a mere mathematical artifact. As a consequence, quantum information theory and quantum computation became powerful tools for analyzing both new and old problems in physics [34, 35, 36]. The most relevant application may be the use of measures such as the entanglement entropy for understanding the physical features of many-body systems [37, 38, 39]. This has been used in the context of non-equilibrium dynamics to determine entanglement growth and the corresponding spreading of correlations [40, 41, 42, 43, 44].

1.2. Quantum Quenches and Equilibration

Among the virtually infinite number of ways of driving a system out of equilibrium, one of the most popular ones is the so-called (global) *quantum quench* [45, 46, 47]. In this protocol, the system is prepared in the ground state $|0\rangle$ of an initial Hamiltonian H_0 , which is then let evolve unitarily according to

$$|\psi(t)\rangle = \exp(-itH_1)|0\rangle, \quad t \geq 0, \quad (1.1)$$

where H_1 is another Hamiltonian that usually differs from H_0 in one or several of its external parameters (such as magnetic field, pressure, or on-site repulsion). Of course, one must ensure that $[H_0, H_1] \neq 0$. Note that we assume that the system remains isolated and the global state is always a pure state. During the evolution, energy will be conserved

$$\langle\psi(t)|H_1|\psi(t)\rangle = \langle\psi(0)|H_1|\psi(0)\rangle > E_0^{(1)}, \quad (1.2)$$

where $E_0^{(1)}$ is the ground state energy of H_1 . This implies that, even though a macroscopically large energy is given to (or taken from) the system at $t = 0$, it is distributed over the excitation levels of H_1 and the dynamics can still be considered isolated.¹

There are other popular protocols for driving a system out of equilibrium [10]: local quenches where the system is not uniformly modified, but rather the sudden change is limited to a bounded region [42, 28]; ramps or sweeps where the Hamiltonian changes in time according to a given schedule [52, 53, 9]; and geometric quenches where the spatial configuration of the system is suddenly changed [54, 55]. For the sake of concreteness, we will focus solely on global quenches.

Our main goal is to study the evolution of expectation values

$$\langle\mathcal{O}\rangle(t) \equiv \frac{\langle\psi(t)|\mathcal{O}|\psi(t)\rangle}{\langle\psi(t)|\psi(t)\rangle}, \quad (1.3)$$

¹The word quench (meaning “extinguish”) comes from the Old English *acwencan*. The use in the original context has steadily declined over the past few centuries and it is used now mostly in the context of material sciences, where it denotes rapidly cooling a material. To the best of my knowledge, the expression “quantum quench” was first introduced in [45] by analogy, in the sense that one of the control parameters is changed abruptly (though the notion of “quench dynamics” for a quantum system was already discussed in [48] as a response to the experimental results obtained in [16]), and the first theoretical calculations of what we may now call quantum quenches were done in the seminal papers by Barouch, McCoy and Dresden about the XY model in 1970 [49, 50, 51].

where \mathcal{O} is a finite product of local operators. The dynamics of a finite system will have Poincaré recurrences [56], so strictly speaking it cannot reach equilibrium. However, for large enough systems and long enough times, local relaxation can be achieved on average. If we assume that H_1 has a spectrum $\{E_n\}$, we have

$$\langle \mathcal{O} \rangle (t) = \sum_{n,m} \langle 0|E_m \rangle \langle E_n|0 \rangle \langle E_m|\mathcal{O}|E_n \rangle e^{-i(E_n-E_m)t}. \quad (1.4)$$

For very long times, all factors with $E_n - E_m \neq 0$ will oscillate rapidly and average to zero, so that, on average,

$$\lim_{T \rightarrow \infty} \frac{1}{T} \int_0^T dt \langle \mathcal{O} \rangle (t) = \sum_{n,m} \langle 0|E_m \rangle \langle E_n|0 \rangle \langle E_m|\mathcal{O}|E_n \rangle \delta_{E_n,E_m}. \quad (1.5)$$

Note that the typical times for these terms to vanish depend on the spectral gaps of H_1 . In particular, gapless systems will require longer relaxation times.

If a subsystem can be described by an equilibrium ensemble, we expect (1.4) to at least fluctuate around a well-defined value. Accordingly, a local operator is said to *equilibrate on average* if its expectation value is arbitrarily close to the equilibrium value (1.5) for almost all times.

We can summarize all the relevant physics for this problem by considering the states themselves. If the long-time behavior of the system can be characterized by some sort of equilibrium, it is tempting to expect that the corresponding density matrix will be close to one of the statistical ensembles that are prescribed in usual statistical mechanics. Given that the exact density matrix

$$\rho = |\psi(t)\rangle \langle \psi(t)| = \sum_{n,m} e^{-i(E_n-E_m)t} \langle 0|E_m \rangle \langle E_n|0 \rangle |E_n\rangle \langle E_m| \quad (1.6)$$

always describes a pure state and that $\lim_{t \rightarrow \infty} \rho(t)$ may not exist, it is customary to define its *infinite time average* [10, 11]

$$\omega \equiv \lim_{T \rightarrow \infty} \frac{1}{T} \int_0^T dt \rho(t) = \sum_{n,m} \delta_{E_n,E_m} \langle 0|E_m \rangle \langle E_n|0 \rangle |E_n\rangle \langle E_m|. \quad (1.7)$$

This is usually called the *diagonal ensemble* because it loses all the coherences between different energies and is exactly diagonal if there are no degeneracies in the eigenvalue spectrum. It can be shown that this state corresponds to the maximum entropy state if all constants of motion are fixed [57]².

A system is said to thermalize if ω can be approximated by a thermal ensemble

$$\rho^{\text{th}} = \frac{1}{Z} \exp(-\beta H_1), \quad (1.8)$$

where $Z = \text{Tr}(\exp(-\beta H_1))$ and β is a Lagrange multiplier fixed by

$$\text{Tr}(\rho^{\text{th}} H_1) = \langle 0|H_1|0 \rangle. \quad (1.9)$$

If the energy is the only conserved quantity with a local density, this will be the ensemble that maximizes the entropy [57, 11].

²Some authors relate this to the principle of maximum entropy (also known as Jaynes principle): the probability distribution which best represents the current state of knowledge is the one with largest entropy, in the context of precisely stated prior data [58, 59].

1.3. Eigenstate Thermalization Hypothesis and Generalized Gibbs Ensembles

Thermalization as described in the previous section has been studied extensively [4, 60, 61, 62]. (For a complete review, see [11, 63].) A priori, one would expect that microcanonical and canonical (i.e. Gibbs) ensembles should be common enough in realistic models given the general success of statistical mechanics. This implies that generic initial states and generic Hamiltonians (with reasonable conditions such as locality) should in principle produce long-time ensembles close to the thermal one.

On the other hand, Eq. (1.7) shows that the diagonal ensemble retains information about the initial state in the coefficients $\langle 0|E_n\rangle$. This suggests in turn that certain states may not equilibrate in a generic way if some other physical constraints are present during the evolution.

The most prominent answer to this dilemma has been formalized by the name of *eigenstate thermalization hypothesis* (ETH) [4, 64, 65, 66]. It is usually stated as [66]:

For a “typical” initial state $|0\rangle$, the infinite time average (1.5) of a finite product of local operators \mathcal{O} will correspond to the value predicted by the microcanonical ensemble³ if the following criteria are met:

1. The diagonal matrix elements

$$\mathcal{O}_{nn} \equiv \langle E_n|\mathcal{O}|E_n\rangle \quad (1.10)$$

change slowly with the state (i.e., smoothly with the energy), with the difference between neighboring values $\mathcal{O}_{n+1,n+1} - \mathcal{O}_{nn}$ being exponentially small in the system size.

2. The off-diagonal terms

$$\mathcal{O}_{nm} \equiv \langle E_n|\mathcal{O}|E_m\rangle, \quad n \neq m, \quad (1.11)$$

are also exponentially small in the system size.

ETH implies thermalization, in the sense that the corresponding diagonal ensemble will give the same results as the microcanonical ensemble. Numerical simulations and experiments with cold atoms suggest that many interacting systems do thermalize in this way, in particular classically chaotic systems [67, 27, 68, 69].

Interestingly, integrable systems do not thermalize in the ETH sense [24, 70, 71, 72, 73, 74, 75, 76, 77, 78, 79]. In a nutshell, integrable systems are defined by having as many (local) integrals of motion $\{I_n\}$ as degrees of freedom, such that⁴

$$[I_n, I_m] = 0, \quad n \neq m. \quad (1.12)$$

³The microcanonical ensemble is the one defined by energy $\bar{E} = \langle 0|H_1|0\rangle$. We must ensure that the energy variance $\overline{\Delta E}$ is algebraically small in the systems size N , i.e., $\overline{\Delta E} \sim N^{-1/2}\bar{E}$ [66]. This is the case for any macroscopic state that can be prepared in a laboratory, so the assumption is motivated.

⁴The definition of quantum integrable models has many subtleties. Given that there are an infinite number of operators that trivially commute with the Hamiltonian H_1 (for instance, the projectors to energy eigenstates $|E_n\rangle\langle E_n|$), it is important to characterize which constructions are valid. Locality is usually used to fix this problem. An integral of motion is said to be local if it can be written as a sum of a local density. However, some models require generalized quasiloc operators [80, 81].

It is assumed that the Hamiltonian H_1 is one of the integrals of motion, or a linear combination of them. Given that all the expectation values $\langle I_n \rangle(t)$ are constant (because $[I_n, H_1] = 0$), the equilibrium ensembles must contain more information. It has been shown that the appropriate description is a so-called *generalized Gibbs ensemble* (GGE) [61, 80, 82, 83]

$$\rho^{\text{GGE}} = \frac{1}{Z} \exp \left(- \sum_n \lambda_n I_n \right), \quad (1.13)$$

where we assume that the set $\{I_n\}$ is complete and $Z = \text{Tr} \exp(-\sum_n \lambda_n I_n)$ is the generalized partition function. Once again, the Lagrange multipliers $\{\lambda_n\}$ are fixed by the initial condition

$$\text{Tr} (\rho^{\text{GGE}} I_n) = \langle 0 | I_n | 0 \rangle. \quad (1.14)$$

In analogy to the thermal state, this is the ensemble that maximizes the entropy subject to the constraints of all the conserved integrals of motion [84, 72, 11].

It should be noted that not all integrable systems equilibrate to this ensemble. In particular, the equilibration of spin chains with certain initial states evolving according to the anisotropic XXZ Hamiltonian cannot be described by a GGE [85, 86].

1.4. Lieb-Robinson Bounds and Entanglement Growth

After the quench, we expect information (in the form of excitations) to propagate around the system. Remarkably, there is a well-defined causal structure given by the so-called *Lieb-Robinson bounds* [87], producing natural “light-cones” similar to the ones obtained in relativistic theories. These bounds limit the speed at which excitations can propagate in a quantum lattice system that is described by a local Hamiltonian. More concretely, if O_A and O_B are two local observables with supports in regions A and B , then

$$\|[O_A(t), O_B]\| \leq c \|O_A\| \|O_B\| \exp(-(d(A, B) - v_{\text{LR}}|t|)), \quad (1.15)$$

where $\|O\|$ is the operator norm⁵, $d(A, B)$ the lattice distance between the regions, c a positive constant that only depends on the size of the spatial supports, and $v_{\text{LR}} \geq 0$ the effective group velocity (independent of both operators). It follows that correlation functions can only grow in a significant manner inside the “light-cone”, while everything outside is exponentially suppressed [91]. Applying this inequality to the local terms of the Hamiltonian, we also see that local changes cannot affect the whole system instantaneously.

Even though these bounds are almost never tight, they can be used to obtain qualitative results about the growth of correlations after a quantum quench. In particular, they can give useful insight about the entanglement dynamics. Assume we divide the whole system into two disjoint parts, A and B . The reduced density matrix of A is defined as

$$\rho_A(t) = \text{Tr}_B (|\psi(t)\rangle \langle \psi(t)|), \quad (1.16)$$

and its *entanglement entropy* (or von Neumann entropy) as

$$S_A(t) = -\text{Tr} [\rho_A(t) \log (\rho_A(t))]. \quad (1.17)$$

⁵This result can be extended to unbounded operators, as we will see in the study of harmonic chains [88, 89, 90].

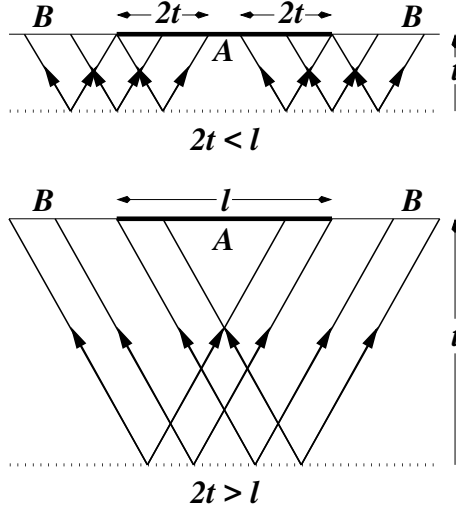


Figure 1.1: Space-time diagram illustrating how the entanglement between a region A and the rest of the system grows linearly and then saturates due to oppositely moving coherent quasiparticles. (Taken from [94].)

It can be shown that [91, 44, 11]

$$S_A(t) - S_A(t=0) \leq C |\partial A| t, \quad (1.18)$$

where $|\partial A|$ denotes the size of the boundary of A and C is a constant that depends on the norm of the Hamiltonian density. In other words, the entanglement entropy satisfies an area law while it grows at most linearly in time. Lieb-Robinson bounds suggest an intuitive picture to explain this: if the initial state $|0\rangle$ is slightly correlated and there is a ballistic propagation (i.e., at maximum speed v_{LR}) of quasi-particles, new correlations will be formed across boundaries at most in a linear fashion [92, 93] (see Figure (1.1)).

This quasiparticle picture assumes that the excitations that are produced at the same point in space are correlated (i.e., entangled), while those far away are incoherent. Subsequently, the entanglement entropy of a subsystem A after a quench is proportional to the total number of quasiparticle pairs that, after being emitted at the same point, are shared between that region and its complement. In Ref. [94], they obtain a phenomenological formula for one-dimensional systems that quantifies this idea

$$S_A(t) = 2t \int_{2|v(\lambda)|t < \ell} d\lambda v(\lambda) s(\lambda) + \ell \int_{2|v(\lambda)|t > \ell} d\lambda s(\lambda), \quad (1.19)$$

where ℓ is the size of region A , λ is the quasi-momentum of the quasiparticles, $v(\lambda)$ the corresponding group velocity, and $s(\lambda)$ is a function that depends on the rate of production of quasiparticles with quasi-momentum $\pm\lambda$ and their individual contribution to the entanglement entropy. Formula (1.19) has been verified analytically and numerically for several systems [40, 95, 43, 96, 97, 98]. Finding a candidate for $s(\lambda)$ is not easy in general, but as we will see in the case of free bosons, it can be estimated from the equilibration properties.

Given that $|v(\lambda)| \leq v_{\text{LR}}$, we can make some generic estimations about the behavior of formula (1.19) [99]. If $t < \ell/v_{\text{LR}}$, the second term vanishes and we expect S_A to grow linearly in time. If $t \gg \ell/v_{\text{LR}}$, the second term dominates and we expect the entanglement entropy to be extensive in the system size $S_A \propto \ell$. As we will see in the next chapter, S_A may saturate to a constant or have a mild logarithmic growth in time.

Quantum Quenches for Bosonic Systems

Most of the results found in this chapter are well established in the literature. We will expand Ref. [1], complementing it with Refs. [93, 100, 101]. We will specialize the conclusions and the notation in order to fit the original results presented in the next chapter.

2.1. A Simple Harmonic Oscillator

Before we address the many-body problem, we will consider the dynamics of a quenched harmonic oscillator (HO). In this context, we want to study the evolution of the ground state of the initial Hamiltonian

$$H_0 = \frac{\hat{p}^2}{2} + \frac{1}{2}\omega_0^2\hat{q}^2, \quad (2.1)$$

described by the Gaussian state

$$\langle x|0\rangle = \left(\frac{\omega_0}{\pi}\right)^{1/4} \exp\left(-\omega_0\frac{x^2}{2}\right), \quad (2.2)$$

under the action of the unitary operator

$$U_t = \exp\left[-it\left(\frac{\hat{p}^2}{2} + \frac{1}{2}\omega^2\hat{q}^2\right)\right] \equiv \exp(-itH_1). \quad (2.3)$$

We can summarize the quenching protocol as

$$H(t) = \begin{cases} H_0, & t < 0, \\ H_1, & t \geq 0, \end{cases} \quad (2.4)$$

assuming that the initial state is the ground state of H_0 . Note that if $\omega \rightarrow 0$, this corresponds to the dynamics of a single particle released from a quadratic potential.

If we use the creation and annihilation operators that diagonalize H_0

$$\hat{q} = \sqrt{\frac{1}{2\omega_0}}(a^\dagger + a), \quad \hat{p} = i\sqrt{\frac{\omega_0}{2}}(a^\dagger - a), \quad (2.5)$$

we can rewrite the Hamiltonian as

$$H_1 = \frac{\omega_0^2 + \omega^2}{2\omega_0} \left(a^\dagger a + \frac{1}{2} \right) - \frac{\omega_0^2 - \omega^2}{4\omega_0} \left((a^\dagger)^2 + a^2 \right). \quad (2.6)$$

This has the form of a generic quadratic bosonic operator. The unwanted $(a^\dagger)^2 + a^2$ can be eliminated by means of a Bogoliubov transformation

$$\begin{pmatrix} a \\ a^\dagger \end{pmatrix} = (\cosh \theta \mathbb{1} - \sinh \theta \sigma^x) \begin{pmatrix} b \\ b^\dagger \end{pmatrix}. \quad (2.7)$$

Setting

$$\cosh \theta = \frac{1}{2} \frac{\omega_0 + \omega}{\sqrt{\omega_0 \omega}}, \quad \sinh \theta = \frac{1}{2} \frac{\omega - \omega_0}{\sqrt{\omega_0 \omega}}, \quad (2.8)$$

we recover the ladder operators that diagonalize H_1 :

$$H_1 = \omega \left(b^\dagger b + \frac{1}{2} \right). \quad (2.9)$$

Using this map between modes, we can go back to the variables that act in a simple manner on the initial state $|0\rangle$. For instance, the time evolved operators are easily computed

$$\begin{aligned} a(t) &= U_t a U_t^\dagger = \cosh(\theta) e^{-i\omega t} b - \sinh(\theta) e^{i\omega t} b^\dagger \\ &= \left(\cos(\omega t) - i \sin(\omega t) \frac{\omega_0^2 + \omega^2}{2\omega_0 \omega} \right) a - i \sin(\omega t) \frac{\omega^2 - \omega_0^2}{2\omega_0 \omega} a^\dagger. \end{aligned} \quad (2.10)$$

Using this result, we obtain all relevant expectation values, in particular

$$\begin{aligned} \langle \hat{q}^2 \rangle(t) &= \frac{\omega_0^2 + \omega^2}{4\omega_0 \omega^2} - \frac{\omega_0^2 - \omega^2}{4\omega_0 \omega^2} \cos(2\omega t), \\ \langle \hat{p}^2 \rangle(t) &= \frac{\omega_0^2 + \omega^2}{4\omega_0} + \frac{\omega_0^2 - \omega^2}{4\omega_0} \cos(2\omega t), \\ \langle \hat{q}\hat{p} \rangle(t) &= \frac{\omega_0^2 - \omega^2}{4\omega_0 \omega} \sin(2\omega t) + \frac{i}{2}. \end{aligned} \quad (2.11)$$

These correlators will be the building blocks we will use to compute all the two-point functions in the many-body system [100, 101].

Thermal State as Initial State

It is easy to generalize the previous results to the case of an initial state set at temperature β_0

$$\rho_0 = \frac{1}{Z(\beta_0, \omega_0)} \exp(-\beta_0 H_0), \quad Z(\beta_0, \omega_0) = \frac{1}{2 \sinh\left(\frac{\beta_0 \omega_0}{2}\right)}. \quad (2.12)$$

Being a simple quadratic theory, most of the calculation follows the same lines, only with different initial conditions

$$\langle \hat{q}^2 \rangle_{\beta_0}(t=0) = \frac{1}{2\omega_0} \coth\left(\frac{\beta_0 \omega_0}{2}\right), \quad \langle \hat{p}^2 \rangle_{\beta_0}(t=0) = \frac{\omega_0}{2} \coth\left(\frac{\beta_0 \omega_0}{2}\right). \quad (2.13)$$

In this setting, temperature allows for a richer interplay with the control parameters (see [100]). However, for the sake of concreteness, from now on we will be working solely at zero temperature (i.e., $\beta_0 = \infty$).

2.2. Model Hamiltonian: the Harmonic Chain

The mass quench of a free bosonic QFT has been studied extensively [102, 100, 101]. One of its main features is that each mode will evolve independently after the quench, with a new frequency determined by the new mass. All the relevant quantities, obtained from the fundamental two-point correlators, can then be reduced to the quenching of independent simple harmonic oscillators (HOs).

We will use a standard UV regularized version of the usual free boson QFT: the harmonic chain. The UV cutoff will be particularly important for the analysis of the scaling of the entanglement entropy after the quench. Unless stated, we will work with a one-dimensional configuration. However, all results can be extended to higher dimensions in a straight-forward way.

Consider a set of N harmonic oscillators described by a set of canonical variables $\{\hat{p}_r, \hat{q}_r\}$ such that

$$[\hat{q}_r, \hat{p}_s] = i\delta_{rs}. \quad (2.14)$$

We define the Hamiltonian

$$H(m) = \frac{1}{2} \sum_{r/a=1}^N [\hat{p}_r^2 + m^2 \hat{q}_r^2 + \Omega^2 (\hat{q}_{r+a} - \hat{q}_r)^2], \quad (2.15)$$

where $a = L/N$ is the UV regularization and we assume periodic boundary conditions. Using the Fourier transform

$$\hat{q}_r = \frac{1}{\sqrt{N}} \sum_k e^{ikr} \hat{q}_k, \quad (2.16)$$

(similarly for \hat{p}_r), where momenta $k = \frac{2\pi}{L}n$ are given by $n = 0, \pm 1, \dots, \pm \frac{N-1}{2}$, we have

$$H(m) = \frac{1}{2} \sum_k \left[\hat{p}_k^\dagger \hat{p}_k + \omega_k^2 \hat{q}_k^\dagger \hat{q}_k \right]. \quad (2.17)$$

The resulting dispersion relation is given by

$$\omega_k^2 = 4\Omega^2 \sin^2 \left(\frac{ka}{2} \right) + m^2. \quad (2.18)$$

Operators \hat{p}_k and \hat{q}_k are not Hermitian, but they satisfy

$$\hat{p}_k^\dagger = \hat{p}_{-k}, \quad \hat{q}_k^\dagger = \hat{q}_{-k} \quad (2.19)$$

Eq. (2.17) implies that $H(m)$ can be studied as a set of N independent HOs, one for each momentum mode. The associated frequency will be determined by the corresponding value of the dispersion relation.

Note that if we want a well-defined continuum limit

$$aN = L \text{ fixed}, \quad N \rightarrow \infty, a \rightarrow 0, \quad (2.20)$$

with a relativistic dispersion relation

$$\omega_k^2 \approx a^2 \Omega^2 k^2 + m^2, \quad (2.21)$$

the associated speed of light will be $c = a\Omega$.

Some Basic Results for Higher Dimensions

Hamiltonian (2.15) can be written in arbitrary dimensions:

$$H^{(d)}(m) = \frac{1}{2} \sum_{\mathbf{r}} \left[\hat{p}_{\mathbf{r}}^2 + m^2 \hat{q}_{\mathbf{r}}^2 + \sum_{s=1}^d \Omega^2 (\hat{q}_{\mathbf{r}+a_s} - \hat{q}_{\mathbf{r}})^2 \right], \quad (2.22)$$

where a_s is a displacement in the d -dimensional (periodical) lattice by one site along the s -th dimension. It is diagonalized in the same way

$$H = \frac{1}{2} \sum_{\mathbf{k}} \left[\hat{p}_{\mathbf{k}}^\dagger \hat{p}_{\mathbf{k}} + \omega_{\mathbf{k}}^2 \hat{q}_{\mathbf{k}}^\dagger \hat{q}_{\mathbf{k}} \right], \quad (2.23)$$

with dispersion relation

$$\omega_{\mathbf{k}}^2 = m^2 + 4\Omega^2 \sum_{s=1}^d \sin^2 \left(\frac{k_s a}{2} \right), \quad (2.24)$$

where $\mathbf{k} = (k_1, \dots, k_d)$ and

$$k_s = \frac{2\pi}{L_s} n, \quad n = 0, \pm 1, \dots, \pm \frac{N_s - 1}{2}. \quad (2.25)$$

Note that in the continuum limit (2.20), the associated speed of light is still $c = a\Omega$.

2.3. Lieb-Robinson Bound for Harmonic Systems

In order to analyze the timescales of propagation after the quench, we can consider the corresponding Lieb-Robinson bounds [87]. For quadratic bosonic systems, the maximum speed of propagation can be obtained from the couplings of the Hamiltonian [88, 89, 90]. We will summarize some results for harmonic systems following [90], focusing only on the type of Hamiltonians discussed in this thesis for the sake of concreteness.

Consider the generic quadratic Hamiltonian

$$H = \frac{1}{2} \sum_{i,j} (\hat{q}_i X_{ij} \hat{q}_j + \hat{p}_i P_{ij} \hat{p}_j), \quad (2.26)$$

where $X, P \in \mathbb{R}^{N \times N}$ are symmetric matrices. For simplicity, we will assume that $P_{ij} = \delta_{ij}$ and a nearest-neighbor Hamiltonian

$$X_{ij} = 0, \quad \text{for } d(i, j) > 1, \quad (2.27)$$

where $d(i, j)$ is the graph-theoretical distance. (Note that we are not assuming that the lattice has a particular spatial dimension.) If we define $\hat{q}_n(t) = e^{itH} \hat{q}_n e^{-itH}$, we have [90]

$$i[\hat{q}_n(t), \hat{q}_m] = \sum_{s=0}^{\infty} \frac{(-1)^s t^{2s+1}}{(2s+1)!} (X^s)_{nm} \equiv C_{nm}^{qq}(t) \mathbb{1}. \quad (2.28)$$

This identity holds even if H is unbounded from below because it is obtained using commutators of \hat{q}_i and \hat{p}_i with $\exp(\alpha H)$ via the Baker-Hausdorff formula [90].

Coefficient $C_{nm}^{qq}(t)$ can be bounded using the locality condition (2.27), so that

$$|C_{nm}^{qq}(t)| \leq \frac{1}{\sqrt{\|X\|}} \sum_{s=0}^{\infty} \frac{\tau^{2s+2d(i,j)+1}}{(2s+2d(i,j)+1)!}, \quad (2.29)$$

where $\|X\|$ is the operator norm and $\tau = \sqrt{\|X\|}t$. For $e\tau < 2c$, for $c \in \mathbb{Z}^+$, we have

$$\sum_{s=c}^{\infty} \frac{\tau^{2s}}{(2s)!} \leq \frac{(e\tau/2c)^{2c}}{\sqrt{2c}(1-(e\tau/2c)^2)}. \quad (2.30)$$

Now, being a finite matrix, $\|X\|$ correspond to its largest eigenvalue in absolute value. We can apply this to Hamiltonian (2.22). In that case, it is easy to diagonalize the corresponding X matrix by a Fourier transform. Assuming $4\Omega^2 \geq |m^2|$, it follows that

$$\|X\| = \max_{\mathbf{k}} |\omega_{\mathbf{k}}| = 4d\Omega^2 + m^2. \quad (2.31)$$

Using (2.30) and (2.31), we have that the Lieb-Robinson bound for Hamiltonian (2.22) is

$$v_{\text{LR}} = ea\sqrt{4d\Omega^2 + m^2}. \quad (2.32)$$

Commutators of operators that are ‘‘space-like’’ separated with respect to v_{LR} will be exponentially suppressed. In particular, if $2r > v_{\text{LR}}t$, we have

$$\begin{aligned} \|[\hat{q}_r(t), \hat{q}_0]\| &\leq \frac{1}{\max |\omega_{\mathbf{k}}|} \frac{e^{-2(r/a)\log(2r/v_{\text{LR}}t)}}{\sqrt{r/a}(1-\frac{v_{\text{LR}}t}{2r})}, \\ \|[\hat{p}_r(t), \hat{p}_0]\| &\leq \max |\omega_{\mathbf{k}}| \frac{e^{-2(r/a)\log(2r/v_{\text{LR}}t)}}{\sqrt{r/a}(1-\frac{v_{\text{LR}}t}{2r})}. \end{aligned} \quad (2.33)$$

Note that all these results hold for $m^2 \mapsto -m^2$. This will be very important when we consider the tachyonic quench in Chapter 3.

The bound will always be larger than the speed of light $c = a\Omega$ as long as $\Omega \gg |m|$. In the case of a one-dimensional harmonic chain, we obtain

$$v_{\text{LR}} \approx 2ec. \quad (2.34)$$

This is consistent with the associated speed of light in the continuum limit (2.20). As we discussed in the previous chapter, Lieb-Robinson bounds are not necessarily tight. In this case, the extra factor of e is due to the fact that this bound is obtained for general lattices [90]).

2.4. Correlators After a Quantum Quench

In this chapter, we will consider regular mass quenches of Hamiltonian (2.15), i.e., a sudden global change in the value of the boson mass so that $m_0, m \geq 0$. We can summarize the protocol as

$$H(t) = \begin{cases} H(m_0), & t < 0, \\ H(m), & t \geq 0, \end{cases} \quad (2.35)$$

starting with the many-body ground state of $H(m_0)$. This quench can be implemented in a straight-forward way. First, note that, for any value of the mass, the Hamiltonian can

be written as a set of N independent HOs (2.17) labelled by momentum k . In analogy to a single HO, all quantities after the quench will be determined by the corresponding frequencies of each mode. Accordingly, we will denote the different dispersion relations as

$$\omega_{0k} = \sqrt{4\Omega^2 \sin^2\left(\frac{ka}{2}\right) + m_0^2}, \quad \omega_k = \sqrt{4\Omega^2 \sin^2\left(\frac{ka}{2}\right) + m^2}. \quad (2.36)$$

For simplicity, we will be working mostly in the so-called *deep quench limit* [101]. It is characterized by an extremely massive initial state $m_0 \gg m$, so that the initial correlation length vanishes and we have an effective product state. In this limit, all the correlations formed after the quench are due to the evolution, allowing for a clear analysis.

For our numerical calculations we will set $a = \Omega = 1$, so that $c = 1$. This choice will give the correct relativistic scale to the time direction. Note that, in order to describe a theory that corresponds to a proper discretization of a non-trivial continuous QFT, we must impose $m \ll \Omega$.

Being a Gaussian state evolving according to a Gaussian unitary, we expect the system to remain Gaussian for all times after the quench. That implies that everything will be determined by the fundamental two-point functions. These correlators can be written as

$$\begin{aligned} \langle \hat{q}_r \hat{q}_s \rangle (t) &= \frac{1}{N} \sum_k e^{ik(r-s)} C_k^{(qq)}(t), \\ \langle \hat{p}_r \hat{p}_s \rangle (t) &= \frac{1}{N} \sum_k e^{ik(r-s)} C_k^{(pp)}(t), \\ \langle \hat{q}_r \hat{p}_s \rangle (t) &= \frac{1}{N} \sum_k e^{ik(r-s)} C_k^{(qp)}(t), \end{aligned} \quad (2.37)$$

where

$$\begin{aligned} C_k^{(qq)}(t) &= \frac{\omega_{0k}^2 + \omega_k^2}{4\omega_{0k}\omega_k^2} - \frac{\omega_{0k}^2 - \omega_k^2}{4\omega_{0k}\omega_k^2} \cos(2\omega_k t), \\ C_k^{(pp)}(t) &= \frac{\omega_{0k}^2 + \omega_k^2}{4\omega_{0k}} + \frac{\omega_{0k}^2 - \omega_k^2}{4\omega_{0k}} \cos(2\omega_k t), \\ C_k^{(qp)}(t) &= \frac{\omega_{0k}^2 - \omega_k^2}{4\omega_{0k}\omega_k} \sin(2\omega_k t) + \frac{i}{2}. \end{aligned} \quad (2.38)$$

These are the corresponding generalizations of the correlators obtained in the previous section for a quenched HO (2.11).

In the deep quench limit, there are some simplifications. The initial mass scale $\omega_{0k} \approx m_0$ decouples in the correlators and we have

$$\begin{aligned} \langle \hat{q}_r \hat{q}_s \rangle (t) &= \frac{m_0}{4N} \sum_k e^{ik(r-s)} \left[\frac{1 - \cos(2\omega_k t)}{\omega_k^2} \right], \\ \langle \hat{p}_r \hat{p}_s \rangle (t) &= \frac{m_0}{4N} \sum_k e^{ik(r-s)} [1 + \cos(2\omega_k t)], \\ \langle \hat{q}_r \hat{p}_s \rangle (t) &= \frac{m_0}{4N} \sum_k e^{ik(r-s)} \left[\frac{\sin(2\omega_k t)}{\omega_k} \right] + \frac{i}{2} \delta_{rs}. \end{aligned} \quad (2.39)$$

Note that these correlators are valid for $|r - s|, t \gg 1/m_0$.

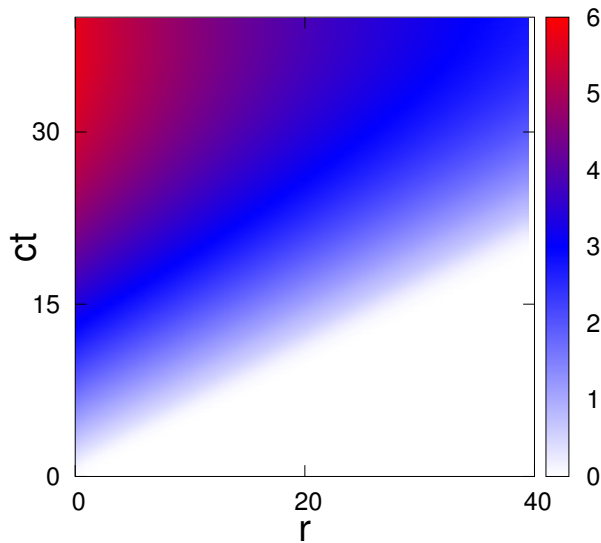


Figure 2.1: Density plot of the correlator $\langle \hat{q}_r \hat{q}_0 \rangle(t)$ after a massive quench using $m_0 = a = \Omega = 1$, $m^2 = 0.001$, and $N = 10000$.

As we see in Fig. (2.1), the correlators respect the causal “light-cone” imposed by the Lieb-Robinson bound. This structure is more explicit in the continuum limit, where causality can be related to usual relativistic invariance. If we set $\Omega = \frac{1}{a}$, we have $\omega_k^2 \rightarrow k^2 + m^2$ as $a \rightarrow 0$ and

$$\frac{\langle \hat{q}_r \hat{q}_s \rangle(t)}{a} \rightarrow \frac{m_0}{4} \int \frac{dk}{2\pi} e^{ik(r-s)} \left[\frac{1 - \cos(2\omega_k t)}{k^2 + m^2} \right]. \quad (2.40)$$

It can be easily shown that this propagator vanishes for $r > 2t$. This follows from evaluating the integral by closing the integration contour in the upper half of the complex k plane, where $\omega_k \rightarrow \sqrt{k^2}$ as $|k| \rightarrow \infty$.

We expect this type of sharp “light-cones” to be generic after massive quenches. Outside the emergent “light-cone”, correlations effectively vanish because of the initial correlation length (which is inversely proportional to the initial mass m_0). Some modes will propagate close to the maximum speed, forming the sharply defined edge at which information is finally shared. Once two points are causally connected, the correlations can build up and eventually saturate.

Massless Quenches

If $m = 0$, the correlator in the continuum limit (2.40) can be computed exactly for all spatial dimensions. Defining $\phi(r) = \lim_{a \rightarrow 0} \hat{q}_r / \sqrt{a}$, we have [101]

1. $d = 1$

$$\langle \phi(r, t) \phi(0, t) \rangle = \begin{cases} 0 & \text{if } r > 2t, \\ \frac{m_0}{8} (2t - r) & \text{if } r \leq 2t. \end{cases} \quad (2.41)$$

2. $d = 2$

$$\langle \phi(r, t) \phi(0, t) \rangle = \begin{cases} 0 & \text{if } r > 2t, \\ \frac{m_0}{8\pi} \log \left[\frac{2t + \sqrt{4t^2 - r^2}}{r} \right] & \text{if } r < 2t. \end{cases} \quad (2.42)$$

3. $d = 3$

$$\langle \phi(r, t) \phi(0, t) \rangle = \begin{cases} 0 & \text{if } r > 2t, \\ \frac{m_0}{16\pi r} & \text{if } r < 2t. \end{cases} \quad (2.43)$$

These correlators enforce strongly the causal structure, so that two points in space a distance r apart remain strictly uncorrelated after the quench until $t = \frac{r}{2}$. Note that for $d = 3$ the value of the correlator is independent of time for $r < 2t$.

In the case of $d = 1$, we must be careful because a massless free bosonic theory is not physically meaningful [46, 101]. Since its canonical dimension vanishes, we can construct all types of local fields using powers of ϕ without introducing a scale. Consistent renormalization requires then that interaction terms are present, so that the truly physical operators are the vertex operators $\exp(iq\phi(r))$. Given that the state is Gaussian, the corresponding correlators are easily computed

$$\begin{aligned} \langle e^{iq\phi(r,t)} e^{-iq\phi(s,t)} \rangle &= \exp \left[-q^2 (\langle \phi(0, t) \phi(0, t) \rangle - \langle \phi(r, t) \phi(s, t) \rangle) \right] \\ &= \begin{cases} \exp \left(-\frac{q^2 m_0 t}{4} \right) & \text{if } r > 2t, \\ \exp \left(-\frac{q^2 m_0 r}{8} \right) & \text{if } r < 2t. \end{cases} \end{aligned} \quad (2.44)$$

We obtain then an exponentially decaying correlation function outside the causal horizon and a static solution inside. This is consistent with the results obtained using conformal field theory (CFT) [45, 46].

2.5. Equilibration After a Massive Bosonic Quench

Generalized Gibbs Ensemble

We can associate as many local conserved charges to Hamiltonian (2.15) as bosonic degrees of freedom. They can be written as [103]

$$\begin{aligned} I_n &= \frac{1}{2} \sum_k \cos(nk) \left[\hat{p}_k^\dagger \hat{p}_k + \omega_k^2 \hat{q}_k^\dagger \hat{q}_k \right] \\ &= \sum_k \omega_k \cos(nk) \left(b_k^\dagger b_k + \frac{1}{2} \right), \end{aligned} \quad (2.45)$$

where we use the creation and annihilation operators

$$b_k = \frac{1}{\sqrt{2\omega_k}} (\omega_k \hat{q}_k + i \hat{p}_k), \quad b_k^\dagger = \frac{1}{\sqrt{2\omega_k}} (\omega_k \hat{q}_{-k} - i \hat{p}_{-k}). \quad (2.46)$$

It is trivial to see that $[I_n, I_m] = 0$ and that $H(m) = I_0$. Locality follows from a simple Fourier transform

$$I_n = \frac{1}{2} \sum_r \left[\hat{p}_r \hat{p}_{r+n} + (m^2 + 2\Omega^2) \hat{q}_r \hat{q}_{r+n} - \Omega^2 (\hat{q}_r \hat{q}_{r+n+1} + \hat{q}_r \hat{q}_{r+n-1}) \right]. \quad (2.47)$$

The momentum representation can be used to obtain

$$\sum_n \tilde{\lambda}_n I_n = \sum_k \left(\omega_k \sum_n \tilde{\lambda}_n \cos(kn) \right) \left(b_k^\dagger b_k + \frac{1}{2} \right) \equiv \sum_k \lambda_k \left(b_k^\dagger b_k + \frac{1}{2} \right). \quad (2.48)$$

This allows us to define a generalized Gibbs ensemble (GGE) (see (1.13)) using the mode occupation numbers [46, 93]

$$\rho^{\text{GGE}} = \frac{1}{Z} \exp \left(- \sum_k \lambda_k b_k^\dagger b_k \right), \quad (2.49)$$

where

$$Z = \text{Tr} \left[\exp \left(- \sum_k \lambda_k b_k^\dagger b_k \right) \right] = \prod_k \frac{1}{1 - e^{-\lambda_k}}. \quad (2.50)$$

By computing $\langle b_k^\dagger b_k \rangle_{\text{GGE}}$, it is easy to fix the Lagrange multipliers from the initial conditions (see (1.14))

$$\frac{1}{e^{\lambda_k} - 1} = \frac{1}{4} \left(\frac{\omega_k}{\omega_{0k}} + \frac{\omega_{0k}}{\omega_k} \right) - \frac{1}{2}. \quad (2.51)$$

Note that $\lambda_k = \lambda_{-k}$, as expected from the parity in Eq. (2.47). Going back to the original variables, we obtain

$$\begin{aligned} \langle \hat{q}_k^\dagger \hat{q}_k \rangle_{\text{GGE}} &= \frac{1}{2\omega_k} \left(\langle b_k^\dagger b_k \rangle_{\text{GGE}} + \langle b_{-k}^\dagger b_{-k} \rangle_{\text{GGE}} \right) \\ &= \frac{\omega_{0k}^2 + \omega_k^2}{4\omega_{0k}\omega_k^2}, \end{aligned} \quad (2.52)$$

which implies

$$\langle \hat{q}_r \hat{q}_s \rangle_{\text{GGE}} = \frac{1}{N} \sum_k e^{ik(r-s)} \frac{\omega_{0k}^2 + \omega_k^2}{4\omega_{0k}\omega_k^2}. \quad (2.53)$$

This corresponds to the infinite-time average of correlator (2.37) after the quench

$$\overline{\langle \hat{q}_r \hat{q}_s \rangle} = \lim_{T \rightarrow \infty} \frac{1}{T} \int_0^T dt \langle \hat{q}_r \hat{q}_s \rangle (t). \quad (2.54)$$

Similar results hold for the other fundamental two-point functions. It follows then that the equilibration values of all observables can be computed using the GGE (2.49). In other words, the long-time behavior of the system after the quench can be effectively described by a simple statistical ensemble. Even though it does not thermalize, the equilibration is guaranteed and well-behaved. As we will see in the next chapter, the dynamics after a tachyonic quench cannot be captured in such simple terms due to the unstabilities of the driving Hamiltonian.

Effective Temperature

Sotiriadis, Calabrese and Cardy [100] obtained an effective temperature for the equilibration of each mode by comparing the infinite-time average of $\langle \hat{q}_r(t_1) \hat{q}_s(t_2) \rangle$ to the Matsubara propagator. It can be written as

$$\beta_{\text{eff}}(k) = \frac{1}{\omega_k} \log \left(\frac{(\omega_k + \omega_{0k})^2}{(\omega_{0k} - \omega_k)^2} \right). \quad (2.55)$$

If we assume the deep quench limit $\omega_{0k} \approx m_0 \gg \omega_k$, we can find a simplified relation

$$\beta_{\text{eff}}(k) \approx \frac{4}{m_0} \left(1 + \frac{\omega_k^2}{3m_0^2} \right). \quad (2.56)$$

The momentum dependence is consistent with the fact that integrable systems (such as free bosons) do not equilibrate globally after a quench. As we already showed, this is due to the presence of a macroscopic number of conserved quantities.

2.6. Evolution of the Entanglement Entropy

Entanglement entropy (EE) is perhaps one of the simplest measures that characterize the information interdependence between subsystems. Given that after a quantum quench a system can survey a big portion of the Hilbert space, the evolution of the EE of a fixed subsystem can be used as a proxy to understand in an unified way the formation of new correlations.

Observables in Gaussian systems are completely determined by the covariance matrix

$$\Gamma_{nm} = \text{Re} \langle \hat{r}_n \hat{r}_m \rangle, \quad (2.57)$$

where $\hat{\mathbf{r}} = (\hat{q}_1, \dots, \hat{q}_N, \hat{p}_1, \dots, \hat{p}_N)$. In particular, all information about a subsystem A , composed of sites $\{i_1, \dots, i_L\}$, can be obtained from the $2L \times 2L$ submatrix

$$\Gamma_{nm}^A = \Gamma_{i_n i_m}, \quad \Gamma_{n+L, m}^A = \Gamma_{i_n + N, i_m}, \quad \text{etc..} \quad (2.58)$$

The EE of subsystem A can be computed from the associated symplectic eigenvalues $\{\sigma_n | n = 1, \dots, L\}$, where $\sigma_n \geq 1/2$. These correspond to the positive spectrum of $i\Gamma^A \Omega_{\text{sym}}$, where Ω_{sym} is the symplectic matrix

$$\Omega_{\text{sym}} = \begin{pmatrix} 0 & \mathbb{1}_L \\ -\mathbb{1}_L & 0 \end{pmatrix}. \quad (2.59)$$

The EE is given by the formula [104, 105, 106]

$$S_A = \sum_{n=1}^L \left(f \left(\sigma_n + \frac{1}{2} \right) - f \left(\sigma_n - \frac{1}{2} \right) \right), \quad (2.60)$$

where $f(x) = x \log(x)$. Note that for very large symplectic eigenvalues $\sigma_n \gg 1$, we have $f(\sigma_n + \frac{1}{2}) - f(\sigma_n - \frac{1}{2}) \approx \log(\sigma_n) + 1$.

We can estimate the asymptotic growth of entanglement by using the values predicted by the GGE. In the case of the ensemble described by ρ^{GGE} , the global entropy is simply

$$S_{\text{GGE}} = -\text{Tr} (\rho^{\text{GGE}} \log \rho^{\text{GGE}}) = \log Z - \sum_k \lambda_k \frac{\partial \log Z}{\partial \lambda_k}. \quad (2.61)$$

Setting $n_k = \langle b_k^\dagger b_k \rangle = 1/(e^{\lambda_k} - 1)$, we have

$$S_{\text{GGE}} = \sum_k [(n_k + 1) \log(n_k + 1) - n_k \log(n_k)]. \quad (2.62)$$

If we use the phenomenological formula for the EE evolution after a quench we introduced in the previous chapter (1.19), we can postulate [99]

$$2\pi s(k) = (n_k + 1) \log(n_k + 1) - n_k \log(n_k), \quad (2.63)$$

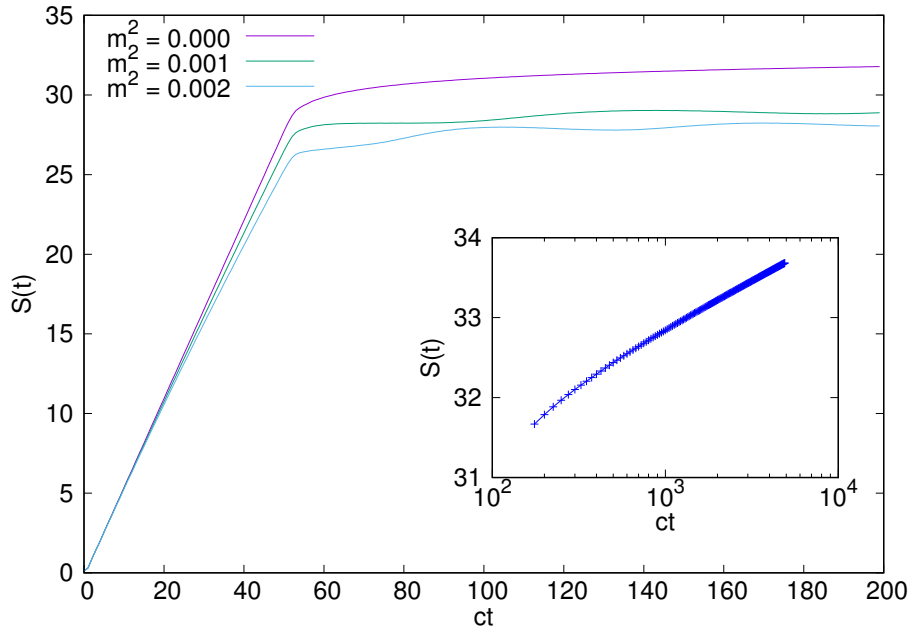


Figure 2.2: Evolution of the EE of a block of size $L = 100$ after a massive bosonic quench with $m^2 = 0.0, 0.001, 0.002$ and $N = 10000$. (We set $a = \Omega = 1$.) Note that for short times, the growth is approximately linear and roughly independent of m until the saturation time $t \approx L/2c$. *Inset*: Semilog plot of the EE for a critical quench $m^2 = 0$. As we see, there is a logarithmic growth instead of a saturation.

so that, in the thermodynamic limit, we can write

$$S_A(t) = 2t \int_{2|v(k)|t < L} dk v(k) s(k) + L \int_{2|v(k)|t > L} dk s(k), \quad (2.64)$$

where $v(k) = d\omega_k/dk$ is the corresponding group velocity. This phenomenological formula has been compared to the exact numerical results with very good agreement [55].

In Fig. (2.2), we plot the evolution of the EE after a massive quench for a block of size $L = 100$ and a system of $N = 10000$ sites. This is obtained from the evolution of the symplectic eigenvalues (2.60) computed from the two-point correlators. We set $m_0 = 1$ and consider $m^2 = 0.0, 0.001, 0.002$. In all cases, we see a linear growth for times shorter than the saturation time $t \approx L/2c$. This is consistent with the ballistic spreading of quasiparticles we discussed in the previous chapter. If $m^2 > 0$, the EE saturates to a constant, with possible fluctuations due to the remaining slow modes [95, 107]. If $m^2 = 0$, there is a remaining logarithmic growth, so that for long times $S \sim \log(t)$ (see inset). It should be noted that there will be revivals for times $t_{\text{rev}} \sim N/2c$ where $S(0) \approx S(t_{\text{rev}})$. This finite-size phenomenon can be interpreted as a recombination of the fastest quasiparticles in the system [108, 109].

In the next chapter, we will consider an unstable tachyonic quench for a free bosonic system. Most of the general formalism we have introduced so far will carry on to that scenario. We will be able to compare the generic results we have shown so far to the ones obtained in that exotic protocol.

Tachyonic Quenches in a Bosonic Field Theory

3.1. Introduction

Tachyonic systems have an exotic history. They were originally proposed as field theories describing particles that could have a group velocity larger than the speed of light [110, 111, 112, 113]. If they are free, they are characterized by the dispersion relation

$$E^2 = p^2 - \mu^2, \tag{3.1}$$

where E is the energy of the particle, p its linear momentum, and μ a real parameter, usually referred to as tachyonic mass. However, these theories were later understood on more physical grounds as instabilities that could still preserve Lorentz causality [114] and be related instead to symmetry breaking or condensation processes [115, 116, 117].

In this chapter, we study a bosonic field theory driven by a free tachyonic Hamiltonian. We will obtain this regime from a theory describing two coupled bosonic fields after a regular quench. We will focus on free (Gaussian) systems [102, 100, 101], so that everything can be characterized analytically. To the best of our knowledge, this type of quench has not been studied in the context of many-body quantum physics. Even though the driving Hamiltonian is unbounded from below, we will argue that the corresponding unitary evolution is well-defined. In particular, we will characterize the evolution of simple correlators, the entanglement entropy of a block, and the mutual information between disconnected subregions. We will show that the causal structure is very similar to the one obtained after a critical quench [101, 118, 92] (see Chapter 2). For short times, physical quantities also resemble the evolution of a massless quench. However, the resulting evolution will be dominated by exponential divergences that prevent the system from being close to a steady state regime. In other words, the system will not equilibrate, even in the sense of generalized Gibbs ensembles [11, 84, 61] (see Chapter 1). Some applications and extensions will then be outlined.

3.2. Coupled bosonic QFT

Consider two bosonic fields described by the Lagrangian density

$$\mathcal{L} = \frac{1}{2}(\partial_\mu \Phi_1)^2 + \frac{1}{2}(\partial_\mu \Phi_2)^2 - \frac{m^2}{2}(\Phi_1^2 + \Phi_2^2) - g\Phi_1\Phi_2. \quad (3.2)$$

We can rewrite this Gaussian theory using another set of bosonic fields $\Phi_\pm = (\Phi_1 \pm \Phi_2)/\sqrt{2}$ to obtain

$$\mathcal{L} = \frac{1}{2}(\partial_\mu \Phi_+)^2 + \frac{1}{2}(\partial_\mu \Phi_-)^2 - \frac{1}{2}m_+^2\Phi_+^2 - \frac{1}{2}m_-^2\Phi_-^2, \quad (3.3)$$

where $m_\pm^2 = m^2 \pm g$. In the new variables, the fields are decoupled and their properties solely determined by their respective masses.

This seemingly trivial manipulation allows us to translate the dynamics from the coupling of the original fields to the masses of the new ones. In particular, note that quenching the coupling of $\Phi_{1,2}$ is equivalent to quenching the masses of Φ_\pm . We can exploit this relation to access regimes that would a priori seem rather artificial.

For instance, consider a global quench where we suddenly change the interaction $g \mapsto g'$ so that $m_-'^2 = m^2 - g' < 0$. The resulting Hamiltonian density for Φ_- ,

$$\mathcal{H}_- = \frac{1}{2} [(\partial_t \Phi_-)^2 + (\nabla \Phi_-)^2 - |m_-'|^2 \Phi_-^2], \quad (3.4)$$

has a negative mass term, i.e., it describes a tachyonic dispersion relation, giving rise to a Hamiltonian that is not bounded from below. Operators with these characteristics are usually considered pathological because the associated systems would be intrinsically unstable. However, as we will argue in more detail in later sections, this quenching procedure can still yield a well-defined unitary evolution in the Hilbert space of the original theory. We can then rigorously study the resulting evolution after the quench, even though the driving Hamiltonian lacks a proper ground state. We will call this quenching protocol an unstable tachyonic quench, or more simply, a *tachyonic quench*.

The most popular way tachyonic field theories are handled in the literature is by adding an extra quartic term $\lambda\Phi^4$. This bounds the Hamiltonian from below while providing a false unstable vacuum around the quadratic maximum [115]. The most prominent use of this potential is in the symmetry-breaking mechanism that gives mass to gauge fields while preserving gauge invariance [84, 119, 120, 121]. Even though we will focus only on free systems, the addition of this term will be briefly discussed in the context of possible realizations.

Free tachyonic systems can also be studied by themselves in a rigorous manner [110, 111, 112, 113]. One feature of these theories is the restriction of momenta, so that only $|\mathbf{k}| \geq m$ is allowed. We will not need these constraints in the context of this thesis because Hamiltonian (3.4) will only be used to define an unitary operator dictating the non-equilibrium evolution of a well-defined physical system.

In order to simplify the discussion, we will focus our analysis only on Φ_- , i.e., on the field whose mass term changes sign after the quench. It should be understood that this is done in the context of the coupled bosonic theory (3.2) which provides a sensible physical realization.

3.3. Quenching the Frequency of a Simple Harmonic Oscillator

As we discussed in Chapter 2, free bosonic theories can be studied as a set of independent harmonic oscillators (HOs) whose frequency can be determined from the parameters in the Hamiltonian. After a (global) quench, the evolution of all relevant quantities can then be reduced to the quenching of each mode. This reduction of the problem still holds in the context of the tachyonic quench. Once again, we consider the single body problem before moving on to the many-body case. For a single HO, we want to study the evolution of the ground state of the initial Hamiltonian

$$H_0 = \frac{\hat{p}^2}{2} + \frac{1}{2}\omega_0^2\hat{x}^2, \quad (3.5)$$

described by the Gaussian state

$$\langle x|0\rangle = \left(\frac{\omega_0}{\pi}\right)^{1/4} \exp\left(-\omega_0\frac{x^2}{2}\right), \quad (3.6)$$

under the action of the unitary operator obtained from an inverted quadratic potential

$$U_t = \exp\left[-it\left(\frac{\hat{p}^2}{2} - \frac{1}{2}\xi^2\hat{x}^2\right)\right] \equiv \exp(-itH_1). \quad (3.7)$$

We can summarize the protocol as

$$H(t) = \begin{cases} H_0, & t < 0, \\ H_1, & t \geq 0. \end{cases} \quad (3.8)$$

This is the single-body version of the unstable tachyonic quench we want to study in the many-body context.

Operator H_1 in (3.7) is unbounded from below, so it is an ill-defined Hamiltonian. However, we can make sense of it as an operator acting on the original Hilbert space. Consider the ladder operators that diagonalize H_0

$$b = \sqrt{\frac{\omega_0}{2}} \left(\hat{x} + \frac{i}{\omega_0}\hat{p} \right).$$

In these variables, we have

$$H_1 = \frac{\omega_0^2 - \xi^2}{2\omega_0} \left(b^\dagger b + \frac{1}{2} \right) - \frac{\omega_0^2 + \xi^2}{4\omega_0} ((b^\dagger)^2 + b^2).$$

We see then that H_1 is a self-adjoint operator that has a simple and well-defined action on the states of the original Hilbert space. Given that the associated unitary (3.7) will have a bounded spectrum, its action is also well-defined for all t ¹.

The propagator for this evolution is given by

$$\begin{aligned} K(x_f, x_i; t) &= \langle x_f | e^{-itH_1} | x_i \rangle \\ &= \sqrt{\frac{\xi}{2\pi i \sinh(\xi t)}} \exp\left[i \frac{\xi \cosh(\xi t)(x_i^2 + x_f^2) - 2x_i x_f}{2 \sinh(\xi t)} \right]. \end{aligned} \quad (3.9)$$

¹Note also that for a regular massive Hamiltonian $\xi \rightarrow i\omega$, the unbounded term can be eliminated via a bosonic Bogoliubov transformation, as we showed in Chapter 2.

It corresponds to the familiar propagator of the simple HO after the analytic continuation $\omega \mapsto i\omega = \xi$ [122]. This remarkable yet natural result can be derived rigorously via the same computational techniques used for the HO [123].

We can compute the equal-time correlators using propagator (3.9)

$$\begin{aligned}\langle \hat{x}^2 \rangle(t) &= \frac{\omega_0^2 + \xi^2}{4\omega_0\xi^2} \cosh(2\xi t) - \frac{\omega_0^2 - \xi^2}{4\omega_0\xi^2}, \\ \langle \hat{p}^2 \rangle(t) &= \frac{\omega_0^2 + \xi^2}{4\omega_0} \cosh(2\xi t) + \frac{\omega_0^2 - \xi^2}{4\omega_0}, \\ \langle \hat{x}\hat{p} \rangle(t) &= \frac{\omega_0^2 + \xi^2}{4\omega_0\xi} \sinh(2\xi t) + \frac{i}{2}.\end{aligned}\tag{3.10}$$

Once again, note that these correspond to analytic continuations of the results obtained from the simple harmonic oscillator (see Chapter 2) [100, 101].

One of the most prominent features of these correlators are that they grow exponentially fast. This means that we cannot associate a long-time stationary behavior to the dynamics. In other words, the system will not equilibrate after the quench [11]. If we use the energy levels of the original Hamiltonian as a reference, the expected occupation will evolve as

$$\langle \hat{N} \rangle(t) = \langle b^\dagger b \rangle = \frac{(\omega_0^2 + \xi^2)^2 \cosh(2\xi t) - 1}{4\omega_0^2\xi^2}.\tag{3.11}$$

Note that quenching to a free particle ($\xi \rightarrow 0$), we obtain a milder growth $\langle \hat{N} \rangle \rightarrow \omega_0^2 t^2 / 2$. This implies that the unstable quench can be characterized both by the exponential divergence of the correlators and the occupation of the original energy levels.

3.4. Tachyonic Quench for the Harmonic Chain

We will use the harmonic chain as the UV regularization of the free boson QFT. Given that we studied this model in detail in Chapter 2, we will just quote the relevant equations. First, we have the Hamiltonian

$$H(m) = \frac{1}{2} \sum_{r/a=1}^N [\hat{p}_r^2 + m^2 \hat{q}_r^2 + \Omega^2 (\hat{q}_{r+a} - \hat{q}_r)^2],\tag{3.12}$$

where $a = L/N$ is the UV regularization and we assume periodic boundary conditions. Using the Fourier transform

$$\hat{q}_r = \frac{1}{\sqrt{N}} \sum_k e^{ikr} \hat{q}_k,\tag{3.13}$$

(similarly for \hat{p}_r), where momenta $k = \frac{2\pi}{L}n$ are given by $n = 0, \pm 1, \dots, \pm \frac{N-1}{2}$, we have

$$H(m) = \frac{1}{2} \sum_k [\hat{p}_k^\dagger \hat{p}_k + \omega_k^2 \hat{q}_k^\dagger \hat{q}_k].\tag{3.14}$$

The resulting dispersion relation is given by

$$\omega_k^2 = 4\Omega^2 \sin^2\left(\frac{ka}{2}\right) + m^2,\tag{3.15}$$

and the associated speed of light is $c = a\Omega$.

Hamiltonian (3.14) implies that we can associate an independent HO to each mode k . If we quench the mass of the system to a tachyonic regime $m_0^2 \mapsto -m^2$, it will be equivalent to changing the frequencies from

$$\omega_{0k} = \sqrt{4\Omega^2 \sin^2\left(\frac{ka}{2}\right) + m_0^2} \quad (3.16)$$

to

$$\omega_k = \sqrt{4\Omega^2 \sin^2\left(\frac{ka}{2}\right) - m^2} \equiv i\xi_k. \quad (3.17)$$

We see that the oscillators will have two possible dynamics:

a) *Stable modes*: If $m \leq 2\Omega|\sin(ka/2)|$, the final frequency ω_k will be real. In that case the evolution will be like a simple quench from a harmonic Hamiltonian to another. These modes will behave qualitatively as regular mass quenches like the ones described in Chapter 2 [100, 101]. In particular, these modes will equilibrate.

b) *Unstable modes*: If $m > 2\Omega|\sin(ka/2)|$, we expect these modes to behave according to the unstable quench we did for the simple HO in the previous section. It follows that they not only do not equilibrate, but also explode exponentially fast. As we will see in later sections, these modes (the low-frequency ones) will dominate the long-time behavior of the whole system. This makes it impossible to define an stationary ensemble that captures the qualitative physical properties after the quench.

3.5. Causal Structure After a Tachyonic Quench

For simplicity, we will be working mostly in the so-called deep quench limit we introduced in Chapter 2, i.e., $m_0 \gg m$. In this case, all the correlations formed after the quench are due to the evolution, allowing for a clear analysis.

The two-point correlators can still be written as

$$\begin{aligned} \langle \hat{q}_r \hat{q}_s \rangle(t) &= \frac{1}{N} \sum_k e^{ik(r-s)} C_k^{(qq)}(t), \\ \langle \hat{p}_r \hat{p}_s \rangle(t) &= \frac{1}{N} \sum_k e^{ik(r-s)} C_k^{(pp)}(t), \\ \langle \hat{q}_r \hat{p}_s \rangle(t) &= \frac{1}{N} \sum_k e^{ik(r-s)} C_k^{(qp)}(t), \end{aligned} \quad (3.18)$$

where

$$\begin{aligned} C_k^{(qq)}(t) &= \frac{\omega_{0k}^2 + \omega_k^2}{4\omega_{0k}\omega_k^2} - \frac{\omega_{0k}^2 - \omega_k^2}{4\omega_{0k}\omega_k^2} \cos(2\omega_k t), \\ C_k^{(pp)}(t) &= \frac{\omega_{0k}^2 + \omega_k^2}{4\omega_{0k}} + \frac{\omega_{0k}^2 - \omega_k^2}{4\omega_{0k}} \cos(2\omega_k t), \\ C_k^{(qp)}(t) &= \frac{\omega_{0k}^2 - \omega_k^2}{4\omega_{0k}\omega_k} \sin(2\omega_k t) + \frac{i}{2}. \end{aligned} \quad (3.19)$$

Note that these functions are even in ω_k , so there is no branch cut in the k complex plane due to the square root in definition (3.17). Also, in the case ω_k^2 is negative, both possible imaginary roots will give the same functions, so there is no ambiguity.

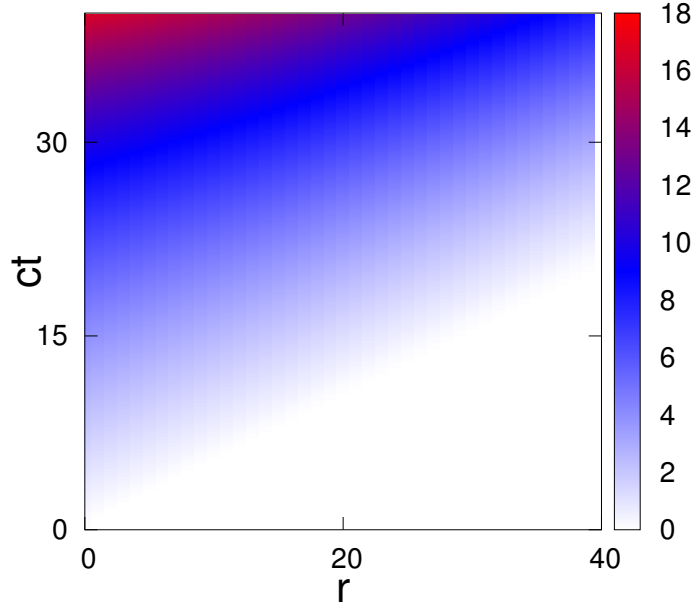


Figure 3.1: Density plot of the correlator $\langle \hat{q}_r \hat{q}_0 \rangle(t)$ after a tachyonic quench using $a = \Omega = m_0 = 1$, $m^2 = 0.001$ and $N = 10000$. Note that the causal structure is strictly preserved.

Even though tachyonic theories are usually associated to superluminal particles, they are better understood as instabilities in causal theories [114, 124, 117, 116, 125]. Propagation is still governed by causal Green functions, in such a way that information cannot move faster than the speed of light. In the context of the tachyonic quench, we can explicitly show that the causal structure is preserved during the evolution.

First, consider the UV regulated Hamiltonian (3.12). Being a local lattice system, the dynamics can be studied using Lieb-Robinson bounds. For quadratic bosonic systems, we saw in Chapter 2 that the maximum speed of propagation can be obtained from the couplings of the Hamiltonian. In the case of the tachyonic Hamiltonian H_1 , we obtain (see section 2.3 for details)

$$v_{\text{LR}} = ea \max |\omega_k| = ea \sqrt{|4\Omega^2 - m^2|} \approx 2ec. \quad (3.20)$$

As we see in Fig. (3.1), correlators agree with this causal light-cone. This is consistent with the associated speed of light $c = a\Omega$.

The structure of the light-cone in the correlators is more explicit in the continuum limit, where causality is also preserved. If we set $\Omega = \frac{1}{a}$, we have

$$\omega_{0k}^2 \rightarrow k^2 + m_0^2, \quad \omega_k^2 \rightarrow k^2 - m^2, \quad (3.21)$$

as $a \rightarrow 0$ and (in the deep quench limit)

$$\frac{\langle \hat{q}_r \hat{q}_s \rangle(t)}{a} \rightarrow \frac{m_0}{4} \int \frac{dk}{2\pi} e^{ik(r-s)} \left[\frac{1 - \cos(2\omega_k t)}{k^2 - m^2} \right]. \quad (3.22)$$

Note that this propagator will vanish for $r > 2t$. This follows from evaluating the integral by taking the principal value around $k = \pm m$ and closing the integration contour in the

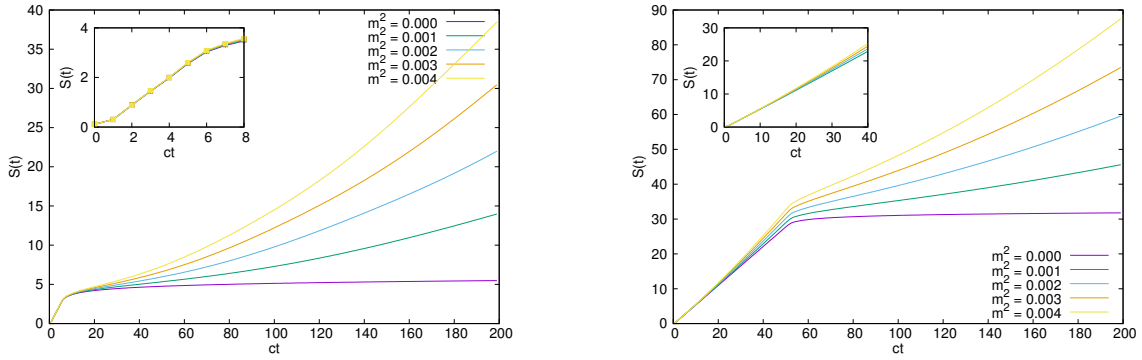


Figure 3.2: Evolution of the EE of a block of size (a) $L = 10$ and (b) $L = 100$ after a tachyonic quench with $m_0 = a = \Omega = 1$, $N = 10000$, and $m^2 = 0.0, \dots, 0.004$. Observe that the EE starts growing in a linear fashion for $mt \gg L$. This implies that for small m the growth will be logarithmically slow until the right scale is reached. *Inset:* For short times, the growth is approximately linear and independent of m .

upper half of the complex k plane. (A similar argument is used in [114] to relate the dynamics of a tachyonic field to instabilities in the theory. See also the end of Section 2.4 for details about the massless case $m \rightarrow 0$.)

3.6. Entanglement and Mutual Information Growth After the Quench

Given that the evolution is described by a Gaussian unitary operator, the state will always remain Gaussian. We can then compute all the relevant physical quantities using the covariance matrix Γ (see Section 2.6). In particular, we will be able to compute the entanglement entropy (EE) of a region A by considering the reduced covariance matrix Γ^A .

Now, before we discuss the evolution of the EE after an unstable tachyonic quench, let us consider the long-time evolution of the correlators. If we take the continuum limit in Equation (3.18), we have

$$\frac{\langle \hat{q}_r \hat{q}_s \rangle (t)}{a} \rightarrow \int \frac{dk}{2\pi} e^{ik(r-s)} C_k^{(qq)}(t). \quad (3.23)$$

For large times $t \gg 1/m$, we have

$$C_k^{(qq)}(t) \approx \frac{m_0}{4\xi_k^2} \exp(2\xi_k t), \quad (3.24)$$

where we also used the deep quench limit. The integrand in (3.23) will be sharply peaked around $k = 0$, so we can do a steepest descent approximation and obtain

$$\log \left(\frac{\langle \hat{q}_r \hat{q}_s \rangle (t)}{a} \right) \rightarrow 2mt + \mathcal{O}(\log(mt)). \quad (3.25)$$

Similarly for $\langle \hat{p}_r \hat{p}_s \rangle$ and $\text{Re} \langle \hat{q}_r \hat{p}_s \rangle$. This implies that, for every region A , all the elements in Γ^A have the same exponentially divergent factor. This will be present in all the

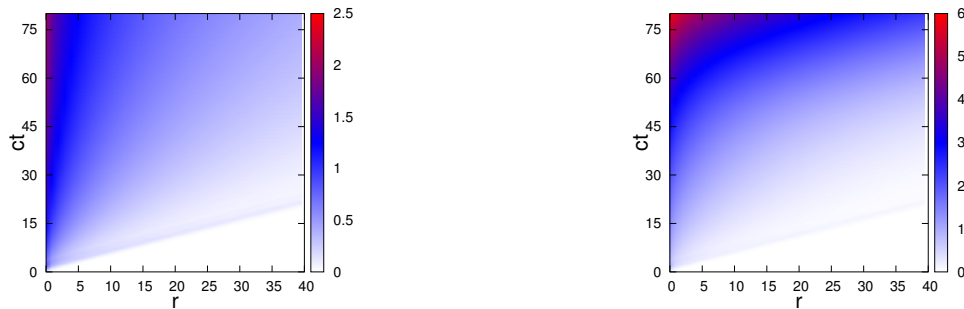


Figure 3.3: Contour plot for the evolution of the mutual information of two blocks consisting of 3 contiguous sites each separated by a distance r for $m_0 = a = \Omega = 1$ and $N = 10000$ after (a) a massless quench $m = 0$ and (b) a tachyonic quench with $m^2 = 0.004$.

associated symplectic eigenvalues $\{\sigma_n | n = 1, \dots, L\}$, which in turn determine the EE according to the formula

$$S_A = \sum_{n=1}^L \left(f \left(\sigma_n + \frac{1}{2} \right) - f \left(\sigma_n - \frac{1}{2} \right) \right), \quad (3.26)$$

where L is the volume of region A . We expect then that for $ct \gg L$, we have

$$S_A \sim 2mLt + \mathcal{O}(\log(mt)), \quad (3.27)$$

where the volumetric factor L comes from the number of symplectic eigenvalues. This behavior is universal. Note that this result is also valid for higher dimensions because the leading divergence of the corresponding correlators will also be an exponential (3.25).

In Fig. (3.2) we see the evolution of $S^A(t)$ after an unstable tachyonic quench for blocks of sizes $L = 10$ and $L = 100$. We see there is a short transient time $t \ll L/c$ during which information propagates ballistically independent of m (see inset). This is the same type of propagation exhibited in the quench dynamics of conformal field theory [118, 92]. However, the instability of the driving Hamiltonian takes over and we end up with a linear growth (3.27). This is qualitatively different to what happens after the regular massive quenches we considered in Chapter 2. In particular, note that the logarithmic growth that singles out the massless quench in Fig. (2.2) is much milder than the linear growth of the tachyonic quench.

We can gain further insight about the growth of correlations by studying the mutual information between subsystems. For two disjoint regions A and B , it is defined as

$$I_{AB} = S_A + S_B - S_{A \cup B}. \quad (3.28)$$

This can be used as a measure of the amount of correlation between A and B , even serving as an upper bound for normalized two-point functions [126].

Figure (3.3) illustrates the evolution of the mutual information after a massless quench ($m^2 = 0$) and a tachyonic quench for two blocks $A = \{1, 2, 3\}$ and $B = \{r+1, r+2, r+3\}$. Both display an unbounded growth with a sharp light-cone. However, the massless quench only grows logarithmically in time, while the tachyonic grows linearly. Figure (3.4) shows this evolution for fixed distances. Note how the mutual information starts

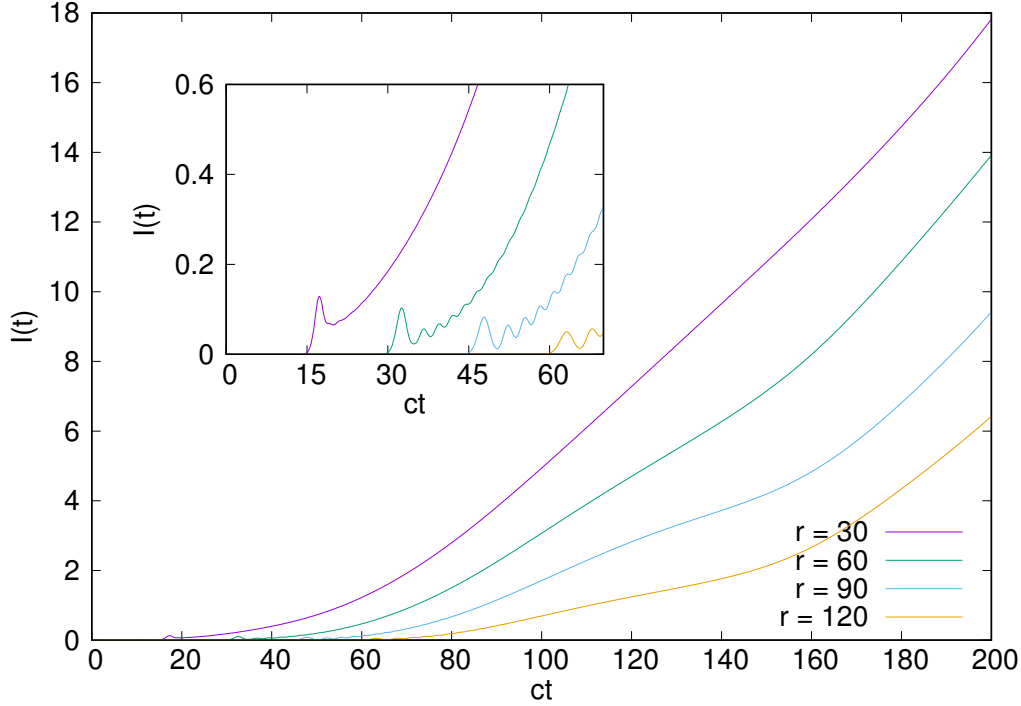


Figure 3.4: Evolution of the mutual information of two blocks consisting of 3 contiguous sites each separated by distances $r = 30, 60, 90, 120$ after a tachyonic quench with $m_0 = a = \Omega = 1$, $m^2 = 0.004$ and $N = 10000$.

growing after $t = r/2c$, as imposed by the causal structure (see inset). In the same fashion as the EE, this implies that the massless modes dominate the dynamics for short times, but the instability ends up leading the behavior.

The linear growth of the mutual information after a tachyonic quench is remarkable because it shows that the divergence in the EE is not a simple artifact due to the size of the local Hilbert space. Also, note that the growth cannot follow from the asymptotic behavior (3.27) because that volumetric contribution cancels.

3.7. Possible Connections to Physical Systems

Given the instabilities of the setting we have described, it is easy to see that any physical realization will have severe constraints. However, it is possible to find regimes that can approximate this type of quenches for certain periods of time. In particular, if we include higher order terms in the Hamiltonian to constrain the instabilities, we expect that tachyonic behavior can be seen for timescales that are shorter than the ones that bound the dynamics.

Consider first an $O(3)$ non-linear σ -model (NLSM) described by the Hamiltonian [127]

$$H = \int dx \left[g^2 \left(\vec{\ell} - \frac{\theta}{4\pi} \partial_x \vec{\phi} \right)^2 + \frac{1}{g^2} \partial_x \vec{\phi}^2 \right], \quad (3.29)$$

where $\vec{\phi} = (\phi_1, \phi_2, \phi_3)$ is constrained by $\vec{\phi}^2 = 1$ and $\vec{\ell} = \vec{\phi} \times \partial_t \vec{\phi}$. If we expand around a classically ordered state $\phi_3^2 \approx 1$, we can approximate the system as two independent

bosonic fields described by the Lagrangian density

$$\mathcal{L} = \frac{1}{g} [(\partial_\mu \phi_1)^2 + (\partial_\mu \phi_2)^2]. \quad (3.30)$$

As we saw in Section 3.2, we can obtain a tachyonic sector by adding a coupling of the form $\phi_1 \phi_2$. We can justify this microscopically by using the well-known map that relates the $O(3)$ NLSM to the antiferromagnetic Heisenberg spin chain [127]

$$S_{2n}^a = s\phi_a(x) + \ell_a(x), \quad S_{2n+1}^a = -s\phi_a(x) + \ell_a(x), \quad (3.31)$$

where S_n^a are the spin operators ($a = 1, 2, 3$), $s \gg 1$ is the total (local) spin, and $x = 2n + \frac{1}{2}$. Setting $\phi_\pm = (\phi_1 \pm \phi_2)/\sqrt{2}$, we have

$$m^2 s^2 \sum_x (\phi_+^2 - \phi_-^2)(x) = m^2 \sum_n [\{S_{2n}^x, S_{2n}^y\} + \{S_{2n+1}^x, S_{2n+1}^y\} - 2S_{2n}^x S_{2n+1}^y - 2S_{2n}^y S_{2n+1}^x]. \quad (3.32)$$

Note that this interaction term will give rise to a proper unstable Hamiltonian in the limit $s \rightarrow \infty$, where we truly have an infinite dimensional local Hilbert space. Yet, the normalization constraint $\vec{\phi}^2 = 1$ will eventually bound the dynamics as soon as the approximation $\phi_3^2 \approx 1$ breaks down.

Consider now a free boson with a quartic interaction

$$\mathcal{H} = \frac{1}{2} \left[(\partial_t \phi)^2 + (\nabla \phi)^2 + m^2 \phi^2 + \frac{1}{4!} \lambda \phi^4 \right]. \quad (3.33)$$

By considering a self-consistent substitution using the Hartree-Fock approximation [128]

$$\phi^4 \rightarrow -3 \langle \phi^2 \rangle^2 + 6 \langle \phi^2 \rangle \phi^2, \quad (3.34)$$

we can define an effective mass [101]

$$m_{\text{eff}}^2 = m^2 + \frac{\lambda}{2} \sum_k \langle \phi_k^2 \rangle. \quad (3.35)$$

If the mass is tachyonic $m^2 \mapsto -m^2$, heuristically we expect the interaction to stop the instability after a characteristic time t_{stable} given by

$$\sum_k \langle \phi_k^2 \rangle (t_{\text{stable}}) \sim 2 \frac{m^2}{\lambda}. \quad (3.36)$$

As we discussed in previous sections, the correlators after a tachyonic quench develop an exponential growth. This implies that the interaction term $\lambda \phi^4$ must be very small compared to the rest of the characteristic terms in order to approximate a tachyonic evolution.

3.8. Discussion

Tachyonic quenches are an exotic alternative for the study of bosonic field theories out of equilibrium. As we saw in all of the computed physical quantities, the causal structure is made manifest in a fashion similar to critical quenches. For short times, the evolution

of observables may even be indistinguishable. However, tachyonic quenches are unstable and exponential divergences end up dominating the behavior. In particular, the low-frequency (unstable) modes $c|k| < m$ are exponentially driven and cannot equilibrate.

Tachyonic (or more generally, unstable) quenches can be used as an intermediate preparation step for many-body states. If the driving Hamiltonian (3.7) is only used for a fixed time T , the resulting state will be highly excited in the low frequency modes while approximately thermal for the high frequency ones. This sets a sharp cut-off around the tachyonic mass, allowing for a dynamical separation of scales. Remarkably, a similar mechanism can be found in the statistical physics of fluids and interfaces, in processes described by the Kuramoto-Sivashinski formula [129].

In order to obtain similar dynamics in other physical systems, the driving Hamiltonian must have some sort of instability. However, being a pathological feature that is generally avoided, this unboundedness is usually absent by construction in physical realizations. For example, extending these constructions to fermions is not straight-forward, at least using free Hamiltonians. This is due to the symmetries of the energy spectrum, that is traditionally interpreted as a Dirac sea. Spin systems could be used, but they would need very large quantum numbers, so that they can be close to the quantum rotor limit. In this case, the parameters must be chosen so that the characteristic times of the instability are shorter than the one imposed by the lower bound of the spectrum of the driving Hamiltonian.

Realizations may also use a $\lambda\phi^4$ potential. However, in order to exploit this resource at its fullest, the parameters must be chosen so that the quartic term becomes relevant after the exponential divergence becomes manifest.

Further work is needed to understand other types of unstable quenches. Interacting terms that produce unbounded Hamiltonians can for example be fine-tuned to obtain other types of long-time divergences. Characterizing approximate realizations using truncated local Hilbert spaces may also provide an interesting setting for future experiments using optical lattices.

Part II

Conformal Blocks

Conformal Blocks as Wave Functions

4.1. Introduction

Developing suitable many-body wave functions has provided remarkable insights into the physics of collective phenomena. Given the complexity of large quantum systems, this is a rather arduous task that demands the use of an extensive theoretical arsenal. In the context of strongly-correlated systems, a tool that has yielded several fruitful results in this direction has been conformal field theory (CFT) [130, 131, 132, 133, 134].

Perhaps the most notorious application of this formalism to the construction of variational wave functions is in the fractional quantum hall (FQH) effect, where a two-dimensional electron gas is subject to a strong magnetic field to form an incompressible quantum liquid (see [135] for a recent review). Remarkably, these systems display topologically robust features and can support quasiparticle excitations with fractional charge, known as *anyons* [136]. The first successful theoretical framework to study these phenomena was the Laughlin wave function [137]. It is used to describe an electron gas when the filling factor of the lowest Landau level is $\nu = 1/q$. Remarkably, it can be derived from a correlator of (chiral) vertex operators of a massless free boson CFT. One of the main predictions from this ansatz is the existence of Abelian fractional statistics for the emergent quasiparticles. This inspired Moore and Read to develop a general framework to describe more exotic filling fractions [138]. Their construction relates the statistics of the quasiparticles to the algebraic properties of certain associated CFT operators. In particular, Moore and Read proposed a Pfaffian wave function for $\nu = 5/2$. This phase has a topological degeneracy and the corresponding low-energy quasiparticles exhibit non-Abelian fractional statistics.

Progress has also been made for lattice systems. Inspired by the so-called matrix product states (MPS), it has been proposed that variational wave functions can be constructed from correlators in a CFT [139]. In this case, (chiral) primary operators $\phi_s(z_i)$ replace the usual finite-dimensional matrices $A_i(s)$ of the original ansatz. The most important examples have made use of Wess-Zumino-Witten (WZW) CFTs, where the internal $SU(2)_k$ symmetry can be exploited to encode the physical (spin) degrees of freedom. This framework has been successfully applied to systems such as the Haldane-Shastry (HS) spin chain in 1D [139, 140, 141, 142, 143, 144, 145, 146, 147] and the Kalmeyer-Laughlin model in 2D [148, 149, 150, 151]. This MPS construction has also inspired sensible numerical truncation schemes for continuous FQH states [152, 153].

The aim of this chapter is to describe a general way of constructing many-body lattice wave functions using chiral correlators, also known as *conformal blocks* (CBs). As we will argue in detail, this can be done for a generic rational CFT, regardless of the existence of an internal symmetry. After a brief motivation of the basic features of the CBs, we will introduce the general formalism in terms of chiral vertex operators (CVOs). We will illustrate these ideas revisiting the Haldane-Shastry spin chain. We will end with a summary of the now classical construction of Moore and Read for FQH systems.

4.2. A Very Brief Primer on 2D Conformal Field Theory

Conformal field theory (CFT) is one of the most conceptually rich tools in theoretical physics [131, 132, 133, 134]. Its development is cemented on concepts derived from renormalization group (RG) techniques, where relations between different energy scales are used to extract relevant physical quantities. CFT has been applied to many domains in physics, from understanding critical phenomena in statistical mechanics; to explaining non-perturbative effects in 1D condensed matter systems using the Luttinger liquid formalism; to describing high-energy scattering processes in exotic mathematical theories. As a matter of fact, several of the basic techniques used in CFT (such as vertex operators and conformal blocks) were originally developed in mathematical physics and string theory.

Broadly speaking, a CFT describes a fixed point of the RG, where the beta functions of the theory vanish [132]. As a consequence, the usual Lorentz invariance of correlators is enlarged to conformal invariance. If we are working with a 2D system, conformal symmetry can be related to all possible analytic mappings of the complex plane [154]. It is then convenient to use complex coordinates to describe our spacetime $z = x_1 + ix_2$, $\bar{z} = x_1 - ix_2$.

Under a conformal transformation $z \mapsto w(z)$, $\bar{z} \mapsto \bar{w}(\bar{z})$, local operators will change in a covariant way. Some operators will transform in a particularly simple way

$$\phi'_n(w, \bar{w}) = \left(\frac{dw}{dz}\right)^{-h_n} \left(\frac{d\bar{w}}{d\bar{z}}\right)^{-\bar{h}_n} \phi_n(z, \bar{z}). \quad (4.1)$$

These are called *primary fields*. The associated exponents h_n are their corresponding *conformal weights*. The action of the conformal group on these operators can be studied by means of the energy-momentum tensor, both its holomorphic $T(z)$ and antiholomorphic $\bar{T}(\bar{z})$ parts. If these fields are expanded in a Laurent series

$$\begin{aligned} T(z) &= \sum_{n \in \mathbb{Z}} z^{-n-2} L_n, & L_n &= \frac{1}{2\pi i} \oint dz z^{n+1} T(z), \\ \bar{T}(\bar{z}) &= \sum_{n \in \mathbb{Z}} \bar{z}^{-n-2} \bar{L}_n, & \bar{L}_n &= \frac{1}{2\pi i} \oint d\bar{z} \bar{z}^{n+1} \bar{T}(\bar{z}), \end{aligned} \quad (4.2)$$

it can be shown that the coefficients obey the famous *Virasoro algebra*

$$\begin{aligned} [L_n, L_m] &= (n - m)L_{n+m} + \frac{c}{12}n(n^2 - 1)\delta_{n+m,0}, \\ [L_n, \bar{L}_m] &= 0, \\ [\bar{L}_n, \bar{L}_m] &= (n - m)\bar{L}_{n+m} + \frac{c}{12}n(n^2 - 1)\delta_{n+m,0}, \end{aligned} \quad (4.3)$$

where c is the central charge of the theory. The action of these operators on the primary fields can be used to obtain complete representations (more correctly, Verma modules) of the conformal group [132]

$$\phi_n^{(m)}(z, \bar{z}) \equiv (L_{-m}\phi_n)(z, \bar{z}), \quad \phi_n^{(\bar{m})}(z, \bar{z}) \equiv (\bar{L}_{-m}\phi_n)(z, \bar{z}). \quad (4.4)$$

These derived fields are called descendant fields. They satisfy, among other relations,

$$\phi_n^{(0)}(z, \bar{z}) = h_n\phi_n(z, \bar{z}), \quad \phi_n^{(1)}(z, \bar{z}) = \partial_z\phi_n(z, \bar{z}), \quad \phi_n^{(-m)}(z, \bar{z}) = 0, m \geq 1. \quad (4.5)$$

In these terms, a CFT is completely determined if one is given the central charge of the theory, the conformal weights of the primary fields and the operator product expansion (OPE) coefficients

$$\phi_n(z, \bar{z})\phi_m(w, \bar{w}) \sim \sum_p \frac{C_{nmp}}{(z-w)^{h_n+h_m-h_p}(\bar{z}-\bar{w})^{\bar{h}_n+\bar{h}_m-\bar{h}_p}} \phi_p(z, \bar{z}). \quad (4.6)$$

Interestingly, some models have extra internal symmetry that goes beyond the Virasoro algebra. This is the case of Wess-Zumino-Witten (WZW) models, where an affine Lie algebra arises as the spectrum-generating algebra [132].

4.3. The Simplest Conformal Blocks

Before we present a general (though somewhat abstract) way of defining and manipulating conformal blocks, let us first consider them in one of their simplest forms: the decomposition of the 4-point function in a CFT ¹. This will provide some basic intuition for the general case. We will work with 2D CFTs, even though most of these results also hold *mutatis mutandis* in higher dimensions.

One of the most powerful results in CFT is that conformal symmetry fully determines some features of all the relevant correlators in the theory [154, 132]. If we have a set of primary fields $\{\phi_n\}$ with conformal weights $\{h_n\}$, we can show that two-point functions necessarily have the form ²

$$\langle \phi_1(z_1, \bar{z}_1)\phi_2(z_2, \bar{z}_2) \rangle = C_{12} \frac{\delta_{h_1, h_2} \delta_{\bar{h}_1, \bar{h}_2}}{z_{12}^{2h_1} \bar{z}_{12}^{2\bar{h}_1}}, \quad (4.7)$$

where $z_{12} = z_1 - z_2$ and $\{C_{nm}\}$ are normalization constants that can be redefined as $C_{nm} = \delta_{nm}$ by linear independence. Similarly, all three-point functions can be written as

$$\begin{aligned} \langle \phi_1(z_1, \bar{z}_1)\phi_2(z_2, \bar{z}_2)\phi_3(z_3, \bar{z}_3) \rangle &= C_{123} \frac{1}{z_{12}^{h_1+h_2-h_3} z_{23}^{h_2+h_3-h_1} z_{13}^{h_1+h_3-h_2}} \\ &\times \frac{1}{\bar{z}_{12}^{\bar{h}_1+\bar{h}_2-\bar{h}_3} \bar{z}_{23}^{\bar{h}_2+\bar{h}_3-\bar{h}_1} \bar{z}_{13}^{\bar{h}_1+\bar{h}_3-\bar{h}_2}}, \end{aligned} \quad (4.8)$$

¹Technically, the simplest conformal blocks are related to the decomposition of the torus partition function into holomorphic and antiholomorphic parts, via the Virasoro characters [155]. We will deal with the 4-point correlators case because it is more illuminating for our purposes.

²There are some exotic CFTs where this is not the case. For instance, theories known as log CFTs exhibit extra logarithmic corrections in the correlators of some of the operators [156]. This is usually understood as a singular limit of “usual” CFTs.

where $\{C_{nml}\}$ is a set of constants that must be determined from the theory using the OPE coefficients (4.6). (We must also impose that the sum of the conformal spins $s_n = h_n - \bar{h}_n$ cancels in order to preserve rotation invariance.) Note that in both cases, the holomorphic and the antiholomorphic parts of the correlator factorize neatly.

Alas, global conformal invariance alone does not fix more complicated correlators. If we define the anharmonic ratio

$$\eta = \frac{z_{12}z_{34}}{z_{13}z_{24}}, \quad (4.9)$$

conformal symmetry dictates that the most general form of a 4-point function is

$$\langle \phi_1(z_1, \bar{z}_1) \phi_2(z_2, \bar{z}_2) \phi_3(z_3, \bar{z}_3) \phi_4(z_4, \bar{z}_4) \rangle = f(\eta, \bar{\eta}) \prod_{n < m} z_{nm}^{h/3 - h_n - h_m} \bar{z}_{nm}^{\bar{h}/3 - \bar{h}_n - \bar{h}_m}, \quad (4.10)$$

where $h = h_1 + \dots + h_4$ and $f(\eta, \bar{\eta})$ is an arbitrary function. In order to obtain more information, let us perform a conformal transformation such that $z_1 = \infty$, $z_2 = 1$, $z_3 = x$, and $z_4 = 0$. This implies $\eta = x$ and we can write correlator (4.10) as a matrix element between two asymptotic states (in the operator-state correspondence [154])

$$\begin{aligned} \lim_{z_1, \bar{z}_1 \rightarrow \infty} z_1^{2h_1} \bar{z}_1^{2\bar{h}_1} \langle \phi_1(z_1, \bar{z}_1) \phi_2(1, 1) \phi_3(x, \bar{x}) \phi_4(0, 0) \rangle \\ \equiv \langle h_1, \bar{h}_1 | \phi_2(1, 1) \phi_3(x, \bar{x}) | h_4, \bar{h}_4 \rangle \equiv G_{34}^{21}(x, \bar{x}), \end{aligned} \quad (4.11)$$

where the order of the super- and subindices in G_{34}^{21} is relevant.

We can further decompose this expression if we use the operator product expansion (OPE) for primary fields. From the 3-point function expansion, we have

$$\phi_3(x, \bar{x}) \phi_4(0, 0) \sim \sum_p C_{34p} x^{h_p - h_3 - h_4} \bar{x}^{\bar{h}_p - \bar{h}_3 - \bar{h}_4} \phi_p(0, 0). \quad (4.12)$$

We can complete this expansion by considering all the descendant fields for every ϕ_p . We can label them as

$$\phi_p^{(k\bar{k})} \equiv L_{-k_1} \dots L_{-k_n} \bar{L}_{-\bar{k}_1} \dots \bar{L}_{-\bar{k}_m} \phi_p, \quad (4.13)$$

where L_n, \bar{L}_m are the generators of the Virasoro algebra and $(k\bar{k})$ stands for the (ordered) collection of indices $(k_1, \dots, k_n; \bar{k}_1, \dots, \bar{k}_m)$. Using this notation, the full OPE becomes

$$\phi_3(x, \bar{x}) \phi_4(0, 0) = \sum_{p, (k\bar{k})} C_{34p}^{(k\bar{k})} x^{h_p - h_3 - h_4 + \sum_j k_j} \bar{x}^{\bar{h}_p - \bar{h}_3 - \bar{h}_4 + \sum_j \bar{k}_j} \phi_p^{(k\bar{k})}(0, 0). \quad (4.14)$$

Since the correlations of descendant operators are built on the correlations of primary fields, one can show using conformal transformations that [132]

$$C_{34p}^{(k\bar{k})} = C_{34p} \beta_{34}^{p(k)} \bar{\beta}_{34}^{p(\bar{k})}, \quad (4.15)$$

where $\beta_{34}^{p(k)}$ (resp. $\bar{\beta}_{34}^{p(\bar{k})}$) can be computed mechanically and depend only on the conformal weights h_3, h_4, h_p (resp. $\bar{h}_3, \bar{h}_4, \bar{h}_p$) and the central charge c .

Going back to the 4-point functions, we can use all these definitions to rewrite (4.11) as [154]

$$G_{34}^{21}(x, \bar{x}) = \sum_p C_{34p} C_{12p} \mathcal{F}_{34}^{21}(p|x) \bar{\mathcal{F}}_{34}^{21}(p|\bar{x}), \quad (4.16)$$

where

$$\mathcal{F}_{34}^{21}(p|x) = x^{h_p - h_3 - h_4} \sum_{(k)} \beta_{34}^{p(k)} x^{\sum_j k_j} \frac{\langle h_1 | \phi_2(1) L_{-k_1} \dots L_{-k_n} | h_p \rangle}{\langle h_1 | \phi_2(1) | h_p \rangle}. \quad (4.17)$$

$$\mathcal{F}_{ij}^{\ell m}(p|x) \overline{\mathcal{F}}_{ij}^{\ell m}(p|\bar{x}) = \begin{array}{c} \begin{array}{ccc} 0 & & 1 \\ & \searrow^i & \nearrow^\ell \\ & & p \\ & \nearrow_j & \searrow_m \\ x & & \infty \end{array} \end{array}$$

Figure 4.1: Graphical representation of the CB for a 4-point function. If we interpret this as a partial wave decomposition, p would stand for an intermediate state formed during the scattering of fields i, j into m, ℓ . (Taken from [157].)

(Similarly for $\overline{\mathcal{F}}_{34}^{21}(p|\bar{x})$.) The functions (4.17) are called *conformal blocks* (CBs). Some remarks:

1. Note that every term in the sum (4.16) is factorized into a holomorphic and antiholomorphic part, in a fashion similar to the 2-point and 3-point functions. In particular, $\mathcal{F}_{34}^{21}(p|x)$ contains all the holomorphic information.
2. Each CB is associated to a possible intermediate fusion channel (see Fig. (4.1)). This can be interpreted as the partial waves found in perturbative scattering theory, where some incoming states interact and produce asymptotic final states [154, 131, 132]. In this picture, p would stand for an intermediate state formed during the scattering. These intermediate channels serve as a resolution of the identity decomposing the original correlator. This analogy will remain useful when we consider the CBs corresponding to N -point functions.
3. As we see, CBs can be computed in principle using only the conformal weights and central charge of the theory. In practice, this can be quite complicated to obtain for all fields at all orders for an arbitrary CFT.
4. In the previous computation, we performed the OPE between ϕ_3 and ϕ_4 . We could have instead fused first ϕ_2 and ϕ_3 . The consistency between these two ways of doing the expansion is an important constraint on the CBs, usually known as crossing symmetry [154].

Let us remark that most of our discussion depends on the particulars of 2D CFT, where symmetry can be powerful enough to constraint the theory to the point of it being exactly solvable. However, this formalism can be extended to higher dimensions, where studying conformal blocks can be related to the conformal bootstrap program [158, 159].

4.4. Chiral Vertex Operators and Conformal Blocks

Now that we have some basic intuition about how CBs appear naturally in the holomorphic decomposition of correlators and how this relates to intermediate fusion channels, we can formalize the procedure using an algebraic construction. This will in turn help us understand how to obtain physical wave functions from these mathematical objects.

We start by consider a chiral algebra \mathcal{A} , the simplest examples being the Virasoro algebra (4.3) and the Kac-Moody algebras [132]³. This algebra will contain only holomorphic fields. We must also define the analogous purely antiholomorphic algebra $\bar{\mathcal{A}}$ that commutes with \mathcal{A} . This decomposition is usually related to the left-handed and right-handed eigenmode expansion of the fields in 2D QFT.

Within this formalism, the Hilbert space of a rational conformal field theory (RCFT) can be written as a finite direct sum [155]

$$\mathcal{H}_{\text{CFT}} = \bigoplus_{i=0}^N \mathcal{H}_i \otimes \bar{\mathcal{H}}_i, \quad (4.18)$$

where \mathcal{H}_i (resp. $\bar{\mathcal{H}}_i$) is an irreducible highest-weight representation of \mathcal{A} (resp. $\bar{\mathcal{A}}$). Using the one-to-one mapping between operators and states, we can associate each representation to a primary field of the RCFT. By definition, the representation \mathcal{H}_0 contains the identity operator and, therefore, the stress energy tensor $T(z)$ and all the operators of \mathcal{A} .

The representation \mathcal{H}_i is infinite dimensional, but it can be split into the direct sum of finite-dimensional subspaces with a fixed value of the Virasoro operator L_0 . Let us call $\mathcal{H}_i^{(0)}$ the subspace with the lowest value of L_0 , denoted h_i . For minimal RCFTs, $\mathcal{H}_i^{(0)}$ will be a one-dimensional subspace generated by the highest-weight vector $L_0 |\phi_i\rangle = h_i |\phi_i\rangle$. In the case of $SU(2)_k$ WZW models, there are $k + 1$ primary fields, labeled $j = 0, \frac{1}{2}, \dots, \frac{k}{2}$, such that $\mathcal{H}_j^{(0)} = \mathbb{C}^{2j+1}$ [132].

Different representations can be related by their fusion properties. This is summarized by the *fusion coefficients* N_{jk}^i , which count the multiplicity of ϕ_i in the operator product expansion (OPE) of ϕ_j, ϕ_k , so that $\phi_j \times \phi_k = \sum_i N_{jk}^i \phi_i$. In order to simplify our discussion, we will always assume $N_{jk}^i = 0, 1$.

We can now define *chiral vertex operators* (CVOs). First, consider three representations i, j, k such that the fusion coefficient N_{jk}^i does not vanish. A CVO is given by a linear map [155]

$$\begin{pmatrix} i \\ j \ k \end{pmatrix}_{z,\beta} : \mathcal{H}_k^{(0)} \rightarrow \mathcal{H}_i^{(0)}, \quad (4.19)$$

where $\beta \in \mathcal{H}_j^{(0)}$ and $z \in \mathbb{C}$. This can be pictured as a vertex operator with two incoming particles with labels j, k and an outgoing particle with label i (Fig. (4.2))⁴. We can also define it by the relation

$$\langle \alpha | \begin{pmatrix} i \\ j \ k \end{pmatrix}_{z,\beta} | \gamma \rangle = t(\alpha \otimes \beta \otimes \gamma) z^{-h_j - h_k + h_i}, \quad (4.20)$$

where $\alpha \in \mathcal{H}_i^{*(0)}$, $\gamma \in \mathcal{H}_k^{(0)}$, and $t : \mathcal{H}_i^{*(0)} \otimes \mathcal{H}_j^{(0)} \otimes \mathcal{H}_k^{(0)} \rightarrow \mathbb{C}$ is an invariant tensor ($\mathcal{H}_i^{*(0)}$ is the dual of $\mathcal{H}_i^{(0)}$). Note that we can extend these constructions to the other subspaces of

³Rigorous definitions of chiral algebras can be quite technical and beyond the reach of this introduction (see [160, 161] for a mathematical treatment).

⁴More precisely, we can picture it as an incoming particle k colliding with a particle j located at position z and producing an outgoing particle i .

$$\begin{array}{c} (j, \beta)(z) \\ | \\ \left(\begin{array}{c} i \\ jk \end{array} \right)_{z, \beta} = \begin{array}{c} \text{---} \\ | \\ \text{---} \\ i \quad \quad \quad k \end{array} \end{array}$$

Figure 4.2: Graphical representation of a vertex operator. As defined in the text, $\beta \in \mathcal{H}_j^{(0)}$.

each representation by acting with the Virasoro algebra and computing the corresponding contour integrals.

In this formalism, a *conformal block* (CB) is a chiral correlator that encodes an allowed fusion channel for a given set of primary fields. If we start with N primaries $\{j_n\}$, a CB can be written as [131, 155]

$$\mathcal{F}_{\mathbf{k}}(\beta_1, \dots, \beta_N; z_1, \dots, z_N) = \langle 0 | \left(\begin{array}{c} 0 \\ j_1 \quad k_1 \end{array} \right)_{z_1, \beta_1} \left(\begin{array}{c} k_1 \\ j_2 \quad k_2 \end{array} \right)_{z_2, \beta_2} \cdots \left(\begin{array}{c} k_{N-1} \\ j_N \quad 0 \end{array} \right)_{z_N, \beta_N} | 0 \rangle, \quad (4.21)$$

where $\mathbf{k} = (k_1, \dots, k_{N-1})$ labels the internal channels and $|z_1| \geq \dots \geq |z_N|$. Note that $k_1 = \bar{j}_1$ and $k_{N-1} = j_N$. The number of conformal blocks of this type depends on the possible allowed fusion channels of the j_n fields. We will often summarize the notation and write the CB as

$$\mathcal{F}_{\mathbf{k}}(\beta_1, \dots, \beta_N; z_1, \dots, z_N) = \left\langle \prod_{n=1}^N \phi_{j_n}^{(\beta_n)}(z_n) \right\rangle_{\mathbf{k}}. \quad (4.22)$$

As expected, these functions allow for a decomposition of N -point correlators into the sum of terms that factorize the holomorphic and antiholomorphic contributions

$$\langle \phi_{j_1, \bar{j}_1}(z_1, \bar{z}_1) \cdots \phi_{j_N, \bar{j}_N}(z_N, \bar{z}_N) \rangle = \sum_{\mathbf{k}} d_{\mathbf{k}} \overline{\mathcal{F}_{\mathbf{k}}}(\{\bar{z}_n\}) \mathcal{F}_{\mathbf{k}}(\{z_n\}), \quad (4.23)$$

where $d_{\mathbf{k}}$ are constants independent of $\{z_n\}$ that can be computed from the fusion matrix [162]. This construction generalizes the calculation we did in the previous section for 4-point functions. Once again, we see that the CBs are labeled by the intermediate fusion channels that get summed over when we compute the full correlator.⁵

Note that the basis in which we express the CBs depends on the order of the CVOs in equation (4.21). We can in principle change the order and fuse the operators in a different way. This procedure must be done with care because of the possible branch cuts of the complex functions. These mathematical subtleties can be encapsulated in the braiding matrices [155, 131], which summarize the monodromy properties of the CBs. We will discuss these objects in more detail in the next chapters, in the context of the Ising CFT.

The algebraic construction we presented can be interpreted in geometrical terms using Riemann surfaces with punctures [155, 131]. Every puncture carries a label corresponding to a representation \mathcal{H}_i . Complicated Riemann surfaces can be obtained by “sewing” three holed spheres and summing over the intermediate states passing through the holes. In this context, the three holed spheres can be associated to the CVOs we defined before. The CBs in turn correspond to basis elements for a vector space associated to the resulting surface. We will not use this geometrical approach in this thesis.

⁵We could generalize the construction even further by considering the notion of *vertex (operator) algebras* [163]. However, this formalism will not be necessary in this thesis.

4.5. Lattice Wave Functions from Conformal Blocks

Many-body lattice systems are notoriously hard to study in the thermodynamic limit. One of the main reasons is that the dimension of the Hilbert space grows exponentially with the number of sites. In the past decades, it has been fruitful to think beyond the Hamiltonian paradigm and propose instead novel trial wave functions that are simpler to compute. There is an extensive bibliography using this approach. For our purposes, we will focus on one of the methods, the so-called *matrix product states* (MPS) (see [164] for a practical review).

Consider a lattice spin system such that the local Hilbert space is $\mathcal{H}_n = \mathbb{C}^d$. A generic wave function can be written as

$$|\psi\rangle = \sum_{\{s_n\}} \psi_{s_1 \cdots s_N} |s_1 \cdots s_N\rangle, \quad (4.24)$$

where $s_n = 1, \dots, d$. Simple counting shows that we need $\mathcal{O}(d^N)$ parameters to characterize this state. A MPS representation can be written as

$$\psi_{s_1 \cdots s_N} = \langle 0_L | A_1[s_1] \cdots A_N[s_N] | 0_R \rangle, \quad (4.25)$$

where $\{A_n[s] \mid n = 1, \dots, N, s = 1, \dots, d\}$ is a set of matrices and $\langle 0_L |, | 0_R \rangle$ are suitable reference vectors. If the matrices are all $D \times D$, then the number of parameters we need to characterize $|\psi\rangle$ is $\mathcal{O}(NdD^2)$. This type of representation is always available for any wave function [165]. However, assuming that D grows at most polynomially with N , we see that this parametrization implies a remarkable reduction in the complexity of the problem.

MPS representations have become very useful to study many-body systems in a non-perturbative way. Even though they can be traced back to the solution of the AKLT model [166] and the ansatz underlying the density matrix renormalization group (DMRG) algorithm [167, 168], it was with the development of quantum information processing that they became a fundamental tool applied to different areas of many-body physics [169, 170].

Definition (4.25) shares some structural similarities with the general definition of a CB (4.21). This was used to propose infinite MPS [139], where matrices $A_n[s]$ are replaced by chiral operators $\phi_n(z_n)$ in a CFT. Extra internal symmetries, such as the one found in $SU(2)_k$ WZW models, can be exploited to find suitable spin representations to model the lattice spins. One may wonder if a CFT with no internal symmetries (as, for instance, the minimal models originally introduced in [154]) can be used to generate useful lattice wave functions. In that case, the only available degrees of freedom are the labels of the different fusion channels. As we will see in detail, these intermediate internal channels can still provide enough structure for this construction to make sense.

We will now present a generalization of the infinite MPS construction using all the features of the CBs [2]. For concreteness, consider a self-conjugate chiral field ϕ , i.e., it satisfies $\phi \times \phi = \mathbb{1} + \dots$, with $\mathbb{1}$ being the identity field (equivalently, self-conjugation implies $N_{\phi\phi}^{\mathbb{1}} = 1$). If we define the incidence matrix $(\Lambda^{(\phi)})_j^i = N_{\phi_j}^i$, the number of different CBs obtained from N ϕ fields is [131]

$$d_{\phi,N} = \left([\Lambda^{(\phi)}]^N \right)_0^0, \quad (4.26)$$

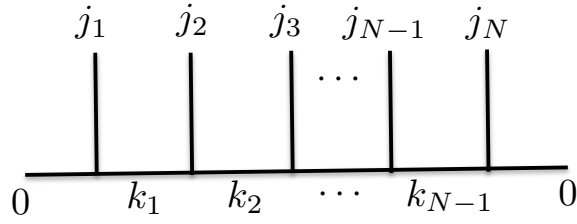


Figure 4.3: Graph representing a conformal block in the multiperipheral basis.

where 0 stands for the identity 1 component. We will use \mathbf{k} to label the intermediate fusion channels. This is the canonical basis, usually called *multiperipheral basis* [162] (see Fig. (4.3))⁶. We will distinguish two cases:

1. *Abelian*: if $d_{\phi,N} = 1$, there is only one CB. It defines a map

$$\mathcal{F} : \mathcal{H}_{\phi}^{(0)} \otimes \cdots \otimes \mathcal{H}_{\phi}^{(0)} \rightarrow \mathbb{C}, \quad (4.27)$$

that allows us to postulate, for a fixed set of coordinates $\{z_i\}$, the wave function

$$|\psi\rangle = \sum_{\{s_i\}} \mathcal{F}(z_1, \dots, z_N; s_1, \dots, s_N) |s_1, \dots, s_N\rangle, \quad (4.28)$$

where $\{|s\rangle : s = 1, \dots, \dim(\mathcal{H}_{\phi}^{(0)})\}$ is an orthonormal basis for $\mathcal{H}_{\phi}^{(0)}$.

2. *Non-Abelian*: if $d_{\phi,N} > 1$, the different CBs must be labelled by the internal fusion channels. This defines a family of maps

$$\mathcal{F}_{\mathbf{k}} : \mathcal{H}_{\phi}^{(0)} \otimes \cdots \otimes \mathcal{H}_{\phi}^{(0)} \rightarrow \mathbb{C}, \quad (4.29)$$

that suggests the wave function

$$|\psi\rangle = \sum_{\{s_i\}, \mathbf{k}} \mathcal{F}_{\mathbf{k}}(z_1, \dots, z_N; s_1, \dots, s_N) |\mathbf{k}\rangle \otimes |s_1, \dots, s_N\rangle, \quad (4.30)$$

where $|\psi\rangle \in W_{\phi,N} \otimes \left(\mathcal{H}_{\phi}^{(0)}\right)^{\otimes N}$, and $W_{\phi,N}$ contains all the auxiliary degrees of freedom (note that $\dim(W_{\phi,N}) = d_{\phi,N}$).

Consider now the special case when $\dim(\mathcal{H}_{\phi}^{(0)}) = 1$ for a non-Abelian theory. Wave function (4.30) can represent a many-body lattice system if the auxiliary Hilbert space $W_{\phi,N}$ can account for all the local physical degrees of freedom. It should be noted that there are different sensible bases for this auxiliary space. As we discussed, these different representations are usually related to the order in which we fuse the primary fields. This implies that there are several lattice wave functions that can be obtained from the same CBs in the non-Abelian case. The most natural option is the multiperipheral basis. However, there are other bases that can be chosen for physical reasons. We will discuss this in more detail in Chapter 6.

⁶This way of characterizing different states by the fusion of successive fields is closely related to the string Hilbert spaces used in restricted solid on solid (RSOS) or face models [171].

One consistency condition we need to check is that the normalization of the state has no monodromy issues with respect to the auxiliary coordinates $\{z_i\}$. This can be stated in terms of the full correlator

$$\langle \psi | \psi \rangle = \langle \phi(z_1, \bar{z}_1) \cdots \phi(z_n, \bar{z}_n) \rangle = \sum_{\mathbf{k}} d_{\mathbf{k}} \overline{\mathcal{F}_{\mathbf{k}}} \mathcal{F}_{\mathbf{k}}. \quad (4.31)$$

In the multiperipheral basis, this implies the necessary condition $\langle \mathbf{k} | \mathbf{k}' \rangle = d_{\mathbf{k}} \delta_{\mathbf{k}, \mathbf{k}'}$.

We will illustrate this general construction with two examples. First, the Haldane-Shastry spin chain from the point of view of the $SU(2)_1$ WZW model. This case has already been studied extensively [139, 140, 141, 142, 143, 144, 145, 146, 147]. We will provide a brief summary for the sake of clarity and analogy. For the non-Abelian case, we will use the Ising CFT. Being non-Abelian and lacking internal symmetry, it provides a good testing ground for encoding physical degrees of freedom using only the internal fusion channels. This will be done extensively in Chapter 6.

4.6. Abelian Case Study: the Haldane-Shastry Chain

The chiral algebra of the $SU(2)_k$ WZW model is the Kac-Moody algebra defined by the conserved chiral currents $J^a(z)$, where a stands for the index labeling the generators of the $SU(2)$ algebra [132]. It contains a representation of the Virasoro algebra that can be obtained from the stress-energy tensor $T(z)$ via the relation

$$T(z) = \frac{1}{2(k+2)} \sum_a (J^a J^a)(z) \quad (4.32)$$

using the Sugawara construction [132]. For this family of models, the conformal symmetry is enriched, allowing for highest-weight representations with more structure.

Consider $SU(2)_1$. This theory has two primary operators, ϕ_0 and $\phi_{1/2}$, satisfying the fusion rules

$$\phi_{1/2} \times \phi_{1/2} = \phi_0, \quad \phi_{1/2} \times \phi_0 = \phi_{1/2}, \quad \phi_0 \times \phi_0 = \phi_0. \quad (4.33)$$

The primary field ϕ_0 corresponds to the identity operator and $\phi_{1/2}$ has a spin- $\frac{1}{2}$ representation, so that $\mathcal{H}_{1/2}^{(0)} = \mathbb{C}^2$. From the fusion rules, we obtain the set of CVOs

$$\phi_{1/2, \text{odd}}^{(s)}(z) = \begin{pmatrix} 0 \\ \frac{1}{2} \quad \frac{1}{2} \end{pmatrix}_{z,s}, \quad \phi_{1/2, \text{even}}^{(s)}(z) = \begin{pmatrix} \frac{1}{2} \\ \frac{1}{2} \quad 0 \end{pmatrix}_{z,s}, \quad (4.34)$$

where we use the third component of the spin $s = \pm 1$ to label the internal degree of freedom. The CB of N $\phi_{1/2}$ fields will alternate both even and odd CVOs (see Fig. (4.4)). This implies that there will only be a single internal fusion channel. Note also that, given the fusion rules, we will only obtain non-trivial results if N is an even number.

The value of the CB can be easily computed if we represent the CVOs as vertex operators in a free bosonic theory [139, 140, 143]

$$\phi_{1/2, \text{odd}}^{(s)}(z) = e^{i\frac{\pi}{2}(s-1)} : \exp\left(i\frac{s}{\sqrt{2}}\varphi(z)\right) :, \quad \phi_{1/2, \text{even}}^{(s)}(z) = : \exp\left(i\frac{s}{\sqrt{2}}\varphi(z)\right) :, \quad (4.35)$$

$$\mathcal{F}(s_1 \cdots s_N) = \begin{array}{c} \left(\frac{1}{2}, s_1\right) \left(\frac{1}{2}, s_2\right) \left(\frac{1}{2}, s_3\right) \left(\frac{1}{2}, s_{N-1}\right) \left(\frac{1}{2}, s_N\right) \\ \begin{array}{c} | \quad | \quad | \quad \cdots \quad | \quad | \\ \hline 0 \quad \frac{1}{2} \quad 0 \quad \cdots \quad \frac{1}{2} \quad 0 \end{array} \end{array}$$

Figure 4.4: Graphical representation of the CB for N $\phi_{1/2}$ fields.

where $\varphi(z)$ is a free boson such that $\langle \varphi(z_1)\varphi(z_2) \rangle = -\log(z_1 - z_2)$. From the N -point correlator, we obtain

$$\mathcal{F}(z_1, \cdots, z_N; s_1, \cdots, s_N) = \rho_{1/2} \prod_{i>j} (z_i - z_j)^{s_i s_j / 2}, \quad \sum_i s_i = 0, \quad (4.36)$$

where $\rho_{1/2} = \exp\left(\frac{i\pi}{2} \sum_{i \text{ odd}} (s_i - 1)\right)$ is a phase that can be interpreted as a Marshall sign factor⁷. The wave function obtained from these CBs corresponds to the Haldane-Shastry (HS) state for the choice $z_n = \exp\left(\frac{i2\pi}{N}n\right)$:

$$\psi_{s_1 \cdots s_N} \propto \rho_{1/2} \prod_{n>m} \left[\sin\left(\frac{\pi(n-m)}{N}\right) \right]^{s_n s_m / 2}. \quad (4.37)$$

The constraints imposed by the current algebra can be exploited to obtain parent Hamiltonians. The general construction relies heavily on the fusion properties of the different representations of the primary fields [140]. For wave function (4.37), the parent Hamiltonian can be related to the HS Hamiltonian [139]

$$H_{HS} = - \sum_{i \neq j} \frac{z_i z_j}{(z_i - z_j)^2} (\vec{\sigma}_i \cdot \vec{\sigma}_j - 1). \quad (4.38)$$

This is an integrable system that is closely connected to the Heisenberg spin chain [172, 173, 174].

Note that the local symmetry derived from the $SU(2)$ algebra allowed for a rather straightforward relation between the primary fields and the physical degrees of freedom of the lattice system. This will not be available in general, as we mentioned before, in particular in non-Abelian theories. In Chapter 6, we will see how to deal with this issue for the Ising CFT.

4.7. Wave Functions for Fractional Quantum Hall Physics

The experimental discovery of the fractional quantum Hall (FQH) effect in 1982 by Daniel Tsui and Horst Störmer [175] had profound implications in the understanding of many-body physics. Certain ideas such as how to define a phase of matter or the importance of a local order parameter derived from symmetry arguments had to be revised, leading to new insights that still dictate research directions [176, 135]. The history and phenomenology of this phenomenon is quite extensive, so we will focus here on the most prominent wave

⁷This ensures the wave function is in a singlet state.

functions that have been proposed for its study. Following the now classical work by Moore and Read [138], these states can be interpreted as CBs obtained from RCFTs. In this context, the complex coordinates stand for the physical positions of the different particles in the condensate. The different internal fusion channels correspond to globally distinct topological sectors.

In a short paper published less than a year after the original FQH experimental results, Laughlin proposed a variational wave function⁸ as an ansatz for the filling fraction $\nu = 1/m$. It can be written as [137]

$$\Psi_m(z_1, \dots, z_N) = \prod_{a < b} (z_a - z_b)^m \times \exp\left(-\sum_a \frac{|z_a|^2}{4}\right). \quad (4.39)$$

If we think of it as a joint probability distribution for all the electrons with a Gibbs form $|\Psi_m|^2 = \exp(-\beta U(z_1, \dots, z_N))$, it can be interpreted as a plasma of particles interacting via Coulomb repulsion in a uniform neutralizing background charge (we must set $\beta = m$)

$$U(z_1, \dots, z_N) = -2 \sum_{a < b} \log |z_a - z_b| + \frac{1}{2m} \sum_a |z_a|^2. \quad (4.40)$$

We can also obtain a similar wave function in the presence of quasiholes. In that case, the Laughlin wave function at filling fraction $\nu = 1/m$ with two quasiholes at positions η_1, η_2 is given by

$$\begin{aligned} \Psi_m(\eta_1, \eta_2; z_1, \dots, z_N) &= |\eta_1 - \eta_2|^{1/m} \prod_{a=1}^N (\eta_1 - z_a)(\eta_2 - z_a) \times \prod_{a < b} (z_a - z_b)^m \\ &\times \exp\left(-\sum_a \frac{|z_a|^2}{4} - \frac{|\eta_1|^2 + |\eta_2|^2}{4m}\right). \end{aligned} \quad (4.41)$$

The connection between Chern-Simmons theories and the topological features of the FQH effect led to interpret these wave functions as holomorphic conformal blocks [176, 135]. In order to show this, we use a free boson CFT such that the basic two-point function is given by $\langle \varphi(z)\varphi(w) \rangle = -\log(z-w)$. We define the vertex operators

$$V(z) =: e^{i\sqrt{m}\varphi(z)} :, \quad H(\eta) =: e^{i\frac{1}{\sqrt{m}}\varphi(\eta)} :, \quad \mathcal{O}_{\text{bg}} = \exp\left(-i\rho\sqrt{m} \int d^2z \varphi(z)\right), \quad (4.42)$$

where \mathcal{O}_{bg} provides a neutralizing background charge, ρ is the constant fermion density, and $: \dots :$ stands for normal ordering. These vertex operators describe primary fields, so computing their correlators corresponds to finding the associated CBs. It is easy to show that

$$\Psi_m(\eta_1, \eta_2; z_1, \dots, z_N) = \langle 0 | H(\eta_1) H(\eta_2) V(z_1) \dots V(z_N) \mathcal{O}_{\text{bg}} | 0 \rangle. \quad (4.43)$$

Moore and Read extended this construction to propose several fractional quantum Hall states with interesting properties [138]. In particular, they proposed a Pfaffian wave functions for a system of electrons

$$\Psi_{\text{MR}}(z_1, \dots, z_N) = \text{Pf}\left(\frac{1}{z_a - z_b}\right) \prod_{a < b} (z_a - z_b)^m \times \exp\left(-\sum_a \frac{|z_a|^2}{4}\right), \quad (4.44)$$

⁸Strictly speaking, the Laughlin wave function is not variational because it has no free parameters [176]. Even the filling fraction is completely determined by the total angular momentum.

where the Pfaffian is defined by (we assume $N = 2M$ electrons)

$$\text{Pf}(\mathbf{Q}) = \sqrt{\det(\mathbf{Q})} = \frac{1}{2^M M!} \sum_{\sigma \in S_{2M}} \text{sgn}(\sigma) \prod_{j=1}^M (\mathbf{Q})_{\sigma(2j-1), \sigma(2j)}, \quad (4.45)$$

and S_{2M} is the permutation group for $2M$ elements.

In the case of $\nu = 1/2$, this wave function can be obtained from the CBs of a CFT composed by an Ising sector and a free boson sector. Electrons are described by the vertex operators

$$\psi_e(z) = \psi(z) : e^{i\sqrt{2}\varphi(z)} :, \quad (4.46)$$

where $\psi(z)$ is a (chiral) Majorana fermion, and quasiholes described by

$$\psi_{\text{qh}}(\eta) = \sigma(\eta) : e^{i\frac{1}{2\sqrt{2}}\varphi(\eta)} :, \quad (4.47)$$

where $\sigma(z)$ is a spin field operator. The presence of quasiholes will produce topological degeneracies that can be codified using the different fusion channels. We will study the Ising CFT in more detail in Section 5.4.

Some Aspects of the Ising Model

5.1. Classical 2D Ising Model

Albeit being one of the simplest models in statistical mechanics, the 2D classical Ising model displays a very rich phenomenology. Since its inception, different mathematical tools have been used to probe its properties, leading in turn to profound physical insights [134]. Its exact solution (obtained by Onsager in 1944 [177]) still serves as a non-trivial testing ground for new ideas in many-body physics.

The general Ising model can be defined on any lattice. However, we will deal here with the 2D regular square lattice. Its Hamiltonian can be written as

$$H = -J \sum_{\langle nm \rangle} \sigma_n \sigma_m, \quad (5.1)$$

where $\sigma_n = \pm 1$ are classical spins and $\langle \dots \rangle$ represents a sum over nearest neighbors. The partition function becomes

$$Z(K) = \sum_{\{\sigma_n\}} \exp \left(K \sum_{\langle nm \rangle} \sigma_n \sigma_m \right), \quad (5.2)$$

where $K = J/T$.

For a long time, it was believed that this model at finite temperature could only describe a trivial paramagnetic (i.e. disordered) phase. This followed from Ising's 1924 solution of the 1D classical model [178]¹. This idea was finally rebutted over a decade later

¹Ernst Ising is sort of a tragic hero (see [179, 180]). His name has been tied to a model he did not devise (it was proposed by his supervisor Wilhelm Lenz) and that he could not solve in a non-trivial form. Even the modern Hamiltonian representation is due to Pauli's contribution to the Solvay conference in 1932. Ising left research in physics shortly after finishing his PhD, convinced that his work had no physical importance. Being Jewish, his life became increasingly difficult during that time. After working as a teacher (his real passion) in several parts of Germany, he eventually had to flee his native country. He spent some time in Luxembourg working odd jobs, until he emigrated with his family to the United States in 1947 (a few years after Onsager's solution). As his son Thomas tells it: "In April 1947, we finally arrived in New York on the freighter 'Lipscomb Lykes'. That spring my father went to a physics convention in Boston to get a job. There he was asked for the first time if he was the 'Ising' of the Ising Model." He eventually became a Physics Professor at Bradley University in Peoria, Illinois. He worked there until his retirement. He never published a second paper.

when Peierls proved that the Ising model in two or higher dimensions develops a non-zero spontaneous magnetization at a low but finite temperature [181]. In 1941, Kramers and Wannier extended this reasoning and managed to find the critical temperature at which the transition happens [182]. Their construction was based on a duality relation between the high-temperature and low-temperature partition functions.

If the system is defined on a $N \times N$ lattice, we can write the partition function as

$$Z(K) = (\cosh K)^{2N} \sum_{\{\sigma_n\}} \prod_{\langle nm \rangle} [1 + \sigma_n \sigma_m \tanh K]. \quad (5.3)$$

In the high-temperature regime (small K), we can expand the sum in powers of $\tanh K$. It is a standard exercise to show that the only nonvanishing terms correspond to configurations where the spins form closed chains of neighbors [134]. These can be characterized as all the polygon lines on the original lattice, so that

$$Z_{\text{high}}(K) = 2^N (\cosh K)^{2N} \sum_{\text{polygons}} (\tanh K)^{\text{length}}. \quad (5.4)$$

The low-temperature regime can be studied using a different expansion. In this case, the spins tend to align themselves with their neighbors, forming regions that share the same spin direction. These “islands” can be separated using lines on the dual lattice. We can then use similar geometrical terms as before, in this case polygons on the dual lattice [134]. We obtain

$$Z_{\text{low}}(K) = 2e^{2NK} \sum_{\text{polygons on dual lattice}} e^{-2K(\text{length})}. \quad (5.5)$$

These expansions suggest the identification of two different temperatures K, K' related by the equation

$$e^{-2K'} = \tanh K \implies \sinh(2K) \sinh(2K') = 1. \quad (5.6)$$

which satisfy

$$\frac{Z(K)}{(\sinh(2K))^{N/2}} = \frac{Z(K')}{(\sinh(2K'))^{N/2}}. \quad (5.7)$$

Note that whenever K is large, K' is small, and viceversa. This implies a physical relation between the high- and low-temperature physics of the model. Kramers and Wannier presented a similar argument (this is its modern form) to suggest that the self-dual point should correspond to the critical point. They obtained

$$K_c = \frac{1}{2} \log(1 + \sqrt{2}) \approx 0.4407, \quad (5.8)$$

which was verified by Onsager’s exact solution.

This result is known as Kramer-Wannier (KW) duality². This feature has been used extensively in the literature. One prominent application is that it can be used to define disorder operators μ_n to study the high-temperature limit [132]. They are related to the spin operators σ_n via a non-local operation that can be interpreted as a topological defect [184, 183]. It has also been extended to more complicated geometries and to other statistical models [185, 186, 187]. We will come back to this duality in the next sections.

²It has been pointed out in the literature that this is not a symmetry in the traditional sense [183]. This is due to the fact that its implementation cannot be represented in general as an unitary operator.

5.2. Ising Transverse Field Spin Chain

While it is possible to study the classical 2D Ising model working directly with the partition function (5.2), it is convenient to find other formulations where an exact solution is readily available. This idea was already at the heart of Onsager's original solution. Most of the modern literature use as a reference the Ising transverse field (ITF) spin chain (first introduced in 1964 in the seminal paper by Schultz, Mattis and Lieb [188])

$$H(h) = - \sum_{n=1}^N \sigma_n^x \sigma_{n+1}^x - h \sum_{n=1}^N \sigma_n^z, \quad (5.9)$$

where σ_n^x, σ_n^z are Pauli matrices acting on the local Hilbert space $\mathcal{H}_n = \mathbb{C}^2$. (We will assume periodic boundary conditions.) This quantum Hamiltonian can be obtained from the transfer matrix of the classical 2D model in the strong anisotropic limit [134, 189]. The external field h can be related to the temperature of the original statistical ensemble ($|h| < 1$ is the symmetry-breaking ferromagnetic phase and $|h| > 1$ the paramagnetic phase).

The exact solution of (5.9) is well-known [190, 189, 134]. The complete spectrum can be obtained by mapping the spin variables to spinless fermions using a Jordan-Wigner (JW) transformation

$$\sigma_n^z = 1 - 2c_n^\dagger c_n, \quad \sigma_n^x = \prod_{m=1}^{n-1} (1 - 2c_m^\dagger c_m) (c_m^\dagger + c_m), \quad (5.10)$$

so that $\{c_n^\dagger, c_m\} = \delta_{nm}$. Using these variables, we obtain

$$H(h) = -h \sum_{n=1}^N (1 - 2c_n^\dagger c_n) - \sum_{n=1}^{N-1} (c_n^\dagger - c_n)(c_{n+1}^\dagger + c_{n+1}) + Q(c_N^\dagger - c_N)(c_1 + c_1^\dagger), \quad (5.11)$$

where we defined the parity operator

$$Q = \prod_{n=1}^N (1 - 2c_n^\dagger c_n) = (-1)^{\sum_{n=1}^N c_n^\dagger c_n}. \quad (5.12)$$

It is easy to show that $[H(h), Q] = 0$. This implies that we can decompose the total Hilbert space into two sectors $\mathcal{H} = \mathcal{H}_0 \oplus \mathcal{H}_1$, where \mathcal{H}_0 (resp. \mathcal{H}_1) contains all states with even (resp. odd) fermionic parity, i.e., such that $\langle Q \rangle = 1$ (resp. $\langle Q \rangle = -1$). We will focus on sector \mathcal{H}_0 unless we state so otherwise. In that case, periodic boundary conditions in the spin variables translates into antiperiodic boundary conditions for the fermions. Hamiltonian (5.11) is a translationally invariant Hamiltonian, so we can Fourier transform the modes

$$c_n^\dagger = \frac{1}{\sqrt{N}} \sum_k e^{ikn} c_k^\dagger, \quad (5.13)$$

where we take³

$$k = \frac{\pi}{N} (2m - N + 1), \quad m = 1, \dots, N. \quad (5.14)$$

³In order to obtain antiperiodic boundary conditions on the fermions, we are assuming that N is even. In case it is odd, we must shift the momenta.

It follows that

$$H(h) = 2 \sum_{k>0} \left[\epsilon_k \left(c_k^\dagger c_k + c_{-k}^\dagger c_{-k} \right) + i \delta_k \left(c_k^\dagger c_{-k}^\dagger + c_k c_{-k} \right) \right], \quad (5.15)$$

up to an additive constant, where

$$\epsilon_k = h - \cos k, \quad \delta_k = \sin k. \quad (5.16)$$

If we use a (fermionic) Bogoliubov transformation

$$\begin{pmatrix} d_k \\ d_{-k}^\dagger \end{pmatrix} = \begin{pmatrix} \cos \left(\frac{\theta_k}{2} \right) \mathbb{1} - i \sin \left(\frac{\theta_k}{2} \right) \sigma^x \end{pmatrix} \begin{pmatrix} c_k \\ c_{-k}^\dagger \end{pmatrix}, \quad (5.17)$$

we can write the Hamiltonian as

$$H(h) = 2 \sum_{k>0} \Delta_k \left(d_k^\dagger d_k + d_{-k}^\dagger d_{-k} - 1 \right) + \text{const.}, \quad (5.18)$$

where we define the dispersion relation

$$\Delta_k = \sqrt{\epsilon_k^2 + \delta_k^2} = \sqrt{(h-1)^2 + h \sin^2 \left(\frac{k}{2} \right)} \quad (5.19)$$

and we impose

$$\cos \left(\frac{\theta_k}{2} \right) = \sqrt{\frac{\Delta_k + \epsilon_k}{2\Delta_k}}, \quad \sin \left(\frac{\theta_k}{2} \right) = -\text{sgn}(\delta_k) \sqrt{\frac{\Delta_k - \epsilon_k}{2\Delta_k}}. \quad (5.20)$$

Note that for small momenta, the dispersion relation (5.19) will have a relativistic form with a mass $m^2 \propto (h-1)^2$. This implies that the critical point $h_c = 1$ can be related to a massless theory. We will come back to this point in more detail when we take the continuum limit of the theory close to the critical point.

The normalized ground state in the original fermionic variables can be found by inverting the Bogoliubov transformation

$$\begin{aligned} |gs(h)\rangle &= \prod_{k>0} \left[\cos \left(\frac{\theta_k}{2} \right) + i \sin \left(\frac{\theta_k}{2} \right) c_k^\dagger c_{-k}^\dagger \right] |0\rangle_c \\ &= \prod_{k>0} \cos \left(\frac{\theta_k}{2} \right) \exp \left[\sum_{k>0} i \tan \left(\frac{\theta_k}{2} \right) c_k^\dagger c_{-k}^\dagger \right] |0\rangle_c, \end{aligned} \quad (5.21)$$

where $|0\rangle_c$ is the state defined by $c_n |0\rangle_c = 0, \forall n$. The ground state (5.21) has the form of a Bardeen-Cooper-Schrieffer (BCS) state. We can construct the rest of the energy eigenstates by acting on $|gs(h)\rangle$ with the creation operators that diagonalize the Hamiltonian. In order to remain in the even sector \mathcal{H}_0 , we must use an even number of these creation operators.

A Primer on BCS States

Now that we know that the ground state of the ITF spin chain (5.21) can be written as a BCS state, let us consider them in their general form. Given a collection of (spinless) fermionic modes $\{c_n\}_{n=1}^N$ on a lattice, we can define the BCS many-body wave function

$$|\psi_{\text{BCS}}\rangle = \prod_{n<m} (u_{nm} + v_{nm} c_n^\dagger c_m^\dagger) |0\rangle_c, \quad (5.22)$$

where $|0\rangle_c$ is the state annihilated by all the operators c_n , and u_{nm}, v_{nm} are complex numbers that satisfy the normalization condition $|u_{nm}|^2 + |v_{nm}|^2 = 1$. Furthermore, we impose $u_{nm} = u_{mn}$ and $v_{nm} = -v_{mn}$. This state can be written as

$$|\psi_{\text{BCS}}\rangle = C_N \exp\left(\sum_{n<m} g_{nm} c_n^\dagger c_m^\dagger\right) |0\rangle_c, \quad (5.23)$$

where $g_{nm} = v_{nm}/u_{nm}$ is the pairing function (or more generally pairing matrix) and $C_N = \prod_{n<m} u_{nm}$ is a normalization constant. Note that g_{nm} is a (generally complex) antisymmetric tensor $g_{nm} = -g_{mn}$.

We can interpret this wave function as a grand canonical state of pairs created by the operator $P = \sum_{n<m} g_{nm} c_n^\dagger c_m^\dagger$. From the fermionic anticommutation relations, it can be shown that the wave function amplitude for $2M$ fermions occupying sites $r(1) < \dots < r(2M)$ is given by

$$\Psi(r(1), \dots, r(2M)) = C_N \text{Pf}(\mathbf{M}), \quad (5.24)$$

where \mathbf{M} is the $2M \times 2M$ antisymmetric matrix

$$(\mathbf{M})_{ij} = g_{r(i), r(j)}, \quad (5.25)$$

and we make use of the Pfaffian

$$\text{Pf}(\mathbf{Q}) = \sqrt{\det(\mathbf{Q})} = \frac{1}{2^M M!} \sum_{\sigma \in S_{2M}} \text{sgn}(\sigma) \prod_{j=1}^M (\mathbf{Q})_{\sigma(2j-1), \sigma(2j)}, \quad (5.26)$$

where S_{2M} is the permutation group for $2M$ elements.

BCS wave functions are Gaussian states that arise naturally from mean-field solutions of Hamiltonians describing superconductivity [189, 191]. In that context, both u_{ij} and v_{ij} can be written in terms of single-particle energies ϵ_k and the pairing interaction potential $V_{k,k'}$. Being spinless fermions, we say that these states correspond to p -wave superconductivity, due to the fact that the wave functions for the spatial degrees of freedom are antisymmetric.

5.3. KW Duality for the Ising Transverse Field Spin Chain

Being a limit of the classical statistical system, we expect Hamiltonian (5.9) to inherit most of its important symmetries. The \mathbb{Z}_2 symmetry associated to the classical global spin flip $\sigma_n \mapsto -\sigma_n$ gets translated into $\sigma_n^x \mapsto -\sigma_n^x$ in the spin chain and as parity preservation in the fermionic variables. The Kramers-Wannier duality also has consequences for the quantum model.

In the spirit of the original relation between high- and low-temperature variables, let us redefine the Hamiltonian using domain walls as the basic variables [192]. In the transverse eigenbasis $\sigma_n^x |\pm\rangle_n = \pm |\pm\rangle_n$, having a domain wall corresponds to adjacent sites having different eigenvalues $\langle \sigma_n^x \sigma_{n+1}^x \rangle = -1$. We define

$$\mu_{n+1/2}^x = \sigma_n^x \sigma_{n+1}^x \quad (5.27)$$

as a natural operator to determine a change of domain. Just as the classical Hamiltonian quantifies the number of domain walls, $\sum_n \mu_{n+1/2}^x$ does the same for the spin chain. On

the other hand, flipping a local spin in the transverse basis $\sigma_n^z |\pm\rangle_n = |\mp\rangle_n$ can create or destroy a local domain. If we define

$$\mu_{n+1/2}^z = \prod_{m=1}^n \sigma_m^z, \quad (5.28)$$

we can write a term that “penalizes” domain walls as

$$\mu_{n-1/2}^z \mu_{n+1/2}^z = \sigma_n^z. \quad (5.29)$$

Using this mapping, we can rewrite the ITF Hamiltonian as

$$H(h) = - \sum_{n=1}^N \mu_{n+1/2}^x - h \sum_{n=2}^N \mu_{n-1/2}^z \mu_{n+1/2}^z - hQ \mu_{N+1/2}^z \mu_{1+1/2}^z. \quad (5.30)$$

Ignoring for a moment the subtleties regarding the boundary term (see [192] for a more detailed explanation), note that the structure of the Hamiltonian is very similar to the one we had in the original variables. We can then propose a mapping

$$\sigma_n^z \mapsto \mu_{n+1/2}^x, \quad \sigma_n^x \mapsto \mu_{n+1/2}^z, \quad h \mapsto \frac{1}{h}, \quad (5.31)$$

(up to an irrelevant scaling constant) that maps the “high-temperature” ($|h| > 1$) phase to the “low-temperature” ($|h| < 1$) phase and viceversa [192]. Note that the self-dual point $h = 1$ indeed corresponds to the critical point.

In order to see the action of this mapping on the fermionic variables, it is illuminating to write the operators in terms of Majorana fermions

$$a_{2n-1} = c_n + c_n^\dagger, \quad a_{2n} = \frac{c_n - c_n^\dagger}{i}. \quad (5.32)$$

Using them, Hamiltonian (5.9) becomes ⁴

$$H(h) = i \sum_n a_{2n} a_{2n+1} + ih \sum_n a_{2n-1} a_{2n}. \quad (5.33)$$

We propose that the action of the KW transformation on the Majorana fermions is given simply by

$$a_r \mapsto a_{r+1}. \quad (5.34)$$

This produces $H(h) \mapsto hH(\frac{1}{h})$ as expected ⁵. As we see, the KW duality can be interpreted naturally as a different way of grouping the Majorana modes into fermionic degrees of freedom: $(2n-1, 2n) \mapsto (2n, 2n+1)$. We will find an analogous relation in the next chapter when we consider the braiding properties of the Ising conformal blocks.

⁴If this Hamiltonian is defined with open boundary conditions, it corresponds to Kitaev’s Majorana wire [193]. The symmetry-breaking ferromagnetic phase of the Ising model $|h| < 1$ gets translated into unpaired Majorana modes at each boundary. They can be used to define a topologically protected (non-local) fermionic mode that can be used in quantum computation.

⁵One must be careful with the term a_{2N} . This is closely related to cumbersome boundary term that appears in the spin variables. Assuming we are in the even parity sector $\langle Q \rangle = 1$, the fermions will have antiperiodic boundary conditions, so $a_{2N} \mapsto -a_1$.

5.4. Majorana Fermions and the (Chiral) Ising CFT

From the dispersion relation (5.19), we expect the low-energy excitations to be around $k = 0$. In that limit, we have

$$\Delta_k^2 \approx (h - 1)^2 + h \left(\frac{|k|}{2} \right)^2. \quad (5.35)$$

We can use this fact to find an effective field theory to describe the thermodynamic limit of Hamiltonian (5.9) by doing a gradient expansion. If we define the complex coordinates $z = x + it$, we can show that the associated action can be written as [134, 189]

$$S = \frac{1}{2\pi} \int d^2z (\psi \bar{\partial} \psi + \bar{\psi} \partial \bar{\psi} + im \bar{\psi} \psi), \quad (5.36)$$

where $\partial = \partial_z = \frac{1}{2}(\partial_x - i\partial_t)$, $\bar{\partial} = \partial_{\bar{z}} = \frac{1}{2}(\partial_x + i\partial_t)$. This action corresponds to a free Majorana fermion [132]. As expected from the dispersion relation, the corresponding dynamics is relativistic. The mass term is proportional to the distance to the critical point $m = (1 - h)$. Note that doing a KW transformation, a small mass implies

$$h = 1 - m \quad \mapsto \quad \frac{1}{h} = \frac{1}{1 - m} \approx 1 + m, \quad (5.37)$$

so that the mass term effectively changes sign.

The classical equations of motion are

$$\bar{\partial} \psi = \frac{im}{2} \bar{\psi}, \quad \partial \bar{\psi} = -\frac{im}{2} \psi. \quad (5.38)$$

This implies that in the massless limit $m = 0$, the field ψ (resp. $\bar{\psi}$) is purely holomorphic (resp. antiholomorphic). Moreover, the theory becomes conformally invariant and can be studied as a CFT [132].

In the conformal limit, the corresponding propagators are easy to compute:

$$\langle \psi(z) \psi(w) \rangle = \frac{1}{z - w}, \quad \langle \bar{\psi}(\bar{z}) \bar{\psi}(\bar{w}) \rangle = \frac{1}{\bar{z} - \bar{w}}. \quad (5.39)$$

The holomorphic part of the energy-momentum tensor is then

$$T(z) = -2\pi T_{zz} = -\frac{1}{2} : \psi \partial \psi : (z), \quad (5.40)$$

where we defined the normal-ordered product

$$: \psi \partial \psi : (z) \equiv \lim_{w \rightarrow z} (\psi(z) \partial \psi(w) - \langle \psi(z) \partial \psi(w) \rangle). \quad (5.41)$$

We can use Wick's theorem to compute the relevant OPEs [132]

$$T(z) \psi(w) \sim \frac{\psi(w)}{2(z-w)^2} + \frac{\partial \psi(w)}{z-w}, \quad T(z) T(w) \sim \frac{1}{4(z-w)^4} + \frac{2T(w)}{(z-w)^2} + \frac{\partial T(w)}{z-w}. \quad (5.42)$$

From these equations, we deduce that the theory has central charge $c = \frac{1}{2}$ and the conformal weights of ψ (resp. $\bar{\psi}$) are $h = \frac{1}{2}$, $\bar{h} = 0$ (resp. $h = 0$, $\bar{h} = \frac{1}{2}$).

Remarkably, we can associate the conformal limit of the Ising model to the simplest example in the family of minimal CFTs. These models have the advantage of having a finite number of irreducible representations of the Virasoro algebra [132]. Their properties can be obtained by imposing consistency conditions on the decoupling of null vectors, i.e., linear combinations of descendant states that vanish as a consequence of unitarity. These constraints can be characterized via the Kac determinant. Relevant to our discussion, some of the resulting theories are associated to the critical point of statistical models with a discrete group symmetry (see [132, 134] for a detailed exposition).

In a nutshell, minimal models can be classified by a pair of coprime integers (i.e., they do not contain common divisors) p, q such that $p > q \geq 2$. The associated central charge is given by

$$c_{pq} = 1 - 6 \frac{(p - q)^2}{pq}. \quad (5.43)$$

The conformal weights of the Virasoro representations ϕ_{rs} can be expressed as

$$h_{rs} = \frac{(rp - sq)^2 - (p - q)^2}{4pq}, \quad 1 \leq r \leq q - 1, 1 \leq s \leq p - 1, \quad (5.44)$$

and they obey the relations

$$h_{rs} = h_{q-r, p-s} = h_{r+q, s+p}. \quad (5.45)$$

The Ising model can be obtained from $(p, q) = (4, 3)$. In that case, $c = \frac{1}{2}$. The primary fields correspond to (we will focus here on the holomorphic sector)

$$\mathbb{1} \leftrightarrow \phi_{1,1} (h_{1,1} = 0), \quad \psi \leftrightarrow \phi_{2,1} \left(h_{2,1} = \frac{1}{2} \right), \quad \sigma \leftrightarrow \phi_{1,2} \left(h_{1,2} = \frac{1}{16} \right). \quad (5.46)$$

Field ψ corresponds to the Majorana fermion we obtained from the low-energy limit of the ITF Hamiltonian. Field σ is related to the original spin variables defined on the lattice. They obey the (non-trivial) fusion rules

$$\sigma \times \sigma = \mathbb{1} + \psi, \quad \psi \times \psi = \mathbb{1}, \quad \sigma \times \psi = \sigma, \quad (5.47)$$

which can be summarized in the fusion coefficients $N_{\sigma\sigma}^{\mathbb{1}} = N_{\sigma\sigma}^{\psi} = N_{\sigma\mathbb{1}}^{\sigma} = N_{\sigma\psi}^{\sigma} = 1$.

5.5. Conformal Blocks of the Ising CFT

We would like to compute all the relevant conformal blocks (CBs) for the Ising CFT. One possible route is similar to the one presented for 4-point functions in Chapter 4. By considering the possible fusion channels, one reduces the problem to a set of second-order partial differential equations. These constraints are derived from the decoupling conditions imposed on the null vectors of the theory [194, 134]. Clearly, this method has the advantage of being completely general and applicable to any minimal CFT. However, going beyond 4-point functions is already quite challenging. We will use instead the fact that two copies of the Ising CFT can be described by a free bosonic theory. This particular ‘‘bosonization’’ was first exploited in 1977 by Zuber and Itzykson in the context of the classical statistical model [195].

If $\phi(z)$ is a holomorphic bosonic field, two copies of the Majorana fermions ψ_1, ψ_2 can be represented as [132]

$$\psi_1(z) + i\psi_2(z) = e^{i\phi(z)}. \quad (5.48)$$

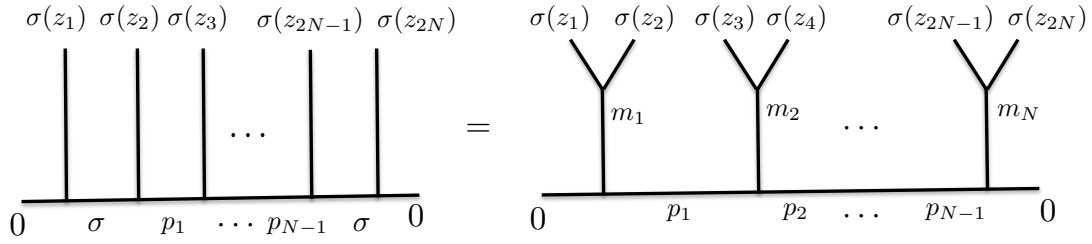


Figure 5.1: A conformal block using only σ field operators grouped in reference pairs $(\sigma(z_{2k-1}), \sigma(z_{2k}))$. The equivalence between the two representations is obtained from the relation $m_k = p_{k-1} + p_k \pmod{2}$.

Note that everything in this relation is already in purely holomorphic terms. Writing the chiral spin operator $\sigma(z)$ is a little more complicated. In this case, we must first consider two copies of the full non-chiral field [194]

$$\sigma_1(z, \bar{z})\sigma_2(z, \bar{z}) = \sqrt{2} \cos\left(\frac{\phi(z) - \bar{\phi}(\bar{z})}{2}\right), \quad (5.49)$$

where we also make use of the antiholomorphic bosonic field $\bar{\phi}(\bar{z})$. Since the two copies do not interact with each other, their joint correlator provide the square of the correlation functions of the original Ising model. This can be used to obtain full correlators such as

$$\langle \sigma(z, \bar{z})\sigma(w, \bar{w}) \rangle^2 = 2 \left\langle \cos\left(\frac{\phi(z) - \bar{\phi}(\bar{z})}{2}\right) \cos\left(\frac{\phi(w) - \bar{\phi}(\bar{w})}{2}\right) \right\rangle = \frac{1}{|z - w|^{1/2}}. \quad (5.50)$$

In a similar fashion, the non-chiral disorder operator μ can be expressed as

$$\mu_1(z, \bar{z})\mu_2(z, \bar{z}) = \sqrt{2} \sin\left(\frac{\phi(z) - \bar{\phi}(\bar{z})}{2}\right). \quad (5.51)$$

These two representations can be used to find their chiral counterparts [196, 197]. The key is to consider both the braiding properties of the fields and their fusion rules.

More concretely, consider $2N$ σ fields located at position z_1, \dots, z_{2N} (radially ordered). If we group them in reference pairs $(\sigma(z_{2k-1}), \sigma(z_{2k}))$, each one will define a local fusion channel $\sigma_{2k-1} \times \sigma_{2k} \rightarrow \mathbb{1} + \psi$. The different global channels can then be labeled using the vector $\mathbf{m} = (m_1, \dots, m_N)$, with $m_n = 0$ (resp. $m_n = 1$) representing an identity operator $\mathbb{1}$ (resp. a fermion ψ) in the n -th local fusion channel. As we discussed in Section 4.3, we can label all the CBs using the intermediate fusion channels. Luckily, the canonical multiperipheral basis can be easily related to the representation in terms of vector \mathbf{m} (see Fig. (5.1)).

Given that the identity $\mathbb{1}$ and the fermions ψ_1, ψ_2 can be represented easily in the holomorphic sector of the bosonic theory, it is natural that fused pairs of σ fields produce suitable holomorphic relations. Indeed, it can be argued that [197]

$$\begin{aligned} \mathcal{F}_{\mathbf{m}}(z_1, \dots, z_{2N})^2 &\equiv \langle \sigma(z_1) \cdots \sigma(z_{2N}) \rangle_{\mathbf{m}}^2 \\ &\propto \left\langle \prod_{j=1}^N \left[\exp\left(i \frac{\phi(z_{2j-1}) - \phi(z_{2j})}{2}\right) + (-1)^{m_j} \exp\left(-i \frac{\phi(z_{2j-1}) - \phi(z_{2j})}{2}\right) \right] \right\rangle. \end{aligned} \quad (5.52)$$

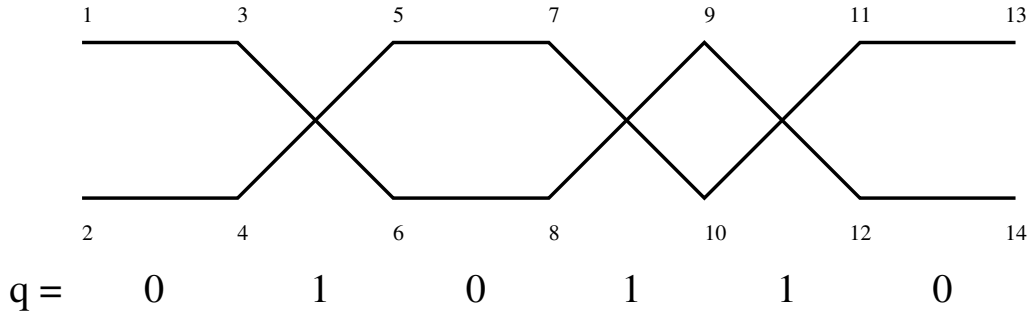


Figure 5.2: Graph representing one of the possible pairs of macrogroups for 14 σ fields, corresponding to $\ell_{\mathbf{q}} = (1, 3, 6, 8, 9, 12, 14)$ and $\ell'_{\mathbf{q}} = (2, 4, 5, 7, 10, 11, 13)$.

As a consistency check, consider the 4-point correlator. Fermionic parity enforces that the fusion channels for both reference pairs are equal, so that $m_1 = m_2 = m$. We have

$$\begin{aligned} \mathcal{F}_m(z_1, \dots, z_4)^2 &\propto \langle e^{i\phi(z_1)/2} e^{-i\phi(z_2)/2} e^{i\phi(z_3)/2} e^{i\phi(z_4)/2} \rangle \\ &\quad + \langle e^{-i\phi(z_1)/2} e^{i\phi(z_2)/2} e^{-i\phi(z_3)/2} e^{i\phi(z_4)/2} \rangle \\ &\quad + (-1)^m \langle e^{i\phi(z_1)/2} e^{-i\phi(z_1)/2} e^{-i\phi(z_3)/2} e^{i\phi(z_4)/2} \rangle \\ &\quad + (-1)^m \langle e^{-i\phi(z_1)/2} e^{i\phi(z_2)/2} e^{i\phi(z_3)/2} e^{-i\phi(z_4)/2} \rangle \\ &= 2 \left(\frac{z_{13} z_{24}}{z_{12} z_{34} z_{14} z_{23}} \right)^{1/4} + (-1)^m 2 \left(\frac{z_{14} z_{23}}{z_{12} z_{13} z_{24} z_{34}} \right)^{1/4}. \end{aligned} \quad (5.53)$$

Defining the cross-ratio $x = \frac{z_{12} z_{34}}{z_{14} z_{32}}$, we can write after some algebra

$$\mathcal{F}_m(z_1, \dots, z_4) \propto \frac{1}{z_{12}^{1/8} z_{34}^{1/8}} \sqrt{(1-x)^{1/4} + (-1)^m (1-x)^{-1/4}}, \quad (5.54)$$

which indeed corresponds to the well-known result [132].

Using the holomorphic representation (5.52) and the multiperipheral basis, all the CBs can be written in a more manageable form [198]. Before stating the general formulas, let us introduce some extra notation. First, we will need certain bipartitions of the σ fields that associate different elements of the same reference pair to different groups. We call these macrogroups $\ell_{\mathbf{q}}, \ell'_{\mathbf{q}}$ and they are generated from an integer $\mathbf{q} = 0, \dots, 2^{N-1} - 1$ according to [199, 198, 3]

$$\ell_{\mathbf{q}}(k) = 2k - \frac{1}{2}(1 + s_k), \quad \ell'_{\mathbf{q}}(k) = 2k - \frac{1}{2}(1 - s_k), \quad (5.55)$$

where q_k are the binary digits of $\mathbf{q} = (q_1, q_2, \dots, q_{N-1})$,

$$s_k = \prod_{i=1}^{k-1} (1 - 2q_i), \quad (5.56)$$

and $s_1 = 1$ by definition. We can represent these bipartitions by combinatorial graphs (see Fig.5.2). Using this notation, we define

$$z_{\mathbf{q}} = \prod_{k < m} z_{\ell_{\mathbf{q}}(k), \ell_{\mathbf{q}}(m)}, \quad (5.57)$$

where $z_{ab} = z_a - z_b$. We will also need the combinatorial sign given by

$$\begin{aligned} \epsilon_{\mathbf{p}\mathbf{q}} &\equiv (-1)^{\sum_k p_k q_k} = \prod_{k=1}^{N-1} (1 - 2p_k q_k) \\ &= \prod_{k=1}^{N-1} (1 + p_k (s_k s_{k+1} - 1)) \equiv \tilde{\epsilon}_{\mathbf{p}\mathbf{s}}, \end{aligned} \quad (5.58)$$

expressed in terms of the binary expansion of both \mathbf{q} and the multiperipheral label $\mathbf{p} = 0, \dots, 2^{N-1} - 1$. All these definitions allow us to write the CBs of $2N$ σ fields (5.52) as [198]

$$\mathcal{F}_{\mathbf{p}}(z_1, \dots, z_{2N}) = \frac{1}{2^{\frac{N-1}{2}}} \prod_{a < b} z_{ab}^{-1/8} \left(\sum_{\mathbf{q}=0}^{2^{N-1}-1} \epsilon_{\mathbf{p}\mathbf{q}} \sqrt{z_{\ell_{\mathbf{q}}} z_{\ell'_{\mathbf{q}}}} \right)^{1/2}. \quad (5.59)$$

Note that in the binary expansion of the multiperipheral label \mathbf{p} , $p_n = 0$ (resp. $p_n = 1$) represent an internal fusion channel carrying an identity operator $\mathbb{1}$ (resp. a fermion ψ) (see Fig. (5.1)). Also, note that the sum inside the square root is the only part that depends on \mathbf{p} via the combinatorial sign $\epsilon_{\mathbf{p}\mathbf{q}}$.

It is important to remark that we are assuming radial ordering

$$|z_1| \geq |z_2| \geq \dots \geq |z_{2N}|. \quad (5.60)$$

Moreover, if $|z_n| = |z_m|$ and $n < m$, we will assume that the angular parts in the polar decomposition are ordered with respect to the principal value of the logarithm. In other words, if $z_n = \exp(a_n + ib_n)$, whenever $a_n = a_m$, we will assume

$$-\pi < b_n < b_m \leq \pi \quad (5.61)$$

if $n < m$.

The ordering of the coordinates will be important because it ensures that we consistently choose the same branches of the (complex) square root. In order to see this, let us define

$$B_{\mathbf{q}} = \prod_{n < m}^N \left[\left(1 - \frac{z_{\ell_{\mathbf{q}}(m)}}{z_{\ell_{\mathbf{q}}(n)}} \right) \left(1 - \frac{z_{\ell'_{\mathbf{q}}(m)}}{z_{\ell'_{\mathbf{q}}(n)}} \right) \right]^{\frac{1}{2}}. \quad (5.62)$$

Using this notation, we note that we can write the \mathbf{p} -dependent part of (5.59) using only the main branch of the square root

$$\mathcal{F}_{\mathbf{p}} \propto \left(\sum_{\mathbf{q}=0}^{2^{N-1}-1} \epsilon_{\mathbf{p}\mathbf{q}} \frac{B_{\mathbf{q}}}{B_0} \right)^{1/2}. \quad (5.63)$$

Note that we can obtain CBs for coordinates which are not radially ordered by analytic continuation of these expressions. This is done consistently by means of the Ising braid matrices [131, 162].

We can also incorporate fermions. The fusion rule $\psi \times \psi \rightarrow \mathbb{1}$ implies that $2M$ Majorana fermions have a single fusion channel. We can compute that CB using Wick's theorem

$$\langle \psi(w_1) \cdots \psi(w_{2M}) \rangle = \text{Pf} \left(\frac{1}{w_n - w_m} \right), \quad (5.64)$$

where Pf is the Pfaffian (5.26). If we also include $2N$ σ fields, we will have in general 2^{N-1} different fusion channels. The CB corresponding to $2M$ fermions and two σ fields was found by Moore and Read [138]. In that context, it was interpreted as a trial wave function for a pair of excitations in a quantum Hall system at filling fraction $\nu = 1/2$. Nayak and Wilczek extended this result to four σ fields and noted that the resulting degeneracy can implement a non-Abelian representation of the braid group [199]. From these results, Ardonne and Sierra found a general expression for $2M$ fermions and $2N$ σ fields [198]

$$\mathcal{F}_{\mathbf{p}}^{(2N,2M)}(z_1, \dots, z_{2N}; w_1, \dots, w_{2M}) = \frac{1}{2^{\frac{N-1}{2}+M}} \prod_{a<b}^{2N} z_{ab}^{-1/8} \left(\sum_{\mathbf{q}=0}^{2^{N-1}-1} \epsilon_{\mathbf{p}\mathbf{q}} \sqrt{z_{\ell_{\mathbf{q}}} z_{\ell'_{\mathbf{q}}}} \right)^{-1/2} \\ \times \left[\sum_{\mathbf{q}=0}^{2^{N-1}-1} \epsilon_{\mathbf{p}\mathbf{q}} \sqrt{z_{\ell_{\mathbf{q}}} z_{\ell'_{\mathbf{q}}}} \text{Pf} \left(\frac{h_{\ell_{\mathbf{q}}, \ell'_{\mathbf{q}}}(w_n, w_m)}{w_n - w_m} \right) \right], \quad (5.65)$$

where

$$h_{\ell, \ell'}(w_n, w_m) = \left[\prod_{a=1}^N \frac{(w_n - z_{\ell(a)})(w_m - z_{\ell'(a)})}{(w_n - z_{\ell'(a)})(w_m - z_{\ell(a)})} \right] + (n \leftrightarrow m). \quad (5.66)$$

We will use expressions (5.59) and (5.65) in Chapter 6 to construct lattice wavefunctions. In the spirit of Section 4.4, we will associate the corresponding physical degrees of freedom to the local fusion channels of the σ fields. Remarkably, we will show that the resulting states for certain coordinate configurations can be related to the low-energy states of the ITF Hamiltonian (5.9) at criticality ($h = 1$). We will also study 2D spin systems and show that their topological properties are consistent with the weak-pairing phase of a $p + ip$ superconductor.

Ising Conformal Blocks as Spin Wave Functions

6.1. Introduction

Even though superconductivity was discovered experimentally in 1911 by Kamerlingh Onnes [200], a sufficiently predictive microscopic theory was not available until the work of Bardeen, Cooper and Schrieffer, published in 1957 [201] (known today as BCS theory). One of the fundamental features of this construction is the realization of the ground state of the system as a grand canonical state of fermionic pairs. Following these steps, several other many-body systems have benefited from these insights and extended the result to other non-trivial Gaussian states.

As we discussed in Section 5.2, current understanding of the 2D classical Ising model is closely related to BCS theory. More concretely, the ground state of the associated one-dimensional quantum spin chain can also be constructed from a condensate of fermionic pairs [190, 189, 134]. This is a remarkable result if we consider that both models have very different descriptions and applications.

BCS theory has remained an important starting point for the analysis of more exotic phenomena. For instance, in the past few decades two-dimensional superconductors have become testbeds for novel topological features, some of them closely related to the fractional quantum Hall (FQH) effect. Read and Green [191, 202, 203] established a connection between the weak pairing regime of the $p+ip$ superconductor and the topological phase defined by the Moore-Read Pfaffian state [138]. The robustness of these phases to local perturbations have turned them into strong candidate schemes for quantum computing [136].

In this chapter, we provide a characterization of many-body lattice wave functions obtained from the chiral conformal blocks (CBs) of the Ising CFT [2, 3]. We show both analytical and numerical evidence that these states can be understood as BCS states. We use this fact to characterize a general family of 1D spin systems and construct their parent Hamiltonians. They are shown to be closely related to the Ising transverse field (ITF) spin chain. Some connections to Temperley-Lieb-Jones (TLJ) algebras will be discussed. This construction provides an analytical proof that the ground state of the finite critical ITF spin chain can be obtained exactly from the CBs of its infinite infrared limit, i.e., from the Ising CFT. We also study 1D excitations by means of wave functions obtained from

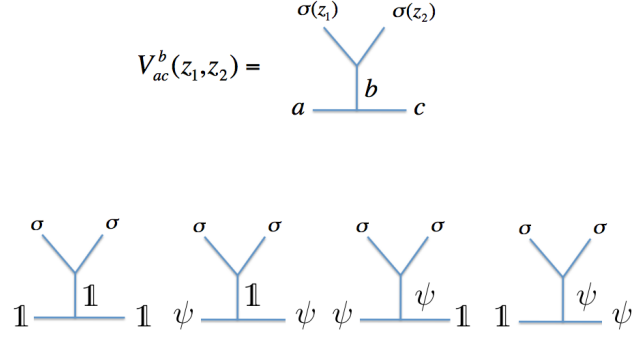


Figure 6.1: Graphical representation of the bilocal vertex operator $V_{ac}^b(z_1, z_2)$.

CBs with different asymptotic boundary conditions. Finally, we provide a brief study of the 2D states obtained from the CBs in the OPE regime. We use both the entanglement spectrum [204] and the scaling of the entanglement entropy to relate these states to the weak pairing phase of the $p + ip$ superconductor.

6.2. Lattice States from the Ising Vertex Operators

We will be interested mainly in wave functions constructed from CBs containing only $2N$ spin operators

$$\mathcal{F}_{\mathbf{p}}^{(2N)}(z_1, \dots, z_{2N}) = \langle \sigma(z_1) \cdots \sigma(z_{2N}) \rangle_{\mathbf{p}}. \quad (6.1)$$

Given the fusion rules, a pair of σ fields can be seen as a single degree of freedom (see Section 5.5 and Fig. (5.1)). This allows us to write the fusion channels in terms of local binary variables.

The reference pairs $(\sigma(z_{2n-1}), \sigma(z_{2n}))$ define local fusion channels $\sigma_{2n-1} \times \sigma_{2n} \rightarrow \mathbb{1} + \psi$. The different CBs can then be labeled using the vector $\mathbf{m} = (m_1, \dots, m_N)$, with $m_n = 0$ (resp. $m_n = 1$) representing an identity operator $\mathbb{1}$ (resp. a fermion ψ) in the n -th local fusion channel. We will use \mathbf{p} to represent the CBs in the multiperipheral basis and \mathbf{m} in the local, pairwise fusion basis.

The local fusion produces bilocal chiral vertex operators

$$V_{ac}^b(z_{2n-1}, z_{2n}) : \mathcal{H}_c \rightarrow \mathcal{H}_a, \quad a, b, c = \mathbb{1}, \psi, \quad (6.2)$$

where $b = m_n$ corresponds to the fusion channel of reference pair $[\sigma(z_{2n-1}), \sigma(z_{2n})]$, \mathcal{H}_a are the Virasoro representations associated to the corresponding primary fields, and we require the conservation of fermionic parity at each vertex (see Fig.(6.1)). We can use these operators to express explicitly the inner structure of each CB.

Let us now consider the 2^N -dimensional Hilbert space \mathcal{H} obtained from N spinless fermionic modes $\{c_n\}_{n=1}^N$ and define the 2×2 operator matrix

$$A^{(n)}(z_{2n-1}, z_{2n}) = \begin{pmatrix} V_{\mathbb{1}\mathbb{1}}^{\mathbb{1}} & c_n^\dagger V_{\mathbb{1}\psi}^\psi \\ c_n^\dagger V_{\psi\mathbb{1}}^\psi & V_{\psi\psi}^{\mathbb{1}} \end{pmatrix}. \quad (6.3)$$

This yields the map

$$A^{(n)}(z_{2n-1}, z_{2n}) : \begin{pmatrix} \mathcal{H}_{\mathbb{1}} \otimes \mathcal{H}_e \\ \mathcal{H}_{\psi} \otimes \mathcal{H}_o \end{pmatrix} \rightarrow \begin{pmatrix} \mathcal{H}_{\mathbb{1}} \otimes \mathcal{H}_e \\ \mathcal{H}_{\psi} \otimes \mathcal{H}_o \end{pmatrix}, \quad (6.4)$$

where \mathcal{H}_e (resp. \mathcal{H}_o) is the Fock space with even (resp. odd) number of fermions

$$\mathcal{H}_e = \left\{ |0\rangle_c, c_{i_1}^\dagger c_{i_2}^\dagger |0\rangle_c, \dots \right\}, \quad \mathcal{H}_o = \left\{ c_{i_1}^\dagger |0\rangle_c, c_{i_1}^\dagger c_{i_2}^\dagger c_{i_3}^\dagger |0\rangle_c, \dots \right\}, \quad (6.5)$$

so that $\mathcal{H} = \mathcal{H}_e \oplus \mathcal{H}_o$. The product of N matrices of type A gives the 2×2 operator matrix

$$\begin{aligned} \Phi^{(N)}(z_1 \cdots, z_{2N}) &= A^{(1)}(z_1, z_2) \cdots A^{(N)}(z_{2N-1}, z_{2N}) \\ &= \begin{pmatrix} \Phi_{ee}^{(N)} & \Phi_{eo}^{(N)} \\ \Phi_{oe}^{(N)} & \Phi_{oo}^{(N)} \end{pmatrix}. \end{aligned} \quad (6.6)$$

Using this notation, we have that the operator $\Phi_{ee}^{(N)}$ acting on $\mathcal{H}_1 \otimes \mathcal{H}_e$ defines the (un-normalized) state

$$|\Psi_{ee}\rangle = \langle 0 | \Phi_{ee}^{(N)} | 0 \rangle | 0 \rangle_c \in \mathcal{H}_e, \quad (6.7)$$

where $\langle 0 | \cdots | 0 \rangle$ corresponds to the expectation value in the vacuum of the CFT. Note that $|\Psi_{ee}\rangle$ is a many-body fermionic state that can be mapped to a lattice spin wave function via a Jordan-Wigner (JW) transformation (5.10).

As noted in Section 4.5, this construction is very similar to matrix product states (MPS) obtained from CFT [139, 140, 141, 142, 143, 144, 145, 146, 147]. In both cases, the ancillary degrees of freedom are described by a quantum field theory and the resulting many-body wave function describes a lattice system. As a matter of fact, note that the wave function amplitudes $|\Psi_{ee}\rangle$ corresponds to CBs, i.e., to chiral correlators

$$\begin{aligned} \Psi_{\mathbf{m}}^{(ee)} &= \langle \mathbf{m} | \Psi_{ee} \rangle \\ &= \langle 0 | V_{1m_1}^{m_1}(z_1, z_2) \cdots V_{m_N 1}^{m_N}(z_{2N-1}, z_{2N}) | 0 \rangle = \mathcal{F}_{\mathbf{m}}(z_1, \dots, z_{2n}), \end{aligned} \quad (6.8)$$

where $|\mathbf{m}\rangle = |m_1 \cdots m_N\rangle$. The present formulation highlights both the inner (i.e., entanglement) structure of these states and its relation to the physical degrees of freedom.

We can also construct other states by adding fermions to the asymptotic states of the CFT (within the operator-state correspondence [132]), in particular

$$|\Psi_{oo}\rangle = \langle \psi | \Phi_{oo}^{(N)} | \psi \rangle | 0 \rangle_c \in \mathcal{H}_e, \quad (6.9)$$

where $|\psi\rangle \in \mathcal{H}_\psi$. As we will see in a later section, these wave functions can be natural ansätze for low-energy excited eigenstates.

6.3. First-Order Analysis: OPE Approximation

The construction we have discussed so far is quite general. In order to get a more intuitive picture of these states, we can consider a first-order approximation using the operator product expansion (OPE). This scheme will allow us to get a glimpse of the structure of state $|\Psi_{ee}\rangle$ using simplified operators.

The full expression of the OPE of two σ fields is given by [132]

$$\sigma(z_1)\sigma(z_2) = \frac{1}{z_{12}^{1/8}} \left(\sum_{\alpha \in \mathcal{V}_1} z_{12}^{h_\alpha} C_{\sigma\sigma}^\alpha \alpha \left(\frac{z_1 + z_2}{2} \right) + \sum_{\beta \in \mathcal{V}_\psi} z_{12}^{h_\beta} C_{\sigma\sigma}^\beta \beta \left(\frac{z_1 + z_2}{2} \right) \right), \quad (6.10)$$

where $z_{12} = z_1 - z_2$, α (resp. β) are the fields with conformal weights h_α (resp. h_β) that generate the Virasoro representation \mathcal{H}_1 (resp. \mathcal{H}_ψ) by acting on the vacuum, and

$C_{\sigma\sigma}^\alpha, C_{\sigma\sigma}^\beta$ are constants fixed by 3-point functions. (Note that we are using a symmetrized version of the OPE, instead of pinning the resulting operators on z_2 .) If we only keep the lowest orders in the expansion, we get the familiar expression

$$\sigma(z_1)\sigma(z_2) \sim \frac{1}{z_{12}^{1/8}} \left(1 + \left(\frac{z_{12}}{2} \right)^{1/2} \psi \left(\frac{z_1 + z_2}{2} \right) \right), \quad (6.11)$$

where we used the fact that $C_{\sigma\sigma}^\psi = 1/\sqrt{2}$.

Assume now that we have N pairs of σ fields, parametrized by

$$z_{2n-1} = w_n - \frac{1}{2}\delta_n, \quad z_{2n} = w_n + \frac{1}{2}\delta_n. \quad (6.12)$$

Using this notation and the OPE, we can write the approximate expression for (6.3)

$$A^{(n)} \sim \frac{1}{\delta_n^{1/8}} \left[\mathbb{1}_2 + \left(\sqrt{\frac{\delta_n}{2}} c_n^\dagger \psi(w_n) \right) \sigma^x \right], \quad (6.13)$$

where $\sigma^x = \begin{pmatrix} 0 & 1 \\ 1 & 0 \end{pmatrix}$ is one of the Pauli matrices. Note that this approximation implies

$$V_{\mathbb{1}\mathbb{1}}^\mathbb{1} = V_{\psi\psi}^\mathbb{1} \sim \frac{1}{\delta_n^{1/8}} \mathbb{1}, \quad V_{\mathbb{1}\psi}^\psi = V_{\psi\mathbb{1}}^\psi \sim \frac{1}{\sqrt{2}} \delta_n^{3/8} \psi(w_n). \quad (6.14)$$

Given that $(c_n^\dagger)^2 = 0$, we have

$$A^{(n)} \propto \exp \left(\sqrt{\frac{\delta_n}{2}} c_n^\dagger \psi(w_n) \sigma^x \right), \quad (6.15)$$

so that (6.6) becomes

$$\Phi^{(N)} \propto \exp \left[\sum_{n=1}^N \left(\sqrt{\frac{\delta_n}{2}} c_n^\dagger \psi(w_n) \right) \sigma^x \right]. \quad (6.16)$$

Now, using the fact that the vacuum of the Ising CFT is a free Gaussian state for the Majorana fermions [132], we employ the familiar identity

$$\langle \exp(A) \rangle_{\text{Gaussian}} = \exp \left(\frac{1}{2} \langle A^2 \rangle_{\text{Gaussian}} \right) \quad (6.17)$$

(assuming $\langle A \rangle_{\text{Gaussian}} = 0$) to obtain

$$\begin{aligned} \langle 0 | \Phi_{ee}^{(N)} | 0 \rangle &\propto \exp \left[\sum_{n < m} \frac{\sqrt{\delta_n \delta_m}}{2} \langle \psi(w_n) \psi(w_m) \rangle c_n^\dagger c_m^\dagger \right] \\ &= \exp \left[\sum_{n < m} \frac{\sqrt{\delta_n \delta_m}}{2(w_n - w_m)} c_n^\dagger c_m^\dagger \right]. \end{aligned} \quad (6.18)$$

Compare this to Eq. (5.23). We conclude then that $|\Psi_{ee}\rangle$ is a BCS state defined by the (real-space) pairing function

$$g_{nm}^{(\text{OPE})} = \frac{\sqrt{\delta_n \delta_m}}{2(w_n - w_m)}. \quad (6.19)$$

Note that this result holds for arbitrary complex coordinates and only depends on the validity of the OPE approximation. One may wonder if this expansion is really needed to guarantee the BCS structure of the lattice wave function. As we will show in a later section, numerical calculations suggests that this result extends beyond the OPE expansion, albeit with a different pairing function. We will also discuss some aspects regarding a full analytical proof of this fact.

If $|z_n| = 1$, it is also convenient to use the conformal transformation that maps the plane to the cylinder

$$z \mapsto \exp(i\theta). \quad (6.20)$$

In this setting, we parametrize the coordinates as

$$\theta_{2n-1} = \phi_n - \frac{1}{2}\epsilon_n, \quad \theta_{2n} = \phi_n + \frac{1}{2}\epsilon_n, \quad (6.21)$$

so that the OPE can be written as

$$\sigma(\theta_{2n-1})\sigma(\theta_{2n}) \sim \left(\frac{1}{2 \sin\left(\frac{\epsilon_n}{2}\right)} \right)^{1/8} \left(1 + \sin^{1/2}\left(\frac{\epsilon_n}{2}\right) \psi(\phi_n) \right). \quad (6.22)$$

Given that on the cylinder we have

$$\langle \psi(\phi_1)\psi(\phi_2) \rangle_{\text{cyl}} = \frac{1}{2 \sin\left(\frac{\phi_1 - \phi_2}{2}\right)}, \quad (6.23)$$

a similar analysis yields a BCS state with the pairing function

$$g_{nm}^{(\text{OPE, cyl})} = \frac{\sqrt{\sin\left(\frac{\epsilon_n}{2}\right) \sin\left(\frac{\epsilon_m}{2}\right)}}{2 \sin\left(\frac{\phi_n - \phi_m}{2}\right)}. \quad (6.24)$$

This representation is particularly useful for lattice configurations which are periodic, such as cylinders. Note again that this analysis holds for arbitrary configurations, allowing for complex θ_n .

6.4. 1D Wave Functions

We focus now on a one-dimensional configuration. For this purpose, we choose the $2N$ coordinates to be given by $z_k = \exp(i\theta_k)$, where (see Fig. (6.2))

$$\theta_k = \frac{2\pi}{2N} (k + (-1)^k \delta - N), \quad (6.25)$$

and $\delta \in (-\frac{1}{2}, \frac{1}{2})$ is a fixed parameter. Using this parametrization and the exact expression for the CBs (5.59), we can rewrite the wavefunction amplitudes (6.8) as

$$\Psi_{\mathbf{p}}^{(ee)}(\delta) = \frac{1}{\tilde{N}_0} \left(\sum_{\mathbf{q}=0}^{2^{N-1}-1} \epsilon_{\mathbf{p}\mathbf{q}} A_{\mathbf{q}}(\delta) \right)^{1/2}, \quad (6.26)$$

where

$$A_{\mathbf{q}} = \prod_{n>m}^N \left[\sin \frac{\theta_{\ell_{\mathbf{q}}(n)} - \theta_{\ell_{\mathbf{q}}(m)}}{2} \sin \frac{\theta_{\ell'_{\mathbf{q}}(n)} - \theta_{\ell'_{\mathbf{q}}(m)}}{2} \right]^{\frac{1}{2}}, \quad (6.27)$$

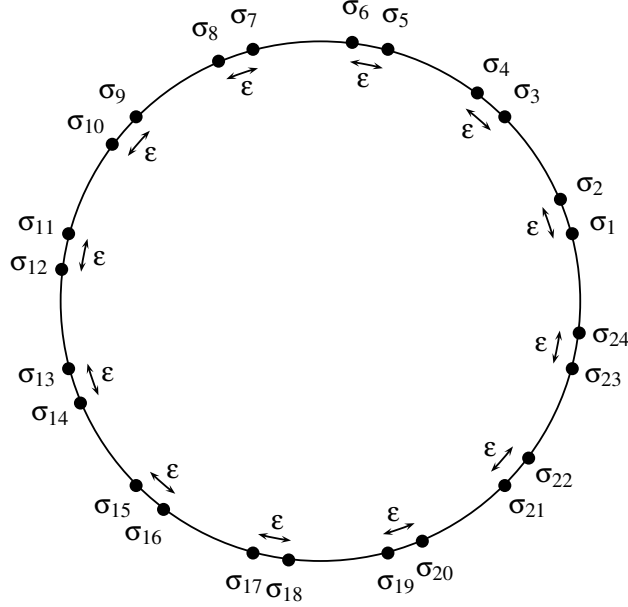


Figure 6.2: Coordinate configuration on the complex plane for a 1D system with 12 spins. Note that the reference pairs are uniformly distributed, so the wave function is translationally invariant for all values of $\epsilon = \delta + \frac{1}{2}$.

and \tilde{N}_0 is a normalization constant

$$\tilde{N}_0^2 = \frac{N^{N/2}}{2^{(N-1)(N-2)/2}}. \quad (6.28)$$

Equation (6.27) follows from the well-known identity

$$z_n - z_m = 2i \exp\left(i \frac{\theta_n + \theta_m}{2}\right) \sin\left(\frac{\theta_n - \theta_m}{2}\right). \quad (6.29)$$

We can massage these expressions to obtain more suitable equations. We will leave all the details for the next two subsections and quote the main results.

First, we can also write (6.27) in terms of the auxiliary spins (5.56)

$$A(\{s_k\}) = \prod_{j>i}^N \sin\left[\frac{\pi}{N} \left(j - i + \frac{1 + 2\delta}{4}(s_j - s_i)\right)\right]. \quad (6.30)$$

Note that for all values of δ , the resulting wave function describes a translationally invariant spin chain with periodic boundary conditions. This is a consequence of the fact that we are describing physical degrees of freedom on the lattice by means of pairs of σ fields. The centers-of-mass of the pairs are uniformly distributed on the circle, while their size is constant for fixed δ

$$\begin{aligned} \theta_{2k} - \theta_{2k-1} &= \frac{2\pi}{N} \left(\frac{1}{2} + \delta\right) \equiv \frac{2\pi}{N} \epsilon, \\ \frac{\theta_{2k} + \theta_{2k-1}}{2} &= \frac{2\pi}{N} \left(k - \frac{2N+1}{2}\right). \end{aligned} \quad (6.31)$$

In this representation, there is an exponentially large number of numerical operations that need to be performed to obtain each wave function amplitude. Luckily, we can obtain a determinant form for these particular configurations that simplifies the calculations. Once again, we make use of the pair-wise fusion basis $\mathbf{m} = (m_1, \dots, m_N)$. It can be shown that the normalized wave function amplitudes can be written as

$$\Psi_{\mathbf{m}}^{(ee)}(\delta) = \left(\frac{\det(F_{\mathbf{m}} * V)}{\det(V)} \right)^{1/2}, \quad (6.32)$$

where $F_{\mathbf{m}} * V$ is the element-wise matrix product (also known as the Hadamard product of matrices)

$$(F_{\mathbf{m}} * V)_{rt} = (F_{\mathbf{m}})_{rt}(V)_{rt}, \quad (6.33)$$

obtained from matrices

$$(V)_{rt} = \exp\left(i \frac{2\pi}{N} r(t-1)\right) \quad (6.34)$$

and

$$(F_{\mathbf{m}})_{rt} = \begin{cases} \cos\left[\frac{\pi}{4N}(1+2\delta)(2t-N-1)\right], & m_r = 0, \\ i \sin\left[\frac{\pi}{4N}(1+2\delta)(2t-N-1)\right], & m_r = 1. \end{cases} \quad (6.35)$$

Determinant expression (6.32) can also allow us to write $|\Psi_{ee}(\delta)\rangle$ as a BCS state. If we define the lattice momenta as

$$k = \frac{\pi}{N}(2m - N - 1), \quad m = 1, \dots, N \quad (6.36)$$

we can write the normalized state as

$$|\Psi_{ee}(\delta)\rangle = C_N(\delta) \exp\left(\sum_{n < m} \tilde{g}_{nm}(\delta) c_n^\dagger c_m^\dagger\right) |0\rangle_c, \quad (6.37)$$

where

$$C_N(\delta) = \prod_k \sqrt{\cos\left[\frac{(1+2\delta)}{4}k\right]}, \quad (6.38)$$

and $\tilde{g}_{nm} = g_{n-m}$ with

$$g_r = (-1)^r \frac{2}{N} \sum_{k>0} \tan\left[\frac{(1+2\delta)}{4}k\right] \sin(kr). \quad (6.39)$$

Note that this result is exact and does not depend on any approximation. We also highlight that this is further evidence that $|\Psi_{ee}\rangle$ as defined in (6.7) has a BCS structure beyond the OPE regime.

Determinant Form for the 1D Wave Function

We can rewrite the wave function amplitudes as (recall that $s_1 = 1$ by definition)

$$\Psi_{\mathbf{p}}^{(ee)}(\delta) = \frac{1}{\tilde{N}_0} \left(\sum_{\{s_1=1, s_2=\pm 1, \dots, s_N=\pm 1\}} \tilde{\epsilon}_{\mathbf{p}\mathbf{s}} A(\{s_k\}) \right)^{1/2} \quad (6.40)$$

where $\tilde{\epsilon}_{\text{ps}}$ was defined in Eq. (5.58) and

$$A(\{s_k\}) = \left(\prod_{j>i}^N \sin \left[\frac{\pi}{N} \left(j - i + \frac{1+2\delta}{4}(s_j - s_i) \right) \right] \right) \sin \left[\frac{\pi}{N} \left(j - i - \frac{1+2\delta}{4}(s_j - s_i) \right) \right]^{1/2}. \quad (6.41)$$

Using the fact that (see Appendix A.1)

$$\prod_{j>i}^N \sin \left[\frac{\pi}{N} \left(j - i + \frac{\alpha}{4}(s_j - s_i) \right) \right] = \prod_{j>i}^N \sin \left[\frac{\pi}{N} \left(j - i - \frac{\alpha}{4}(s_j - s_i) \right) \right], \quad (6.42)$$

for arbitrary real α , we can eliminate the square root in $A(\{s_k\})$ and lift the restriction on s_1 noting that

$$\sum_{\{s_1=1,\dots\}} \tilde{\epsilon}_{\text{ps}} A(\{s_k\}) = \frac{1}{2} \sum_{\{s_1=\pm 1,\dots\}} \tilde{\epsilon}_{\text{ps}} A(\{s_k\}). \quad (6.43)$$

Putting all the pieces together, we have

$$\Psi_{\mathbf{p}}^{(ee)}(\delta) = \frac{1}{N_0} \left(\sum_{\{s_k\}} \tilde{\epsilon}_{\text{ps}} A(\{s_k\}) \right)^{1/2}, \quad (6.44)$$

where now

$$A(\{s_k\}) = \prod_{j>i}^N \sin \left[\frac{\pi}{N} \left(j - i + \frac{1+2\delta}{4}(s_j - s_i) \right) \right] \quad (6.45)$$

and

$$N_0^2 = 2\tilde{N}_0^2 = 2^N \left(\frac{N}{2^{N-1}} \right)^{N/2}. \quad (6.46)$$

Using the identities

$$\sum_{\sigma \in S_N} \text{sgn}(\sigma) \prod_{n=1}^N \alpha_n^{\sigma(n)-1} = \prod_{n>m}^N (\alpha_n - \alpha_m) \quad (6.47)$$

and

$$\sin \left(\frac{\theta_n - \theta_m}{2} \right) = \exp \left(-i \frac{\theta_n + \theta_m}{2} \right) \left(\frac{z_n - z_m}{2i} \right), \quad (6.48)$$

we have

$$\begin{aligned} A(\{s_k\}) &= \prod_{j>i}^N \left[\exp \left(-i \frac{\theta_j + \theta_i}{2} \right) \left(\frac{z_j - z_i}{2i} \right) \right] \\ &= C_N \sum_{\sigma \in S_N} \text{sgn}(\sigma) \left(\prod_{j=1}^N a_{j,\sigma(j)} \right) \left(\prod_{j=1}^N b_{j,\sigma(j)} \right), \end{aligned} \quad (6.49)$$

where

$$(V)_{r,t} = a_{r,t} = \exp \left(i \frac{2\pi}{N} r(t-1) \right) \quad (6.50)$$

defines a Vandermonde matrix,

$$b_{r,t} = \exp\left(i\frac{\pi}{4N}s_r(1+2\delta)(2t-N-1)\right) \quad (6.51)$$

contains all the dependence on $\{s_k\}$, and

$$C_N = (2i)^{-N(N-1)/2} e^{-i\frac{\pi}{2}(N^2-1)}. \quad (6.52)$$

Coming back to $\Psi_{\mathbf{p}}^{(ee)}$, we can now sum over the auxiliary spins $\{s_k\}$

$$\sum_{\{s_k\}} \tilde{\epsilon}_{\mathbf{ps}} A(\{s_k\}) = C_N \sum_{\sigma \in S_N} \text{sgn}(\sigma) \prod_{j=1}^N a_{j,\sigma(j)} \left(\sum_{\{s_k\}} \tilde{\epsilon}_{\mathbf{ps}} \prod_{j=1}^N b_{j,\sigma(j)} \right).$$

We can perform the sum

$$\sum_{\{s_k\}} \tilde{\epsilon}_{\mathbf{ps}} \prod_{j=1}^N b_{j,\sigma(j)} = 2^N \prod_{j=1}^N f_{j,\sigma(j)}. \quad (6.53)$$

where

$$f_{r,t}(\delta) = \begin{cases} \cos\left[\frac{\pi}{4N}(1+2\delta)(2t-N-1)\right], & m_r = 0, \\ i \sin\left[\frac{\pi}{4N}(1+2\delta)(2t-N-1)\right], & m_r = 1, \end{cases} \quad (6.54)$$

and we make use again of the pair-wise basis $\mathbf{m} = (m_1, \dots, m_N)$. In other words, we have a cosine whenever the r -th reference pair fuses to the identity and sine when it fuses to a Majorana fermion. We can now clean everything up. Note first that

$$\begin{aligned} N_0^2 &= 2^N \prod_{j>i}^N \sin\left(\frac{\pi}{2N}(j-i)\right) \\ &= 2^N C_N \sum_{\sigma \in S_N} \text{sgn}(\sigma) \left(\prod_{j=1}^N a_{j,\sigma(j)} \right) \\ &= 2^N C_N \det(V), \end{aligned} \quad (6.55)$$

where V is the Vandermonde matrix defined by $a_{r,t}$. If we define the matrix $F_{\mathbf{m}}$ by the elements $f_{r,t}$, we have

$$\Psi_{\mathbf{m}}^{(ee)}(\delta) = \left(\frac{\det(F_{\mathbf{m}} * V)}{\det(V)} \right)^{1/2}, \quad (6.56)$$

where $F_{\mathbf{m}} * V$ is the Hadamard product

$$(F_{\mathbf{m}} * V)_{r,t} = a_{r,t} f_{r,t}. \quad (6.57)$$

BCS State for 1D Wave Functions

In order to show that the wave function amplitudes (6.32) correspond to a BCS state, we need to write them as Pfaffians obtained from a given pairing function. We will accomplish this by using the multilinearity of the determinant.

First, consider the matrix

$$(U)_{r,t} = \frac{1}{\sqrt{N}} \exp \left(i \frac{2\pi}{N} r \left(t - \frac{1}{2} \right) \right). \quad (6.58)$$

It is easy to show that U is a unitary matrix. Also, by multilinearity of the determinant, we can relate this matrix to the Vandermonde matrix V (6.50)

$$(\Psi_{\mathbf{m}}^{ee})^2(\delta) = \frac{\det(F_{\mathbf{m}} * V)}{\det(V)} = \frac{\det(F_{\mathbf{m}} * U)}{\det(U)}. \quad (6.59)$$

Now, note that we can use once again the multilinearity of the determinant to write

$$\det(F_{\mathbf{m}} * U) = C_N(\delta)^2 \det(H_{\mathbf{m}} * U), \quad (6.60)$$

where

$$C_N(\delta)^2 = \prod_{m=1}^N \cos \left[\frac{\pi}{4N} (1 + 2\delta) (2m - N - 1) \right], \quad (6.61)$$

and $H_{\mathbf{m}}$ is defined by matrix elements

$$(H_{\mathbf{m}})_{r,t}(\delta) = \begin{cases} 1, & m_r = 0, \\ i \tan \left[\frac{\pi}{4N} (1 + 2\delta) (2t - N - 1) \right], & m_r = 1. \end{cases} \quad (6.62)$$

We can further simplify this expression. If we define $M_{\mathbf{m}} = ((H_{\mathbf{m}} * U)U^\dagger)$ and

$$\begin{aligned} g_r(\delta) &= (-1)^r \frac{i}{N} \sum_{m=1}^N \tan \left[\frac{\pi(1 + 2\delta)}{4N} (2m - N - 1) \right] e^{i \frac{2\pi}{N} m r} \\ &= (-1)^r \frac{2}{N} \sum_{k>0} \tan \left((1 + 2\delta) \frac{k}{4} \right) \sin(kr), \end{aligned} \quad (6.63)$$

(using momenta k as defined in (6.36)), it is easy to see that

$$(M_{\mathbf{m}})_{r,t} = \begin{cases} \delta_{r,t}, & m_r = 0, \\ g_{r-t}, & m_r = 1. \end{cases} \quad (6.64)$$

Note that g_r is an anti-symmetric function. Taking into account that $\sum m_n = 2R$ is an even number, assume that the 1's are located at positions $r(1) < \dots < r(2R)$. In order to compute the determinant of $M_{\mathbf{m}}$, note that

$$\det(M_{\mathbf{m}}) = \det(\mathbf{G}_{\mathbf{m}}) \quad (6.65)$$

where $(\mathbf{G}_{\mathbf{m}})_{ij} = g_{r(i)-r(j)}$ is the $2R \times 2R$ anti-symmetric matrix obtained from $M_{\mathbf{m}}$ by keeping only the rows and columns corresponding to $r(1), \dots, r(2R)$. Being anti-symmetric, note also that

$$\det(\mathbf{G}_{\mathbf{m}}) = \text{Pf}^2(\mathbf{G}_{\mathbf{m}}). \quad (6.66)$$

Summing up, we have

$$\begin{aligned} (\Psi_{\mathbf{m}}^{ee})^2(\delta) &= C_N(\delta)^2 \frac{\det(H_{\mathbf{m}} * U)}{\det(U)} \\ &= C_N(\delta)^2 \det(M_{\mathbf{m}}) \\ &= (C_N(\delta) \text{Pf}(\mathbf{G}_{\mathbf{m}}))^2. \end{aligned} \quad (6.67)$$

Given that this result holds for all \mathbf{m} , we conclude that $|\Psi_{ee}(\delta)\rangle = \sum_{\mathbf{m}} \Psi_{\mathbf{m}}^{ee} |\mathbf{m}\rangle$ corresponds to a BCS state defined by pairing function (6.63).

6.5. Fixed Point Ground States of the ITF Model from CBs

We will now show that the three RG fixed points of the ITF spin chain, namely (1) ferromagnetic ($h \rightarrow 0$), (2) paramagnetic ($h \rightarrow \infty$), and (3) critical ($h = 1$) can be obtained exactly from $|\Psi_{ee}(\delta)\rangle$. This is a highly non-trivial result, in particular for the critical case, suggesting a deep connection between finite lattice systems and CBs obtained in the infrared thermodynamic limit.

Consider first $\delta \rightarrow -1/2$. From the OPE, we know that the identity will be more dominant than the fermion in each reference pair. Since in this limit $z_{2k-1} = z_{2k}$, we have that

$$z_{\ell_{\mathbf{q}}} z_{\ell'_{\mathbf{q}}} = z_{\ell_{\mathbf{q}}}^2 = z_{\ell_0}^2. \quad (6.68)$$

so

$$\Psi_{\mathbf{p}}^{(ee)} \left(\delta \rightarrow -\frac{1}{2} \right) = \delta_{\mathbf{p},0}, \quad (6.69)$$

i.e., a trivial product state $|\Psi_{ee}(\delta \rightarrow -\frac{1}{2})\rangle = |0\rangle$.

Now, take $\delta \rightarrow 1/2$. In this limit, $z_{2k} = z_{2k+1}$. Given that for $\mathbf{q} \neq 0$ there will be at least one difference that vanishes (for instance, if $q_1 = 1$, then $z_{\ell'_{\mathbf{q}}} = 0$ because it contains the factor $z_2 - z_3$), we have

$$z_{\ell_{\mathbf{q}}} z_{\ell'_{\mathbf{q}}} = \delta_{\mathbf{q},0} z_{\ell_0} z_{\ell'_0}. \quad (6.70)$$

This implies that all the configurations have equal weight. In the pair-wise fusion basis, this is a ferromagnetic state projected onto the even parity sector, more precisely

$$\left| \Psi_{ee} \left(\delta \rightarrow \frac{1}{2} \right) \right\rangle = \frac{1}{\sqrt{2}} \left(|+\rangle^{\otimes N} + |-\rangle^{\otimes N} \right), \quad (6.71)$$

where $\sigma^x |\pm\rangle = \pm |\pm\rangle$.

These two limiting cases correspond to the (even parity) trivial phases of the Ising transverse field (ITF) spin chain

$$H(h) = - \sum_{n=1}^N \sigma_n^x \sigma_{n+1}^x - h \sum_{n=1}^N \sigma_n^z, \quad (6.72)$$

i.e., $h \rightarrow \infty$ and $h = 0$, respectively.

Remarkably, we can also obtain the ground state for the critical value $h = 1$. In order to show this, let us first specialize the exact solution we obtained for the ITF spin chain in Section 5.2 to the case $h = 1$. The normalized ground state has a BCS structure

$$\begin{aligned} |gs\rangle &= \prod_{k>0} \left[\cos \left(\frac{\theta_k}{2} \right) + i \sin \left(\frac{\theta_k}{2} \right) c_k^\dagger c_{-k}^\dagger \right] |0\rangle_c \\ &= \prod_{k>0} \cos \left(\frac{\theta_k}{2} \right) \exp \left[\sum_{k>0} i \tan \left(\frac{\theta_k}{2} \right) c_k^\dagger c_{-k}^\dagger \right] |0\rangle_c, \end{aligned} \quad (6.73)$$

where the Bogoliubov angles become

$$\cos \left(\frac{\theta_k}{2} \right) = \sqrt{\frac{1 + \sin \left| \frac{k}{2} \right|}{2}}, \quad \sin \left(\frac{\theta_k}{2} \right) = -\text{sgn}(k) \sqrt{\frac{1 - \sin \left| \frac{k}{2} \right|}{2}}. \quad (6.74)$$

This implies that the normalization constant is

$$\begin{aligned} \prod_{k>0} \cos\left(\frac{\theta_k}{2}\right) &= \prod_{k>0} \sqrt{\frac{1 + \sin\left(\frac{k}{2}\right)}{2}} \\ &= \prod_{m=1}^N \sqrt{\cos\left[\frac{\pi}{4N}(2m - N - 1)\right]}. \end{aligned} \quad (6.75)$$

We can also compute the real-space pairing function by doing a Fourier transform of $g_k = i \tan\left(\frac{\theta_k}{2}\right)$

$$\begin{aligned} g_r &= \frac{2}{N} \sum_{k>0} \frac{1 - \sin\left(\frac{k}{2}\right)}{\cos\left(\frac{k}{2}\right)} \sin(kr) \\ &= (-1)^r \frac{2}{N} \sum_{k>0} \tan\left(\frac{k}{4}\right) \sin(kr), \quad r \in \mathbb{Z}, \end{aligned} \quad (6.76)$$

where the second expression is obtained from the first one by replacing $k \mapsto \pi - k$.

Now, coming back to the wave functions obtained from the Ising CBs, note that these expressions correspond to the normalization constant (6.38) and the pairing function (6.39) obtained in the previous section when $\delta = 0$, so that

$$|gs(h = 1)\rangle = |\Psi_{ee}(\delta = 0)\rangle. \quad (6.77)$$

This is a remarkable result given that the expression for the CBs (5.59) was obtained using the Ising CFT. It is non-trivial that it would agree with the ground state of a finite-size lattice system. We can understand this result in a more profound way by considering the algebraic properties inherited by the wave function from the operators in the CFT. In particular, we will consider the Kramers-Wannier duality obtained from braiding the operators and the associated Hamiltonian derived from the Temperley-Lieb-Jones algebra.

6.6. Braiding and Kramers-Wannier Duality

The braiding of fields will in general mix different CBs, $\mathcal{F}_k = \sum_{k'} B_{k,k'} \mathcal{F}_{k'}$, where $B_{k,k'}$ is a representation of the braiding operation [162, 131]. Geometrically, we expect that cyclic permutation of primary fields located on the unit circle according to (6.25) will yield useful algebraic properties.

If we take $\sigma(z_{2N})$ and braid it with all the other $2N - 1$ fields, so that it becomes the first operator, we obtain the same CB up to a relabeling $z_k \rightarrow z_{k+1}$ (identifying $2N + 1 \equiv 1$), so that

$$\mathcal{F}_p(\delta) = \sum_{p'} U_{pp'} \mathcal{F}_{p'}(-\delta), \quad (6.78)$$

where U is the operator obtained from the braiding. Note that there are no radial ordering issues because all the operators are on the unit circle.

This process can be decomposed into pair-wise permutations. Call ω_i the operator that interchanges $\sigma(z_i)$ and $\sigma(z_{i+1})$. The set $\{\omega_i | i = 1, \dots, 2N - 1\}$ will satisfy the *braid group* relations

$$\omega_i \omega_{i+1} \omega_i = \omega_{i+1} \omega_i \omega_{i+1}, \quad \omega_i \omega_j = \omega_j \omega_i, \quad |i - j| \geq 2. \quad (6.79)$$

$$\begin{array}{ccc}
 \sigma_{2n-1} & \sigma_{2n} & \\
 \cdots & \begin{array}{c} | \\ \hline \end{array} & \begin{array}{c} | \\ \hline \end{array} & \cdots & = e^{-i\pi/8} (\delta_{p_{n-1}, p_n} + i \delta_{p_{n-1}, 1-p_n}) & \cdots & \begin{array}{c} \sigma_{2n} & \sigma_{2n-1} \\ | & | \\ \hline \end{array} & \cdots \\
 p_{n-1} & \sigma & p_n & & & & p_{n-1} & \sigma & p_n
 \end{array}$$

$$\begin{array}{ccc}
 \sigma_{2n} & \sigma_{2n+1} & \\
 \cdots & \begin{array}{c} | \\ \hline \end{array} & \begin{array}{c} | \\ \hline \end{array} & \cdots & = \sum_{q=0,1} B_{p_n, q} & \cdots & \begin{array}{c} \sigma_{2n+1} & \sigma_{2n} \\ | & | \\ \hline \end{array} & \cdots \\
 \sigma & p_n & \sigma & & & & \sigma & q & \sigma
 \end{array}$$

Figure 6.3: Braiding operators for \mathcal{F}^{2N} . We define $B = \frac{e^{i\pi/8}}{\sqrt{2}} (\mathbb{1}_{2 \times 2} + i\sigma^x)$ and use the convention $\sigma_i = \sigma(z_i)$.

It can be shown that [162]

$$\omega_1 \cdots \omega_{2N-1}^2 \cdots \omega_1 = \exp(-4i\pi h_\sigma) \quad (6.80)$$

where $h_\sigma = \frac{1}{16}$ is the scaling dimension of σ and the sign of the phase depends on the direction of the exchange. This allows us to define the unitary operator

$$U = e^{2i\pi h_\sigma} \omega_1 \cdots \omega_{2N-1} = e^{-2i\pi h_\sigma} \omega_1^\dagger \cdots \omega_{2N-1}^\dagger, \quad (6.81)$$

which is independent of the convention for the pair-wise exchange.

We can obtain a representation of these operators from the fusion matrix F and the braid operator R [131, 136] (see Fig. (6.3)). The action of this operation can be better understood using the pair-wise fusion basis. In that case, the operator U corresponds to the Kramers-Wannier transformation restricted to the even parity sector ($\langle Q \rangle = \langle \prod_n \sigma_n^z \rangle = 1$) (see Section 5.3)

$$U \sigma_n^z U^\dagger = \sigma_n^x \sigma_{n+1}^x, \quad U \sigma_n^x U^\dagger = \sigma_1^z \cdots \sigma_n^z. \quad (6.82)$$

This duality is known to be non-invertible in the odd parity sector [183]. Note also that iterating this process, i.e. braiding the whole last reference pair, corresponds to a one-site translation in the pair-wise fusion basis.

Relation (6.78) implies that $|\Psi_{ee}(\delta = 0)\rangle$ will be self-dual. As we discussed in Section 5.3, this is also the case for the (even parity) ground state of the critical (ITF) Hamiltonian as a consequence of the self-duality of the critical Ising model. We see then that KW duality motivates that these two states are the same.

6.7. The Temperley-Lieb-Jones Algebra

As we mentioned before, minimal models lack internal symmetries. This makes it hard for us to construct a parent Hamiltonian for wave functions obtained from CBs. However, we can associate an integrable model to a given minimal RCFT using the properties of the CBs. This is due to the fact that the constraints imposed by the braiding and fusion of operators can be related to the Yang-Baxter algebra [131].

We first need some general definitions. A *Temperley-Lieb-Jones* (TLJ) algebra is an unital, complex algebra closely related to the braid group. It is generated by operators $\{e_i | i = 1, \dots, M\}$ satisfying

$$\begin{aligned} e_i^\dagger &= e_i, & e_i e_{i\pm 1} e_i &= e_i, \\ e_i^2 &= \sqrt{\beta} e_i, & e_i e_j &= e_j e_i, \quad \text{for } |i - j| \geq 2, \end{aligned} \quad (6.83)$$

where β is a free parameter which for the Ising model takes the value $\beta_{\text{Ising}} = 2$. Let $\{|\mathbf{p}\rangle = |p_1, \dots, p_{N-1}\rangle\}$ be the basis of the Hilbert space of the model. The action of the TLJ operators on this basis is given by [131]

$$\begin{aligned} e_{2n-1} |\mathbf{p}\rangle &= \sqrt{2} \delta_{p_{n-1}, p_n} |\dots p_n \dots\rangle, & n &= 1, \dots, N, \\ e_{2n} |\mathbf{p}\rangle &= \frac{1}{\sqrt{2}} (|\dots p_{n-1}, p_n \dots\rangle + |\dots p_{n-1}, 1 - p_n \dots\rangle), & n &= 1, \dots, N - 1, \\ e_{2N} |\mathbf{p}\rangle &= \frac{1}{\sqrt{2}} (|\mathbf{p}\rangle + |\mathbf{p}'\rangle), \end{aligned} \quad (6.84)$$

where $\mathbf{p}' = (1 - p_1, 1 - p_2, \dots, 1 - p_{N-1})$. The last element, e_{2N} , is an extension of the TLJ algebra to periodic systems [205]. The TLJ operators can also be expressed in the spin basis $\{|\mathbf{m}\rangle = |m_1, \dots, m_N\rangle\}$, where $m_k = p_k + p_{k-1} \pmod{2}$ (recall Fig. 5.1). They become

$$\begin{aligned} \sqrt{2} e_{2n-1} - 1 &= \sigma_n^z, \\ \sqrt{2} e_{2n} - 1 &= \sigma_n^x \sigma_{n+1}^x, \end{aligned} \quad (6.85)$$

where $n = 1, \dots, N$ and we impose periodic boundary conditions $\sigma_{N+1}^x = \sigma_1^x$. One can verify that the operator U that implements the KW duality satisfies

$$e_{n+1} = U e_n U^\dagger, \quad n = 1, \dots, 2N. \quad (6.86)$$

Using equations (6.85), it is clear that the critical ITF Hamiltonian corresponds to the Temperley-Lieb Hamiltonian

$$H_{TL} = - \sum_{i=1}^{2N} \left(\sqrt{2} e_i - 1 \right). \quad (6.87)$$

We expect then that the many-body state constructed from the CBs of the Ising model (6.26) will be closely related to the spin chain Hamiltonian (6.87). Since this Hamiltonian is translationally invariant, one is led to the 1D configuration $z_n = e^{2\pi i n / (2N)}$. This also guarantees that the state is self-dual under a KW transformation. In other words, we are led to try $|\Psi_{ee}(\delta = 0)\rangle$ as a trial wave function for the critical ITF Hamiltonian.

It is important to highlight that this argument does not constitute a rigorous proof of the result we presented in Section 6.5, although it serves as further motivation. For comparison, in the case of the Haldane-Shastry wave function, the associated parent Hamiltonian was derived using the algebraic constraints imposed by the null vectors of the Kac-Moody algebra $SU(2)_1$. We expect that this type of construction could be extended to minimal CFTs by considering other algebraic relations.

6.8. Parent Hamiltonians for 1D

Going back to the 1D states (6.26), we have checked numerically that for $\delta \neq 0$ we can find parent Hamiltonians that can also be mapped to a quadratic fermionic form. We consider the following family of Hamiltonian terms

$$\begin{aligned} Z &= - \sum_n \sigma_n^z, \\ X_r &= - \sum_n \sigma_n^x \sigma_{n+1}^z \cdots \sigma_{n+r-1}^z \sigma_{n+r}^x, \\ Y_r &= - \sum_n \sigma_n^y \sigma_{n+1}^z \cdots \sigma_{n+r-1}^z \sigma_{n+r}^y, \end{aligned} \quad (6.88)$$

with $r = 1, \dots, N/2$. (Note that X_1 is the usual Ising term.) Given that $|\Psi_{ee}(\delta)\rangle$ is translationally invariant and describes a system with periodic boundary conditions, we impose the same constraints on the Hamiltonian terms.

This particular choice for the family of Hamiltonian terms corresponds to those that will yield quadratic forms in fermionic variables. If we use the Jordan-Wigner transformation

$$\begin{aligned} \sigma_n^z &= 1 - 2c_n^\dagger c_n, \\ \sigma_n^x &= \prod_{m=1}^{n-1} (1 - 2c_m^\dagger c_m) (c_m^\dagger + c_m), \\ \sigma_n^y &= i \prod_{m=1}^{n-1} (1 - 2c_m^\dagger c_m) (c_m^\dagger - c_m), \end{aligned} \quad (6.89)$$

we obtain

$$\begin{aligned} Z &\mapsto - \sum_n (1 - 2c_n^\dagger c_n), \\ X_r &\mapsto - \sum_n (c_n^\dagger - c_n) (c_{n+r}^\dagger + c_{n+r}), \\ Y_r &\mapsto \sum_n (c_n^\dagger + c_n) (c_{n+r}^\dagger - c_{n+r}). \end{aligned} \quad (6.90)$$

We know that the variational wavefunctions obtained from the CBs of the Ising model behave nicely under a Kramers-Wannier (KW) duality transformation. In particular, we have that

$$|\Psi_{ee}(\delta)\rangle \mapsto |\Psi_{ee}(-\delta)\rangle. \quad (6.91)$$

Something similar can be said about the Hamiltonian terms we are considering.

The action of the KW transformation can be summarized in the map

$$\sigma_n^z \mapsto \sigma_n^x \sigma_{n+1}^x, \quad \sigma_n^x \mapsto \sigma_1^z \cdots \sigma_n^z. \quad (6.92)$$

From these relations, it is easy to compute the action of the KW transformation (for the even-parity sector of the Hilbert space $\langle Q \rangle = \langle \prod_n \sigma_n^z \rangle = 1$)

$$\begin{aligned} Z &\mapsto X_1, & X_1 &\mapsto Z, \\ X_r &\mapsto -Y_{r-1}, \quad (r = 2, \dots, N/2), & Y_r &\mapsto -X_{r+1}, \quad (r = 1, \dots, N/2). \end{aligned} \quad (6.93)$$

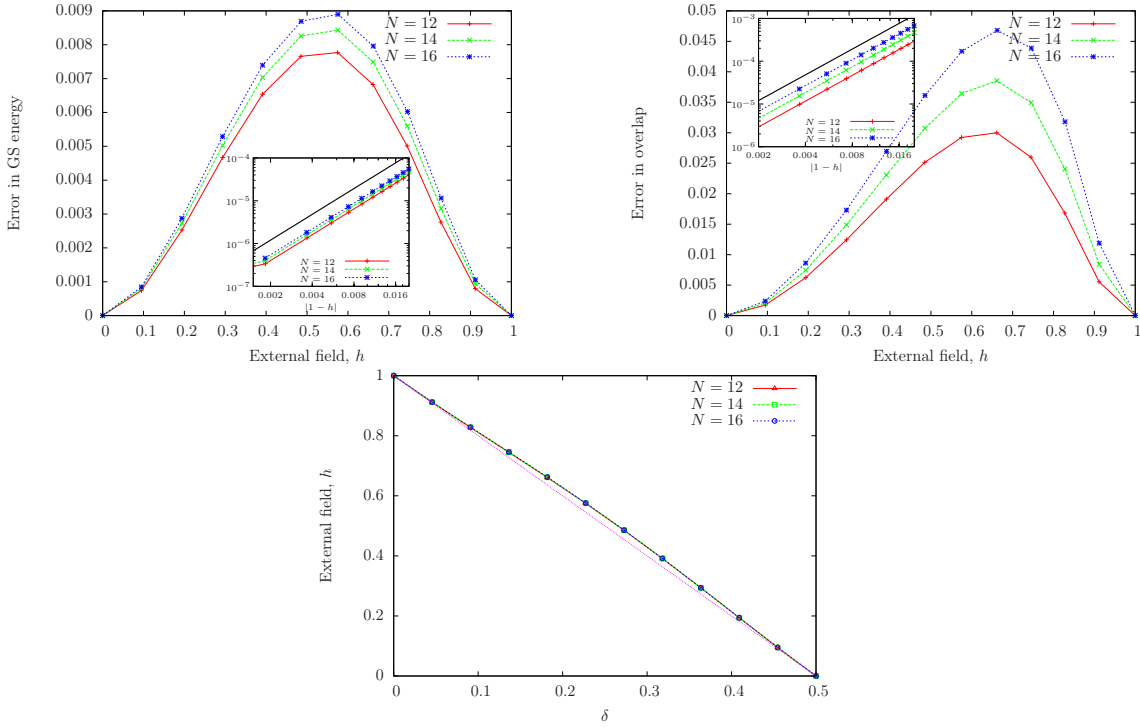


Figure 6.5: Errors of (a) the variational energy and (b) the overlap. Both plots use the value of δ that optimizes the overlap with the ground state of $H(h)$. The insets correspond to the scaling near $h_c = 1$. In both cases, the error scales as $|1 - h|^2$ (the black thick line serves as reference for a quadratic scaling). (c) Relation between the variational parameter δ and the value of the external field h that optimizes the overlap. (The dotted purple line is a reference straight line.) Note that the behavior is virtually independent of the system size. .

Forcing the ITF Hamiltonian

For $|\delta| \approx 0$, all the Hamiltonian terms that change sign under a KW transformation are very small compared to \tilde{H}_1 . Given that the whole Hamiltonian family $\{\tilde{H}_r\}$ respect the basic Ising symmetries, this implies that $|\Psi_{ee}(\delta)\rangle$ approximates small massive perturbations away from criticality. If we drop the Hamiltonian terms for $r > 2$, we see that in this vicinity the corresponding transverse field will be given by

$$h = \frac{1 - a_2}{1 + a_2} \approx 1 - 2a_2 + \mathcal{O}(a_2^2). \quad (6.98)$$

It is tempting to relate the variational parameter δ to the external magnetic field h in the usual ITF Hamiltonian (6.72). In order to study this, we computed for different system sizes the value of h that maximizes the overlap between $|\Psi_{ee}(\delta)\rangle$ and the ground state $|gs(h)\rangle$. (We limit our analysis to $0 \leq \delta \leq \frac{1}{2}$. Negative values of δ have a similar behavior due to the KW duality.)

First, we note that the optimal value of h behaves in an almost linear fashion as a function of δ , independent of the system size (Fig. (6.5)). However, there is a qualitative difference in the computed error for the overlap $1 - \langle gs(h) | \Psi_{ee}(\delta) \rangle$ and the expectation value of the Hamiltonian

$$\text{Error} = \frac{|E_{\text{exact}}(h) - \langle \Psi_{ee}(\delta) | H(h) | \Psi_{ee}(\delta) \rangle|}{|E_{\text{exact}}(h)|}. \quad (6.99)$$

Within numerical machine precision, the optimized variational wavefunction (6.26) corresponds to the exact ground state only for $h = 0$ and $h_c = 1$, while errors are considerable for other values of h . We also see that the scaling of the errors close to $h_c = 1$ is quadratic. This implies that the variational minimum is located smoothly at $\delta = 0$.

Some Algebraic Properties of the Hamiltonian Family

It is illuminating to write the operators of the Hamiltonian family in terms of Majorana fermions

$$a_{2n-1} = c_n + c_n^\dagger, \quad a_{2n} = \frac{c_n - c_n^\dagger}{i}. \quad (6.100)$$

Note that, for the even parity sector $\langle Q \rangle = \langle \prod_n \sigma_n^z \rangle = 1$, we have antiperiodic boundary conditions for the fermions $c_{N+m} = -c_m$ after a Jordan-Wigner transformation. Antiperiodic boundary conditions on the fermions imply $a_{2N+r} = -a_r$. In these variables, we have

$$\begin{aligned} Z &= i \sum_n a_{2n-1} a_{2n}, \\ X_r &= i \sum_n a_{2n} a_{2(n+r)-1}, \\ Y_r &= -i \sum_n a_{2n-1} a_{2(n+r)}. \end{aligned} \quad (6.101)$$

Now, let us consider the variational Hamiltonian family defined in (6.94). Using the Majorana variables, we obtain

$$\begin{aligned} \tilde{H}_1 &= i \sum_n a_n a_{n+1}, \\ \tilde{H}_r &= i \sum_n (-1)^n a_n a_{n+2(r-1)-1}, \end{aligned} \quad (6.102)$$

with $r = 2, \dots, N/2 + 1$. As discussed in Section 5.3, the action of the KW transformation on the Majorana fermions is simply

$$a_r \mapsto a_{r+1}, \quad (6.103)$$

which acts as expected on the Hamiltonian family. Note that this action mimics the interpretation of the KW transformation for the CBs as braiding of sigma fields (see Section 6.6).

The Hamiltonian family we have used is very similar to the conserved quantities of the Ising model, seen as an integrable model [206]. Those can be obtained from

$$E_p = (-1)^p \frac{i}{2p} \sum_n a_n a_{n+p}. \quad (6.104)$$

Note that $\tilde{H}_1 = -2E_1$ and that $[E_p, E_q] = 0$. It has been shown that formal manipulations of $\{E_p\}$ can yield lattice representations of the Virasoro algebra [206, 207].

6.9. Excited States

We can extend the previous discussion to other states obtained from operator matrix (6.6). Let us first consider state $|\Psi_{oo}\rangle$, defined in (6.9). In this case, the asymptotic states of the CFT are fermions

$$\Psi_{\mathbf{p}}^{(oo)} \propto \langle \psi | \sigma(z_1) \cdots \sigma(z_{2N}) | \psi \rangle_{\mathbf{p}}. \quad (6.105)$$

Assuming radial ordering, we can obtain the CBs for this state by adding two fermions at $z = 0, \infty$. Starting from the exact expression (5.65) and taking the appropriate limit, the corresponding amplitudes for the associated wave function are given by

$$\Psi_{\mathbf{p}}^{(oo)} = \frac{1}{\tilde{N}_2} \left(\sum_{\mathbf{q}=0}^{2^{N-1}-1} \epsilon_{\mathbf{p}\mathbf{q}} A_{\mathbf{q}} \right)^{-1/2} \left[\sum_{\mathbf{q}=0}^{2^{N-1}-1} \epsilon_{\mathbf{p}\mathbf{q}} A_{\mathbf{q}} \left(\sqrt{\prod_{k=1}^N \frac{z_{\ell_{\mathbf{q}}(k)}}{z_{\ell'_{\mathbf{q}}(k)}}} + \sqrt{\prod_{k=1}^N \frac{z_{\ell'_{\mathbf{q}}(k)}}{z_{\ell_{\mathbf{q}}(k)}}} \right) \right]. \quad (6.106)$$

If we use the homogeneous 1D configuration (6.25), we can rewrite these amplitudes as

$$\Psi_{\mathbf{p}}^{(oo)} = \frac{1}{N_2} \left(\sum_{\{s_k\}} \tilde{\epsilon}_{\mathbf{p}\mathbf{s}} A(\{s_k\}) \right)^{-1/2} \left(\sum_{\{s_k\}} \tilde{\epsilon}_{\mathbf{p}\mathbf{s}} A(\{s_k\}) \cos \left[\frac{\pi}{2N} (1 + 2\delta) \sum_{k=1}^N s_k \right] \right), \quad (6.107)$$

They can also be written in terms of determinants. Define the matrix

$$(J_{\mathbf{m}}(q))_{r,t} = \exp \left(i \frac{2\pi}{N} r(t-1) \right) (F_{\mathbf{m}}(q))_{r,t}, \quad (6.108)$$

where

$$(F_{\mathbf{m}}(q))_{r,t} = \begin{cases} \cos \left[\frac{\pi}{4N} (1 + 2\delta) (2t - N - 1 + q) \right], & m_r = 0, \\ i \sin \left[\frac{\pi}{4N} (1 + 2\delta) (2t - N - 1 + q) \right], & m_r = 1. \end{cases} \quad (6.109)$$

We can easily show that

$$\Psi_{\mathbf{m}}^{(oo)} \propto \frac{1}{(\det(J_{\mathbf{m}}(0)))^{1/2}} [\det(J_{\mathbf{m}}(2)) + \det(J_{\mathbf{m}}(-2))]. \quad (6.110)$$

Given that this wave function can be written in terms of real amplitudes (up to a possible overall phase that does not depend on \mathbf{p}), it is easy to compute the overlap with $|\Psi_{ee}\rangle$

$$\langle \Psi_{ee}(\delta) | \Psi_{oo}(\delta) \rangle = \sum_{\mathbf{p}} \Psi_{\mathbf{p}}^{(ee)} \Psi_{\mathbf{p}}^{(oo)} \propto \cos \left(\frac{\pi}{2} (1 + 2\delta) \right) = -\sin(\pi\delta). \quad (6.111)$$

This implies that the two states will be orthogonal if and only if $\delta = 0$. (Recall that we are assuming $|\delta| < 1/2$.) This is exactly the case for which $|\Psi_{ee}\rangle$ describes the ground state of the critical ITF spin chain.

We have checked numerically the action of this Hamiltonian on $|\Psi_{oo}(\delta = 0)\rangle$ for sizes up to $N = 20$ spins using a Lanczos algorithm. We found that it corresponds within machine precision to the first excited state of the even-parity sector of the critical ITF Hamiltonian.

These results reflect the relation between the finite-size spectrum of the Ising spin chain and the operator content of the corresponding CFT [208, 190, 209]. It is known that the classification of the low-energy states of the even-parity sector of the critical ITF Hamiltonian with periodic boundary conditions corresponds to the Virasoro towers of operators $\mathbb{1}$ and ϵ^1

$$H_0^{(0)} \leftrightarrow (0, 0) + \left(\frac{1}{2}, \frac{1}{2}\right). \quad (6.112)$$

The rest of the Virasoro towers correspond to other excited states within the same sector of the Hamiltonian. Starting from $|\Psi_{ee}(\delta = 0)\rangle$ and $|\Psi_{oo}(\delta = 0)\rangle$, we can in principle construct most of this spectrum by acting on them with the corresponding representation of the Virasoro algebra. Luckily, these operators can be obtained on the lattice using the local Hamiltonian density, which in turn is related to the TLJ algebra [206, 207].

It is tempting to extend this construction to the odd-parity sector of the ITF Hamiltonian. Finite-size scaling using periodic boundary conditions relate the spectrum of this sector to the Virasoro tower of σ [190]

$$H_1^{(0)} \leftrightarrow \left(\frac{1}{16}, \frac{1}{16}\right). \quad (6.113)$$

We tried to obtain the ground state of this sector from the Ising CBs postulating two natural candidates:

- a) using a single fermion on the asymptotic states, either at $z = 0, \infty$, so that the CFT degrees of freedom are traced out by $\langle 0 | \cdots | \psi \rangle$ or $\langle \psi | \cdots | 0 \rangle$;
- b) using a pair of σ fields on the asymptotic states $\langle \sigma | \cdots | \sigma \rangle$, both forming a reference pair.

In both scenarios, the amplitudes obtained using configuration (6.25) for $\delta = 0$ contained complex amplitudes that cannot be factored to an overall phase. This implies that these states cannot be used naively to describe ground states of real Hamiltonians. Moreover, using σ for both asymptotic states can yield wave functions that are not translationally invariant even if the degrees of freedom are arranged uniformly on the circle. This suggests that there is a richer structure underlying the general framework that needs to be understood in further work.

6.10. 2D Wave Functions

So far, we have used coordinate configurations for the σ fields that are constrained to the unit circle. We will now study 2D configurations on the complex plane. Unfortunately, we cannot use the same procedure we described in Section 6.4 to write the amplitudes as a determinant. In principle, this would limit the system sizes we can consider numerically. However, we can get around this impasse by considering the OPE approximation we discussed in Section 6.3.

We will relate $|\Psi_{ee}\rangle$ for a 2D configuration to the weak pairing phase of the effective mean-field Hamiltonian that describes $p + ip$ superconductivity [191]

$$H = \sum_{\mathbf{k}} \left[\xi_{\mathbf{k}} c_{\mathbf{k}}^\dagger c_{\mathbf{k}} + \frac{1}{2} (\Delta_{\mathbf{k}}^* c_{-\mathbf{k}} c_{\mathbf{k}} + h.c.) \right], \quad (6.114)$$

¹ $H_a^{(b)}$ stands for Hamiltonian (6.72) with $h = 1$ in the $a = 0, 1$ parity sector with boundary conditions $\sigma_{N+n}^x = (-1)^b \sigma_n^x$.

where

$$\xi_{\mathbf{k}} = \frac{1}{2m} \mathbf{k}^2 - \mu, \quad \Delta_{\mathbf{k}} = \hat{\Delta}(k_x - ik_y), \quad (6.115)$$

μ is the chemical potential, and $\hat{\Delta}$ is a constant defining the gap function. The (normalized) ground state of this theory is obtained by usual BCS methods and can be written as

$$|gs\rangle = \prod_{\mathbf{k}}' \left((u_{\mathbf{k}} + v_{\mathbf{k}} c_{\mathbf{k}}^{\dagger} c_{-\mathbf{k}}^{\dagger}) |0\rangle \right), \quad (6.116)$$

where the prime on the product indicates that each pair $(\mathbf{k}, -\mathbf{k})$ appears only once, and $u_{\mathbf{k}}, v_{\mathbf{k}}$ are the Bogoliubov functions obtained from the Bogoliubov-de Gennes (BdG) equations

$$E_{\mathbf{k}} u_{\mathbf{k}} = \xi_{\mathbf{k}} u_{\mathbf{k}} - \Delta_{\mathbf{k}}^* v_{\mathbf{k}}, \quad E_{\mathbf{k}} v_{\mathbf{k}} = -\xi_{\mathbf{k}} v_{\mathbf{k}} - \Delta_{\mathbf{k}} u_{\mathbf{k}}. \quad (6.117)$$

This reduces to

$$E_{\mathbf{k}} = \sqrt{\xi_{\mathbf{k}}^2 + |\Delta_{\mathbf{k}}|^2}, \quad (6.118)$$

$$|u_{\mathbf{k}}|^2 = \frac{1}{2} \left(1 + \frac{\xi_{\mathbf{k}}}{E_{\mathbf{k}}} \right), \quad |v_{\mathbf{k}}|^2 = \frac{1}{2} \left(1 - \frac{\xi_{\mathbf{k}}}{E_{\mathbf{k}}} \right).$$

The ground state can then be rewritten as

$$|gs\rangle = \left(\prod_{\mathbf{k}} |u_{\mathbf{k}}|^2 \right) \exp \left(\frac{1}{2} \sum_{\mathbf{k}} g_{\mathbf{k}} c_{\mathbf{k}}^{\dagger} c_{-\mathbf{k}}^{\dagger} \right) |0\rangle, \quad (6.119)$$

where

$$g_{\mathbf{k}} = \frac{v_{\mathbf{k}}}{u_{\mathbf{k}}} = -\frac{E_{\mathbf{k}} - \xi_{\mathbf{k}}}{\Delta_{\mathbf{k}}^*}. \quad (6.120)$$

(Note there is no restriction on \mathbf{k} , except maybe for $\mathbf{k} = 0$.) Using the fermionic statistics, the amplitudes of the ground state can be written as Pfaffians (5.26) using the real-space pairing function

$$g(\mathbf{r}) = \frac{1}{N^2} \sum_{\mathbf{k}} e^{i\mathbf{k}\cdot\mathbf{r}} g_{\mathbf{k}}. \quad (6.121)$$

If $\mu > 0$, the system will be in the so-called weak pairing phase [191, 202, 203]. For small momenta, we have $\xi_{\mathbf{k}} < 0$ and

$$g_{\mathbf{k}} \sim -\frac{2\mu}{\hat{\Delta}(k_x + ik_y)}. \quad (6.122)$$

The leading behaviour of the real-space pairing function is given by (see next subsection for details)

$$g(\mathbf{r}) \sim -\left(\frac{2a^2\mu}{2\pi i \hat{\Delta}} \right) \frac{1}{x + iy}, \quad (6.123)$$

where a is the lattice spacing. Note that this analysis is done on the torus, assuming a very large system size. However, the leading singular term gives the qualitative infrared behavior that determines the phase of the system.

Pairing function (6.123) is similar to the one obtained from $|\Psi_{ee}\rangle$ using an OPE approximation (6.19). This suggests that $|\Psi_{ee}\rangle$ can be related to the weak pairing phase of (6.114) as long as the OPE regime yields a good approximation of the CBs. The set of

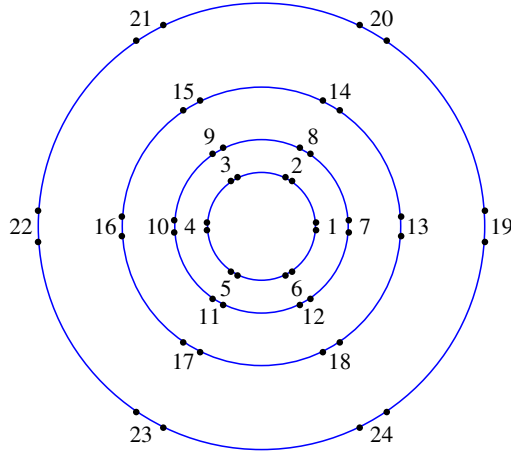


Figure 6.6: 2D configuration corresponding to 48 σ fields arranged on a cylinder with $N_x = 6$ and $N_y = 4$. We represent it on the plane according to the exponential map $z \mapsto \exp(i\theta)$. For clarity, we label the 24 physical spins, each one obtained from a pair of σ fields. Using coordinates (6.124), spins with equal y_n are located at the same radius.

distances between the σ fields in each reference pair can then be related to the chemical potential of the $p+ip$ superconductor. We expect then that $|\Psi_{ee}\rangle$ can describe the topological weak pairing phase of (6.114), which has been associated to the Moore-Read Pfaffian state in the fractional quantum Hall effect [191, 202, 203].

Based on the previous analysis, we focus now on 2D spin systems on finite cylinders. The lattice will contain N_y spins along the longitudinal direction and N_x spins along the periodic one (see Fig. (6.6)). We use the identification $z_n = \exp(i\theta_n)$ according to the cylinder coordinates (6.21). We parametrize them as

$$\phi_n = \frac{2\pi}{N_x}(x_n - iRy_n) \quad (6.124)$$

where $n = 1, \dots, N_x N_y$ labels the spin sites, $x_n \in \{1, \dots, N_x\}$ and $y_n \in \{1, \dots, N_y\}$ are positive integers that define the lattice on the cylinder, and R is the anisotropy factor (we will use $R = 1$ for a regular square lattice). We also set

$$\epsilon_n = \frac{2\pi}{N_x}\epsilon. \quad (6.125)$$

We can use complex values for ϵ , but the radial ordering leads to subtleties when we extrapolate to the exact regime. We will focus then on real values, noting that the OPE regime corresponds to $0 < \epsilon \ll 1$.

Using this notation, the OPE pairing function becomes

$$g_{nm} = \frac{\sin\left(\frac{\pi}{N_x}\epsilon\right)}{2 \sin\left(\frac{\pi}{N_x}(x_n - x_m - iR(y_n - y_m))\right)}. \quad (6.126)$$

Note that, for large values of N_x , we can approximate this expression by a power law, so the leading singular term is similar to (6.123).

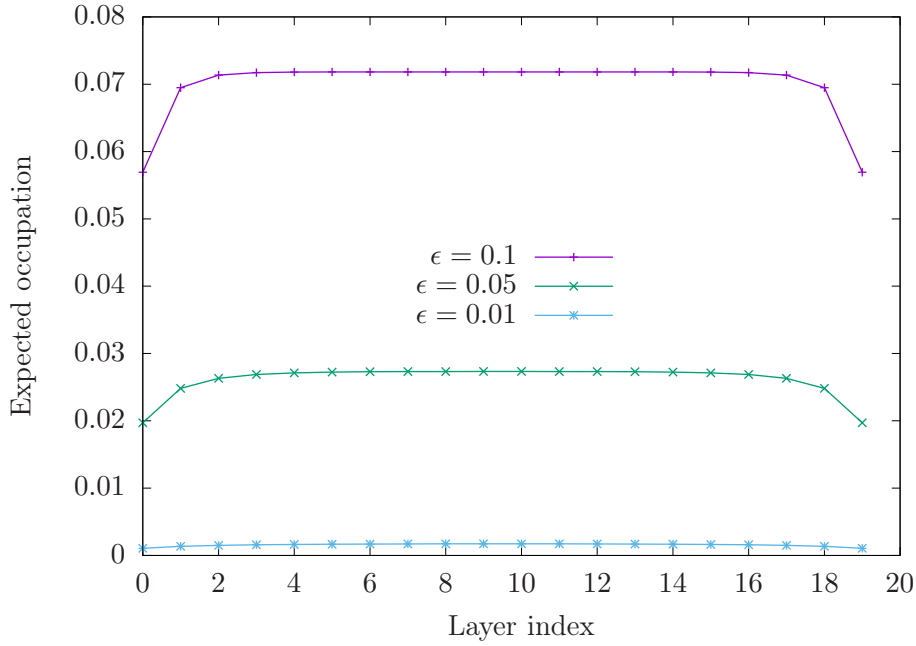


Figure 6.7: Expected occupation per site for different values of ϵ . The layer correspond to the longitudinal y -direction in the cylinder.

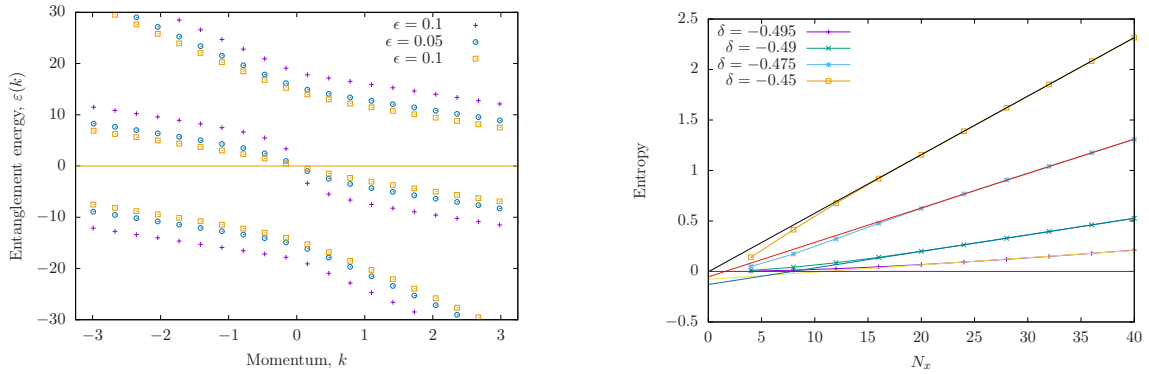


Figure 6.8: (a) Entanglement (single-body) spectrum for different values of ϵ . (b) Scaling of the entanglement entropy as a function of the circumference of the cylinder for different values of ϵ .

In order to characterize these wave functions, we study the entanglement spectrum [204] and the entanglement entropy obtained from the reduced density matrix ρ_{cyl} of half a cylinder. Being a BCS state, we know that ρ_{cyl} can be written as [210, 211]

$$\rho_{\text{cyl}} = \frac{1}{Z} \exp \left(\sum_m \epsilon_m b_m^\dagger b_m \right), \quad (6.127)$$

where $\{b_m\}$ are fermionic modes and Z the normalization constant. In Appendix A.3, we describe a general algorithm to obtain both the spectrum $\{\epsilon_m\}$ and the fermionic modes from the pairing function g_{nm} .

We compute the expected occupation per site for different values of ϵ (see Fig. (6.7)). We see that the boundaries do not affect the physics deep inside the bulk for large enough N_y . Given that in the limit $\epsilon \rightarrow 0^+$ the state corresponds to a trivial vacuum, the occupation is small in the OPE regime.

The periodicity in the x -direction is preserved in ρ_{cyl} , so that we can associate a momentum k to each mode. We can then write the single-body spectrum as a dispersion relation. In Fig. (6.8)(a), we see the single-body spectrum for different values of ϵ . It corresponds to a chiral free fermion. For values close to $\epsilon \rightarrow 0$, there is a gap in the dispersion that closes at around $\epsilon \sim 0.1$. This behavior is in agreement with the entanglement spectrum of $p + ip$ superconductors in the weak pairing phase [212].

From the entanglement spectrum, we computed the scaling of the entanglement entropy for different values of ϵ by changing the circumference of the cylinder (see Fig. (6.8)(b)). In all cases, the scaling follows an area law $S(N_x) \sim cN_x$, with non-universal slopes. According to the scaling, there is no topological correction in the entanglement entropy. Once again, this is in agreement with the behavior of $p + ip$ superconductors [212, 213].

Fourier Transform of 2D Pairing Function

If $\mu > 0$, we have $\xi_{\mathbf{k}} > 0$ for small momenta and

$$g_{\mathbf{k}} \sim -\frac{2\mu}{\hat{\Delta}(k_x + ik_y)}. \quad (6.128)$$

Let us try to fix the constants in the Fourier transform, at least in an asymptotic way. Taking $L = aN$ to be the length of the systems (so that the total number of sites is $N \times N$), we can define

$$k_x = \frac{2\pi(n - \frac{1}{2})}{aN}, \quad k_y = \frac{2\pi(m - \frac{1}{2})}{aN}, \quad (6.129)$$

where $n, m = -N/2, -N/2 + 1 \dots, N/2$. Using this, we have

$$\frac{1}{N^2} \sum_{k_x, k_y} \frac{\exp[i(k_x x + k_y y)]}{k_x + ik_y} \rightarrow \frac{a^2}{(2\pi)^2} \int_{-\pi/a}^{\pi/a} dk_x \int_{-\pi/a}^{\pi/a} dk_y \frac{\exp[i(k_x x + k_y y)]}{k_x + ik_y}. \quad (6.130)$$

Here we need to be careful. We will both take the limit $a \rightarrow 0^+$ and keep it explicitly in the prefactor. (This can be fixed by changing the normalization of the Fourier transform.) Note that for $y > 0$

$$\int_{-\infty}^{\infty} \frac{dk_y \exp[i(k_x x + k_y y)]}{2\pi i (k_y - ik_x)} = \Theta(k_x) \exp[ik_x (x + iy)], \quad (6.131)$$

where $\Theta(k)$ is the Heaviside function. Using this, we have

$$g(\mathbf{r}) \rightarrow -\frac{2a^2\mu}{2\pi i \hat{\Delta}} \frac{1}{x + iy}. \quad (6.132)$$

For a fixed number of fermions, this corresponds to the Moore-Read state for the FQHE. In this phase, the ground state of the $p + ip$ conductor is then a grand-canonical state of fermions with this pairing.

6.11. BCS Structure Beyond OPE: General Observations

We have seen that the OPE expansion of the CBs yields many-body wave functions with a BCS structure, and that this remains true in the exact case for translationally invariant 1D configurations. One may wonder if this result still holds true for the exact CBs using an arbitrary configuration (assuming, of course, radial ordering). In order to check this, let us consider $N = 4$ spins described by $|\Psi_{ee}\rangle$. This provides the smallest system size in which a BCS wave function is non-trivial and it allows us to understand the problem in more detail.

First, consider a general BCS wave function for $N = 4$. If we write it in full detail, we have

$$|\Psi_{\text{BCS}}\rangle \propto \left(1 + \sum_{n < m} g_{nm} c_n^\dagger c_m^\dagger + g_{1234} c_1^\dagger c_2^\dagger c_3^\dagger c_4^\dagger \right) |0\rangle_c, \quad (6.133)$$

where we define for convenience

$$g_{1234} = g_{12}g_{34} - g_{13}g_{24} + g_{14}g_{23}. \quad (6.134)$$

Note that this definition relates explicitly to Wick theorem for fermions. If $|\Psi_{ee}\rangle$ does indeed describe a BCS state, we expect its amplitudes to fulfill this constraint.

In order to check this, let us write the operator matrix (6.3) as (we omit the coordinates for simplicity)

$$A^{(n)} = \begin{pmatrix} V_{00} & c_n^\dagger V_{01} \\ c_n^\dagger V_{10} & V_{11} \end{pmatrix}. \quad (6.135)$$

Using this notation, it is easy to see that condition (6.134) will be fulfilled for $|\Psi_{ee}\rangle$ if and only if (see Fig. (6.9))

$$\begin{aligned} \langle V_{00} V_{00} V_{00} V_{00} \rangle \langle V_{01} V_{10} V_{01} V_{10} \rangle = & \\ \langle V_{01} V_{10} V_{00} V_{00} \rangle \langle V_{00} V_{00} V_{01} V_{10} \rangle & \\ - \langle V_{01} V_{11} V_{10} V_{00} \rangle \langle V_{00} V_{01} V_{11} V_{10} \rangle & \\ + \langle V_{01} V_{11} V_{11} V_{10} \rangle \langle V_{00} V_{01} V_{10} V_{00} \rangle. & \end{aligned} \quad (6.136)$$

We may call this condition a *generalized Wick theorem*. Note first that this equation is trivially satisfied if all V_{ij} are numbers. Also, if we use the OPE approximation (6.14), the equation reduces to the usual Wick theorem for free fermions. If we write equation (6.136) using the exact amplitudes in the pair-wise fusion basis, we get

$$\mathcal{F}_{0000} \mathcal{F}_{1111} = \mathcal{F}_{1100} \mathcal{F}_{0011} - \mathcal{F}_{1010} \mathcal{F}_{0101} + \mathcal{F}_{1001} \mathcal{F}_{0110}. \quad (6.137)$$

We have checked numerically the condition for random configurations using the exact CBs and they do indeed describe BCS wave functions. Unfortunately, we cannot provide a general proof even for such a small system size. One possible route is to expand the vertex operators using the full OPE expansion (6.10). In that case, condition (6.136) can be recast into a perturbative expression. Some subtleties regarding this approach are discussed in Appendix A.4.

6.12. Moving Beyond the Ising CFT

As we discussed in Section 4.5, CBs can be used to construct lattice wave function using both the intermediate fusion channels and the available representations of the symmetry

Figure 6.9: Graphical representation of equation (6.136).

groups. In this chapter, we have illustrated this formalism using only the fusion channels provided by the σ fields of the Ising model. It is natural to try to extend this construction to other minimal models. In general, we would still lack an internal symmetry group to codify the physical degrees of freedom of the lattice system, so we would need to rely solely on the fusion algebra.

Unfortunately, exact expressions for CBs containing an arbitrary number of fields are not available in the literature for other CFTs. Some particular cases can in principle be computed using bosonization methods, as well as coset constructions using WZW models [132]. Even though we cannot provide detailed results, we can still speculate about the nature of the resulting wave functions using the fusion rules of the primary operators. We will do this exercise for the tricritical Ising model and the 3-state Potts model.

Consider first the tricritical Ising model. Using the standard parametrization of the minimal models (see Section 5.4), this corresponds to $(p, q) = (5, 4)$ and $c_{5,4} = \frac{7}{10}$. It contains 6 primary fields, two of which can be interpreted as spin operators:

$$\sigma \leftrightarrow \phi_{2,2} \left(h_{2,2} = \frac{3}{8} \right), \quad \sigma' \leftrightarrow \phi_{2,1} \left(h_{2,1} = \frac{7}{16} \right). \quad (6.138)$$

There is a fermionic field ²

$$\psi'' \leftrightarrow \phi_{3,1} \left(h_{3,1} = \frac{3}{2} \right) \quad (6.139)$$

²The tricritical Ising model is one of the few physically relevant supersymmetric models [214]. Once this extra symmetry is present, it can be shown that field ψ'' can be related to the supersymmetric partner of the energy-momentum tensor T .

that closes a subalgebra with σ'

$$\sigma' \times \sigma' = \mathbb{1} + \psi'', \quad \psi'' \times \psi'' = \mathbb{1}, \quad \psi'' \times \sigma' = \sigma'. \quad (6.140)$$

This resembles the algebra we had in the Ising CFT, although with different conformal weights. We expect then that the CBs associated with σ' will also characterize a spin chain, but probably in a different phase. Finding a parent Hamiltonian in this case would not be canonical, given that there are several microscopic models that give rise to this fixed point [215].

The fusion rules for the other spin field σ involve all the primaries of the theory. In particular, there are 4 different fusion channels when two σ fields are fused. This suggests that the total Hilbert space of the corresponding lattice system is not a simple tensor product of spin- $\frac{1}{2}$ spaces. Given the fusion rules, it seems that it would be more natural to work with string Hilbert spaces [171] and possibly a face Hamiltonian.

The 3-state Potts model can be characterized by some of the operators contained in the minimal model corresponding to $(p, q) = (6, 5)$ and $c_{6,5} = \frac{4}{5}$. The representation theory of this model is subtle, so the partition function has to be constructed grouping the different operators according to certain criteria dictated by modular invariance [132]. This leads to an extension of the model that contains six operators

$$\mathbb{1} (h_{\mathbb{1}} = 0), \quad \epsilon \left(h_{\epsilon} = \frac{2}{5} \right), \quad \sigma_1, \sigma_2 \left(h_{\sigma} = \frac{1}{15} \right), \quad Z_1, Z_2 \left(h_Z = \frac{2}{3} \right). \quad (6.141)$$

The fusion rules of the spin operators show that they are not self-conjugate fields

$$\sigma_1 \times \sigma_1 = \sigma_2 + Z_2, \quad \sigma_2 \times \sigma_2 = \sigma_1 + Z_1, \quad \sigma_1 \times \sigma_2 = \mathbb{1} + \epsilon. \quad (6.142)$$

This can in principle be fixed by alternating both σ fields in the CBs. We also note that the Z fields implement a \mathbb{Z}_3 symmetry

$$Z_1 \times Z_1 = Z_2, \quad Z_2 \times Z_2 = Z_1, \quad Z_1 \times Z_2 = \mathbb{1}. \quad (6.143)$$

We can use this fact to construct a spin-1 wave function using correlators built from these fields

$$|\Psi_3\rangle = \sum_{\{s_n\}} \langle Z_{s_1} \cdots Z_{s_N} \rangle |s_1 \cdots s_N\rangle \quad (6.144)$$

where $s_n = 0, 1, 2$ and we define $Z_0 = \mathbb{1}$. These correlators can in principle be obtained using a coset construction starting from the $SU(3)_k$ WZW model [132]. Note that we would not be encoding the physical degrees of freedom in the fusion algebra, but rather in the choice of operators (in a fashion similar to Abelian theories such as the Haldane-Shastry model we discussed in Section 4.6). Another possible route would be to use parafermions to implement the \mathbb{Z}_3 symmetry we expect in a Potts model realization [216, 217, 218].

6.13. Conclusions and Discussion

We have presented a characterization of many-body states for lattice systems constructed from the CBs of the chiral Ising CFT. The basic feature of the construction is the use of pairs of σ fields to describe single localized spins. Writing these CBs using local vertex

operators enables us to relate this formalism to usual matrix product states. This rewriting makes explicit the relation between the ancillary CFT degrees of freedom and the lattice fermionic modes. The states we obtain inherit some algebraic properties from the CFT, such as the well-known KW duality and a representation of the TLJ algebra.

We have provided evidence that states constructed from CBs using only σ fields can be written as BCS states. A partial proof of this fact can be obtained whenever an OPE approximation is valid. In this case, an explicit BCS form can be obtained using the local vertex operator formalism. In the case of translationally invariant 1D configurations, we can go beyond the approximation and write a full non-perturbative proof. This also allows us to obtain a whole family of quasi-local parent Hamiltonians that can be written as quadratic fermionic forms. They are closely related to the critical ITF Hamiltonian.

We presented a proof that the ground state of the critical ITF spin chain can be obtained exactly from the Ising CBs. This is a remarkable result that connects the physics described by quantum field theories in the infrared limit to the physics of small, lattice models. Given that information is lost during the RG flow, it is non-trivial that we can recover exact features of the microscopic model. We hope that this result can be extended to other CFTs, in particular to the minimal models related to known spin systems. Given that the first excited state of the even-parity sector of this Hamiltonian can also be obtained using CBs with fermions in the asymptotic CFT states, we expect that the connection should extend to part of the full energy spectrum.

We used an approximation based on the OPE expansion to understand the inner structure of the CBs. This allowed us to study large 2D spin configurations. By placing the degrees of freedom on finite cylinders, we have related the states obtained from the CBs in the OPE regime to the weak pairing phase of the $p + ip$ superconductor. This has been done via the entanglement spectrum obtained from the reduced density matrix of half of the cylinder.

Further work is needed to deepen the connection between CBs and the ground states of finite systems. In the case of the Ising CFT, this would mean a general proof that $|\Psi_{ee}\rangle$ describes a BCS wave function regardless of the coordinate configuration. A deeper understanding of the formalism may produce other physically relevant states, such as the ground state of the 1D odd parity sector of the ITF Hamiltonian, or vortices in 2D superconductors. In addition, generalizations to other rational CFTs, such as the tricritical Ising model, the 3-state Potts model or the \mathbb{Z}_n model [130, 131, 132], are worth studying. Due to the algebraic constraints, we expect those constructions to be related to anyon chains [219, 220], statistical face models [171] or parafermions [216, 221].

Part III

Appendices and General Conclusions

APPENDIX A

Appendices

A.1. A Useful Relation

We want to prove

$$\prod_{j>i}^N \sin \left[\frac{\pi}{N} \left(j - i + \frac{\alpha}{4} (s_j - s_i) \right) \right] = \prod_{j>i}^N \sin \left[\frac{\pi}{N} \left(j - i - \frac{\alpha}{4} (s_j - s_i) \right) \right]. \quad (\text{A.1})$$

Consider the complex function

$$f(z) = \prod_{j>i}^N \sin \left[\frac{\pi}{N} (j - i) + \frac{z}{2} (s_j - s_i) \right], \quad (\text{A.2})$$

where $s_i = \pm 1$, for all $i = 1, \dots, N$. Given that $s_j - s_i = 0, \pm 2$, note that $f(z + 2\pi) = f(z)$. Also, being the product of analytic functions, $f(z)$ is also analytic on the whole complex plane.

We would like to prove that $f(z)$ is an even function. This holds trivially if $s_j = 1$ for all $j = 1, \dots, N$. For the general case, let us define the sets

$$A_{\pm} = \{j \mid s_j = \pm 1\}, \quad (\text{A.3})$$

so that $A_+ \cup A_- = \{1, \dots, N\}$. Using this notation, we can write the ratio

$$\frac{f(z)}{f(-z)} = \prod_{j \in A_+} \left[\prod_{\substack{i \in A_- \\ i < j}} \frac{\sin \left(\frac{\pi}{N} (N + i - j) - z \right)}{\sin \left(\frac{\pi}{N} (j - i) - z \right)} \prod_{\substack{i \in A_- \\ i > j}} \frac{\sin \left(\frac{\pi}{N} (i - j) - z \right)}{\sin \left(\frac{\pi}{N} (N + j - i) - z \right)} \right]. \quad (\text{A.4})$$

Let us now define the (non-symmetric) functions

$$d_R(i, j) = \begin{cases} i - j & i \geq j, \\ N + i - j & i < j, \end{cases} \quad (\text{A.5})$$

$$d_L(i, j) = \begin{cases} N + j - i & i > j, \\ j - i & i \leq j. \end{cases} \quad (\text{A.6})$$

These functions can be interpreted geometrically. Assume the integers $\{1, \dots, N\}$ are evenly distributed on a circle in a clockwise ascending order. Then, $d_R(i, j)$ (respectively $d_L(i, j)$) is the distance from j to i going only in the clockwise (respectively, anticlockwise) direction. (Note that $d_R(i, j) = d_L(j, i)$.)

We can then write (A.4) as

$$\frac{f(z)}{f(-z)} = \prod_{j \in A_+} \prod_{i \in A_-} \frac{\sin\left(\frac{\pi}{N} d_R(i, j) - z\right)}{\sin\left(\frac{\pi}{N} d_L(i, j) - z\right)}. \quad (\text{A.7})$$

In this formulation, $f(z)$ will be an even function if the lists of integers

$$\begin{aligned} R &= (d_R(i, j) \mid i \in A_-, j \in A_+), \\ L &= (d_L(i, j) \mid i \in A_-, j \in A_+) \end{aligned} \quad (\text{A.8})$$

contain the same elements with the same multiplicities. In other words, we must prove that the set of all the distances from every element of A_+ to every element in A_- counting clockwise is the same as the list counting anticlockwise.

In order to prove this statement, note that if $d_R(i, j) = r$, then $d_L(i, j) = N - r$. This implies that R and L will be equal if we can pair the elements within the same list as $(r, N - r)$. (If N is even, this statement is true except if $r = N/2$. In that case, the element is trivially in both lists and does not need pairing.) We will then focus on pairing the elements in list R .

Consider the matrix defined by

$$[D(P, Q)]_{i,j} = d_R(p_i, q_j), \quad (\text{A.9})$$

where $P = \{p_i\}$ and $Q = \{q_i\}$ are two subsets of $\{1, \dots, N\}$. We will say $D(P, Q)$ is a *balanced* matrix if there are the same number of matrix elements that take the value r (with $r \neq 0$) and $N - r$. (Once again, if N is even, we also need $r \neq N/2$.)

It is easy to see that $D(A_+, A_+ \cup A_-)$ is a balanced matrix because we can always pair $d_R(i, j)$ with $d_R(i, N - j)$. Likewise, $D(A_+, A_+)$ is also balanced because $d_R(i, j)$ pairs with $d_R(j, i)$. We have then that $D(A_+, A_-)$ is a submatrix of $D(A_+, A_+ \cup A_-)$ than can be obtained by removing a balanced submatrix. This implies that $D(A_+, A_-)$ is balanced.

Using this result, we see that for every $i \in A_+, j \in A_-$ such that $d_R(i, j) = r$, there exist $i' \in A_+, j' \in A_-$ such that $d_R(i', j') = N - r$, or equivalently, $d_L(i', j') = r$. So both R and L are equal and

$$f(z) = f(-z), \quad (\text{A.10})$$

which is what we wanted to prove.

A.2. Finding a Parent Hamiltonian

Consider a family of Hamiltonian terms

$$H_\alpha = \sum_{i_1, \dots, i_k} h_{i_1, \dots, i_k}^{(\alpha)} \quad (\text{A.11})$$

which can be either local or non-local. For convenience, we set $H_0 = \mathbb{1}$. Given a wavefunction $|\Psi\rangle$, we would like to find a linear superposition of these operators that will have $|\Psi\rangle$ as an eigenstate. In other words, we want to find coefficients J_α such that

$$\left(\sum_{\alpha} J_\alpha H_\alpha \right) |\Psi\rangle = 0. \quad (\text{A.12})$$

In order to solve this, consider the matrix

$$(M)_{\alpha\beta} = \langle \Psi | H_\alpha H_\beta | \Psi \rangle. \quad (\text{A.13})$$

It is easy to see that condition (A.12) will be satisfied for a certain set of coefficients $\{J_\alpha\}$ if and only if M has a non-trivial kernel. (Note that M is positive-definite.) The coefficients of the vectors that span this kernel will satisfy condition (A.12).

A.3. Bogoliubov Transformation from a BCS Pairing Matrix

Let us consider a fermionic system with on-site creation operators $c_i^\dagger, i \in \{1, \dots, N\}$ and annihilation operators c_i . We will adopt the following notation:

$$\{C_l\}_{l=1}^{2N} = \{c_1, \dots, c_N, c_1^\dagger, \dots, c_N^\dagger\}. \quad (\text{A.14})$$

Thus, creation and annihilation operators are bundled together. Let us consider a different set of creation and annihilation operators,

$$\{B_l\}_{l=1}^{2N} = \{b_1, \dots, b_N, b_1^\dagger, \dots, b_N^\dagger\} \quad (\text{A.15})$$

with $B_l = \sum_p M_{lp} C_p$. The linear transformation will be a Bogoliubov transformation if the b^\dagger and b are bona-fide creation and annihilation operators, with the expected anticommutation and adjoint relations. The first condition is that M is unitary. If that is the case, the Bogoliubov matrix M can be naturally split:

$$\begin{pmatrix} b \\ b^\dagger \end{pmatrix} = \begin{pmatrix} D & E \\ E^* & D^* \end{pmatrix} \begin{pmatrix} c \\ c^\dagger \end{pmatrix}, \quad (\text{A.16})$$

where D and E are $N \times N$ complex matrices, D^* and E^* are their complex conjugates (not Hermitian adjoints!) and they must fulfill

$$DD^\dagger + EE^\dagger = \mathbb{1}, \quad DE^T + ED^T = 0 \quad (\text{A.17})$$

so that matrix M will be unitary. Notice that A^\dagger is the Hermitian adjoint, and A^T is merely the transpose.

In our case, the BCS state is defined via the pairing function g_{ij} , which is anti-symmetric, $g_{ij} = -g_{ji}$,

$$|\Psi\rangle = \exp\left(\sum_{ij} g_{ij} c_i^\dagger c_j^\dagger\right) |0\rangle_c \equiv \exp(P) |0\rangle_c \quad (\text{A.18})$$

where the last relation defines the pairing operator P . This state is the vacuum of a certain Bogoliubov set of operators, $\{B_l\}_{l=1}^{2N} = \{b_1^\dagger, \dots, b_N^\dagger, b_1, \dots, b_N\}$, which means that

$$b_k |\Psi\rangle = 0, \quad k \in \{1, \dots, N\}. \quad (\text{A.19})$$

Let us impose that condition in order to find the Bogoliubov transformation M . By definition,

$$b_k = \sum_i D_{ki} c_i + E_{ki} c_i^\dagger, \quad (\text{A.20})$$

so our condition becomes

$$0 = b_k \exp(P) |0\rangle = (\exp(P)b_k + [b_k, \exp(P)]) |0\rangle. \quad (\text{A.21})$$

Remember that b_k can be expanded as a linear combination of c_i and c_i^\dagger . Using

$$[c_i, f(\{c_j, c_j^\dagger\})] = \frac{\partial f}{\partial c_i^\dagger}, \quad (\text{A.22})$$

we find that

$$[c_i, \exp(P)] = \exp(P) \left(\sum_j g_{ij} c_j^\dagger \right). \quad (\text{A.23})$$

Of course, c_i^\dagger commutes with $\exp(P)$. Thus, the annihilation condition becomes

$$\exp(P) \left\{ \sum_i D_{ki} c_i + \sum_{ij} D_{ki} g_{ij} c_j^\dagger + \sum_i E_{ki} c_i^\dagger \right\} |0\rangle = 0. \quad (\text{A.24})$$

which implies the following relation between D , E and g :

$$\sum_i D_{ki} g_{ij} + E_{kj} = 0. \quad (\text{A.25})$$

Thus, in order to find the Bogoliubov transformation given the pairing matrix g , we have to solve the following matrix equations:

$$\begin{aligned} Dg + E &= 0, \\ DD^\dagger + EE^\dagger &= \mathbb{1}, \\ DE^T + ED^T &= 0, \end{aligned} \quad (\text{A.26})$$

From the first equation we get $E = -Dg$, which when inserted into the third equation yields $D(g^T + g)D = 0$. But this relation is trivial due to the antisymmetry of g . Then, the only non-trivial equation becomes

$$D (\mathbb{1} + gg^\dagger) D^\dagger = \mathbb{1}. \quad (\text{A.27})$$

This equation can be easily solved in the eigenbasis of $\mathbb{1} + gg^\dagger$, which is self-adjoint and positive-definite.

A.4. Towards a Generalized Wick Theorem

The OPE of two σ fields is given by (6.10). One can easily identify the fields $\alpha(z)$ as the ones appearing in the fusion channel of the CVOs V_{00} and $V_{\chi\chi}$, while the fields $\beta(z)$ are the ones appearing in the CVOs $V_{0\chi}$ and $V_{\chi 0}$. This implies that (6.136) holds provided the fields $\alpha(z_i)$ and $\beta(z_i)$ satisfy the relation

$$\begin{aligned} \langle \alpha_1 \alpha_2 \alpha_3 \alpha_4 \rangle \langle \beta_1 \beta_2 \beta_3 \beta_4 \rangle &= \langle \beta_1 \beta_2 \alpha_3 \alpha_4 \rangle \langle \alpha_1 \alpha_2 \beta_3 \beta_4 \rangle \\ &\quad - \langle \beta_1 \alpha_2 \beta_3 \alpha_4 \rangle \langle \alpha_1 \beta_2 \alpha_3 \beta_4 \rangle \\ &\quad + \langle \beta_1 \alpha_2 \alpha_3 \beta_4 \rangle \langle \alpha_1 \beta_2 \beta_3 \alpha_4 \rangle, \end{aligned} \quad (\text{A.28})$$

where $\alpha_i = \alpha(z_i)$ and $\beta_i = \beta(z_i)$. This equation coincides with the standard Wick theorem if $\alpha(z) = \mathbb{1}$ and $\beta(z) = \chi(z)$. Let us provide other examples.

Suppose $\alpha_1 = T(z_1)$ with $T(z)$ the stress tensor [132], $\alpha_2 = \alpha_3 = \alpha_4 = \mathbb{1}$ and $\beta_i = \chi(z_i)$. Using this, (A.28) becomes

$$\langle T_1 \rangle \langle \chi_1 \chi_2 \chi_3 \chi_4 \rangle = \langle \chi_1 \chi_2 \rangle \langle T_1 \chi_3 \chi_4 \rangle - \langle \chi_1 \chi_3 \rangle \langle T_1 \chi_2 \chi_4 \rangle + \langle \chi_1 \chi_4 \rangle \langle T_1 \chi_2 \chi_3 \rangle. \quad (\text{A.29})$$

The left hand side of the equation vanishes because on the plane $\langle T(z) \rangle = 0$. To find $\langle T \chi \chi \rangle$, we use Ward identities [154] to conclude

$$\langle T(z_1) \chi(z_2) \chi(z_3) \rangle = \frac{z_{23}}{2z_{12}^2 z_{13}^2}. \quad (\text{A.30})$$

Plugging these equations into (A.28) yields

$$\frac{1}{z_{12}} \frac{z_{34}}{2z_{13}^2 z_{14}^2} - \frac{1}{z_{13}} \frac{z_{24}}{2z_{12}^2 z_{14}^2} + \frac{1}{z_{14}} \frac{z_{23}}{2z_{12}^2 z_{13}^2} = \frac{z_{12}z_{34} - z_{13}z_{24} + z_{14}z_{23}}{2(z_{12}z_{13}z_{14})^2} = 0, \quad (\text{A.31})$$

so that the condition is satisfied.

As a more elaborate example, choose $\alpha_i = \mathbb{1}$, $\beta_1 = L_{-n}\chi(z_1)$ with L_{-n} the mode operator of the stress tensor that belongs to the representation of the Virasoro algebra [132], and $\beta_i(z) = \chi(z_i)$ ($i = 2, 3, 4$). Equation (A.28) becomes

$$\begin{aligned} \langle (L_{-n}\chi_1) \chi_2 \chi_3 \chi_4 \rangle &= \langle (L_{-n}\chi_1) \chi_2 \rangle \langle \chi_3 \chi_4 \rangle - \langle (L_{-n}\chi_1) \chi_3 \rangle \langle \chi_2 \chi_4 \rangle \\ &\quad + \langle (L_{-n}\chi_1) \chi_4 \rangle \langle \chi_2 \chi_3 \rangle, \end{aligned} \quad (\text{A.32})$$

where

$$L_{-n}\chi_1(z_1) = \oint_{z_1} d\zeta (\zeta - z_1)^{-n+1} T(\zeta) \chi(z_1), \quad n \geq 1 \quad (\text{A.33})$$

(We have suppressed the denominator $2\pi i$ in the integral.) Equation (A.28) can be written as

$$\Omega_n \equiv \oint_{z_1} d\zeta (\zeta - z_1)^{-n+1} f(\zeta, \{z_i\}) = 0, \quad (\text{A.34})$$

with

$$\begin{aligned} f(\zeta, \{z_i\}) &= \langle T(\xi) \chi_1 \chi_2 \chi_3 \chi_4 \rangle - \langle T(\xi) \chi_1 \chi_2 \rangle \langle \chi_3 \chi_4 \rangle \\ &\quad + \langle T(\xi) \chi_1 \chi_3 \rangle \langle \chi_2 \chi_4 \rangle - \langle T(\xi) \chi_1 \chi_4 \rangle \langle \chi_2 \chi_3 \rangle. \end{aligned} \quad (\text{A.35})$$

We now use the familiar identity for general fields ϕ_i with conformal weights h_i [132]

$$\left\langle T(\zeta) \prod_i \phi_i(z_i) \right\rangle = \left[\sum_i \left(\frac{h_i}{(\zeta - z_i)^2} + \frac{1}{\zeta - z_i} \frac{\partial}{\partial z_i} \right) \right] \left\langle \prod_i \phi_i(z_i) \right\rangle, \quad (\text{A.36})$$

to find

$$f(\zeta, \{z_i\}) = \left(\frac{\zeta - z_1}{(\zeta - z_2)(\zeta - z_3)(\zeta - z_4)} \right)^2 \frac{z_{23}z_{24}z_{34}}{2z_{12}z_{13}z_{14}}. \quad (\text{A.37})$$

Hence, equation (A.34) becomes

$$\begin{aligned} \Omega_n &= \oint_{z_1} d\zeta (\zeta - z_1)^{-n+1} \left(\frac{\zeta - z_1}{(\zeta - z_2)(\zeta - z_3)(\zeta - z_4)} \right)^2 \\ &= \oint_{z_1} d\zeta \frac{(\zeta - z_1)^{-n+3}}{[(\zeta - z_2)(\zeta - z_3)(\zeta - z_4)]^2} = 0. \quad (n \geq 1) \end{aligned} \quad (\text{A.38})$$

This equation holds for $n = 1, 2, 3$ but for $n = 4$ one has

$$\Omega_4 = \oint_{z_1} d\zeta \frac{(\zeta - z_1)^{-1}}{[(\zeta - z_2)(\zeta - z_3)(\zeta - z_4)]^2} = \frac{1}{(z_{12}z_{13}z_{14})^2} \quad (\text{A.39})$$

It seems that $\Omega_n \neq 0$ for $n \geq 4$. Hence in these cases (A.28) does not hold.

The characters of the Verma modules \mathcal{V}_1 and \mathcal{V}_χ are given by

$$\begin{aligned} \chi_0(q) &= \text{Tr}_{\mathcal{V}_1} q^{L_0 - c/24} \\ &= q^{-\frac{1}{48}} (1 + q^2 + q^3 + 2q^4 + 2q^5 + 3q^6 + \dots), \end{aligned} \quad (\text{A.40})$$

$$\begin{aligned} \chi_1(q) &= \text{Tr}_{\mathcal{V}_\chi} q^{L_0 - c/24} \\ &= q^{-\frac{1}{48} - \frac{1}{2}} (1 + q + q^2 + q^3 + 2q^4 + 2q^5 + \dots). \end{aligned} \quad (\text{A.41})$$

Notice that at level $n = 4$ there are two states in the Majorana sector. As a matter of fact, the descendants we had considered above correspond to the derivatives of the field $\chi(z)$,

$$(L_{-n}\chi)(0) = \frac{n+1}{2}\chi_{-n-\frac{1}{2}} \quad (\text{A.42})$$

The conclusion is that equation (6.136) reduces to equation (A.28) only if the fields α and β that appear in the OPE (6.10) are unique at a given level. Otherwise one has to consider all the fields appearing at the same level.

Summary and Conclusions

The first part of this thesis studied the consequences of a tachyonic quench in a free bosonic system. This type of quenching protocol had not been considered in the literature to the best of our knowledge. It provides an exotic regime where the driving Hamiltonian is inherently unstable, so the long-time dynamics cannot equilibrate to a known statistical ensemble, such as the generalized Gibbs ensembles proposed for integrable systems.

Our analysis was based on the harmonic chain, a model that can be solved exactly via standard techniques. We characterized all the relevant correlators of the theory and showed that the resulting causal structure is very similar to one obtained after critical quenches. We also showed that the instabilities lead to a linear growth of the entanglement entropy for all subregions of the chain. We considered the mutual information between disjoint regions to show that the growing correlations come from a collective phenomenon that can be understood from the exponential occupation of the low-frequency modes. This produces strong, non-local correlations once the instabilities start dominating the dynamics.

Part of the motivation for this work came from the realization that coupled bosonic theories can produce tachyonic sectors. We expect that the ideas described here can be implemented in physical systems where an effective tachyonic regime is available, even if it is only valid during a limited period of time. This can be done using either fine-tuned microscopic interactions in semiclassical spin systems or using moderate quartic interactions that constraint the long-time instabilities.

The second part of this thesis presented a general construction for obtaining many-body wave functions from the conformal blocks (CBs) of rational conformal field theories (CFTs). We argued that the physical degrees of freedom can be encoded both in representations obtained from the local symmetry groups and the intermediate fusion channels obtained from the primary fields of the theory.

We illustrated how to use these internal fusion channels by studying the CBs obtained from the spin field operator σ in the Ising CFT. The resulting states describe spin- $\frac{1}{2}$ systems that inherit some of the properties of the original theory, such as the Kramers-Wannier duality. We presented analytical and numerical evidence that these wave functions correspond to BCS states. In particular, 1D configurations give rise to states related to the Ising transverse field (ITF) Hamiltonian and 2D configurations to $p + ip$ superconductors in the weak-pairing phase.

The most remarkable result that we present in this part is an analytical proof that the ground state of the critical ITF spin chain can be obtained exactly from the CBs of the Ising CFT. This suggests that there is a deep connection between the physics described by certain quantum field theories in the infrared limit and the physics of small, integrable lattice models. Even though the CFT is describing a fixed point that has little information about the microscopic physics, we were able to obtain a complete description of the cor-

responding finite spin chain. We expect that this result can be extended to other CFTs, in particular those related to known statistical models such as the tricritical Ising model and the 3-state Potts model.

Resumen y Conclusiones

La primera parte de esta tesis estudia las consecuencias de un “quench” taquiónico en un sistema bosónico libre. Este tipo de protocolo no se había estudiado antes en la literatura y proporciona un régimen exótico donde el hamiltoniano que dicta la dinámica es inherentemente inestable, de forma tal que el sistema no equilibra después de tiempos suficientemente largos. En particular, no llega a un ensamble estadístico estable, como los ensambles de Gibbs generalizados propuestos para sistemas integrables genéricos.

Nuestro análisis se basa en la cadena armónica, un modelo que puede estudiarse de forma exacta a partir de técnicas estándar. Caracterizamos todos los correladores relevantes para la teoría y mostramos que la estructura causal es muy parecida a la obtenida después de “quenches” críticos (sin masa). Mostramos también que las inestabilidades llevan a un crecimiento lineal en la entropía de entrelazamiento para todas las subregiones del sistema. Consideramos también la información mutua entre regiones disconexas para mostrar que el crecimiento de las correlaciones viene de un fenómeno colectivo que puede interpretarse a partir de la ocupación exponencial de los modos de baja frecuencia. Esto implica fuertes correlaciones causales pero no locales que surgen después de que la dinámica esté dictada por las inestabilidades.

Parte de la motivación para este trabajo viene de los sectores taquiónicos que pueden obtenerse a partir de teorías libres de bosones acoplados. Esperamos que las ideas descritas aquí puedan implementarse en otros sistemas físicos que tengan regímenes taquiónicos efectivos, incluso si estos solo están disponibles durante un periodo de tiempo limitado. En particular, este comportamiento se puede obtener usando interacciones microscópicas ajustadas en sistemas de espines semiclásicos o usando interacciones cuárticas débiles para restringir las inestabilidades después de tiempos suficientemente largos.

La segunda parte de esta tesis presenta una construcción general para obtener funciones de onda colectivas a partir de los bloques conformes (BC) de las teorías de campos conformes (TCC) racionales. Argumentamos que los grados de libertad se pueden cifrar tanto en las representaciones obtenidas a partir de los grupos de simetría locales como en los canales de fusión intermedios obtenidos a partir de los campos primarios de la teoría.

Ilustramos el uso de los canales de fusión estudiando los BC obtenidos a partir del operador de campo de espín σ en la TCC del modelo de Ising. Los estados resultantes describen sistemas de espín $\frac{1}{2}$ que heredan algunas de las propiedades de la teoría original, como la dualidad de Kramers-Wannier. Presentamos evidencia analítica y numérica de que estas funciones de onda corresponden a estados BCS. En particular, las configuraciones 1D dan paso a estados relacionados con la cadena de Ising con campo transversal (ICT) y las configuraciones 2D a los superconductores $p + ip$ en la fase de apareamiento débil.

El resultado más notable que presentamos es una prueba analítica de que el estado fundamental de la cadena ICT crítica puede obtenerse de forma exacta a partir de los BC del modelo de Ising. Esto sugiere una conexión profunda entre la física descrita por las teorías

de campos en el límite infrarrojo y la física de los sistemas integrables en el retículo con pocos grados de libertad. A pesar de que la TCC está describiendo un punto fijo del grupo de renormalización y tiene poca información sobre la física microscópica, fuimos capaces de obtener una descripción completa de la cadena de espines correspondiente. Esperamos que este resultado se pueda extender a otras TCC, en particular aquellas relacionadas a modelos estadísticos conocidos como el modelo de Ising tricrítico y el modelos de Potts de tres estados.

Bibliography

- [1] S. Montes, G. Sierra and J. Rodríguez-Laguna, *Tachyonic quench in a free bosonic field theory*, Journal of Statistical Mechanics: Theory and Experiment **2018** (2018) 023102.
- [2] S. Montes, J. Rodríguez-Laguna, H.-H. Tu and G. Sierra, *Many-body lattice wave functions from conformal blocks*, Physical Review B **95** (2017) 085146.
- [3] S. Montes, J. Rodríguez-Laguna and G. Sierra, *BCS wave function, matrix product states, and the Ising conformal field theory*, Physical Review B **96** (2017) 195152.
- [4] J. M. Deutsch, *Quantum statistical mechanics in a closed system*, Physical Review A **43** (1991) 2046–2049.
- [5] L. Boltzmann, *Weitere Studien über das Wärmegleichgewicht unter Gasmolekülen*, in *Kinetische Theorie II: Irreversible Prozesse Einführung und Originaltexte*, pp. 115–225. Vieweg+Teubner Verlag, Wiesbaden, 1970.
- [6] J. Uffink, *Boltzmann’s Work in Statistical Physics*, in *The Stanford Encyclopedia of Philosophy* (E. N. Zalta, ed.). Metaphysics Research Lab, Stanford University, 2017 ed., 2017.
- [7] J. v. Neumann, *Beweis des Ergodensatzes und des H-Theorems in der neuen Mechanik*, Zeitschrift für Physik **57** (1929) 30–70.
- [8] J. Gemmer, M. Michel and G. Mahler, *Quantum Thermodynamics - Emergence of Thermodynamic Behavior Within Composite Quantum Systems*. Lecture Notes in Physics. Springer-Verlag Berlin Heidelberg, Berlin, 2009.
- [9] A. Polkovnikov, K. Sengupta, A. Silva and M. Vengalattore, *Colloquium: Nonequilibrium dynamics of closed interacting quantum systems*, Reviews of Modern Physics **83** (2011) 863–883.
- [10] J. Eisert, M. Friesdorf and C. Gogolin, *Quantum many-body systems out of equilibrium*, Nature Physics **11** (2015) 124–130.
- [11] C. Gogolin and J. Eisert, *Equilibration, thermalisation, and the emergence of statistical mechanics in closed quantum systems*, Reports on Progress in Physics **79** (2016) 056001.
- [12] J. Goold, M. Huber, A. Riera, L. d. Rio and P. Skrzypczyk, *The role of quantum information in thermodynamics—a topical review*, Journal of Physics A: Mathematical and Theoretical **49** (2016) 143001.

- [13] F. Dalfovo, S. Giorgini, L. P. Pitaevskii and S. Stringari, *Theory of Bose-Einstein condensation in trapped gases*, *Reviews of Modern Physics* **71** (1999) 463–512.
- [14] I. Bloch, J. Dalibard and W. Zwerger, *Many-body physics with ultracold gases*, *Reviews of Modern Physics* **80** (2008) 885–964.
- [15] I. Bloch, *Ultracold quantum gases in optical lattices*, *Nature Physics* **1** (2005) 23–30.
- [16] M. Greiner, O. Mandel, T. Esslinger, T. W. Hänsch and I. Bloch, *Quantum phase transition from a superfluid to a Mott insulator in a gas of ultracold atoms*, *Nature* **415** (2002) 39–44.
- [17] D. Porras and J. I. Cirac, *Effective Quantum Spin Systems with Trapped Ions*, *Physical Review Letters* **92** (2004) 207901.
- [18] A. K. Tuchman, C. Orzel, A. Polkovnikov and M. A. Kasevich, *Nonequilibrium coherence dynamics of a soft boson lattice*, *Physical Review A* **74** (2006) 051601.
- [19] A. Friedenauer, H. Schmitz, J. T. Glueckert, D. Porras and T. Schaetz, *Simulating a quantum magnet with trapped ions*, *Nature Physics* **4** (2008) 757–761.
- [20] M. Aidelsburger, M. Atala, S. Nascimbène, S. Trotzky, Y.-A. Chen and I. Bloch, *Experimental Realization of Strong Effective Magnetic Fields in an Optical Lattice*, *Physical Review Letters* **107** (2011) 255301.
- [21] J. W. Britton, B. C. Sawyer, A. C. Keith, C.-C. J. Wang, J. K. Freericks, H. Uys, M. J. Biercuk and J. J. Bollinger, *Engineered two-dimensional Ising interactions in a trapped-ion quantum simulator with hundreds of spins*, *Nature* **484** (2012) 489–492.
- [22] U. Bissbort, D. Cocks, A. Negretti, Z. Idziaszek, T. Calarco, F. Schmidt-Kaler, W. Hofstetter and R. Gerritsma, *Emulating Solid-State Physics with a Hybrid System of Ultracold Ions and Atoms*, *Physical Review Letters* **111** (2013) 080501.
- [23] M. Greiner, O. Mandel, T. W. Hänsch and I. Bloch, *Collapse and revival of the matter wave field of a Bose–Einstein condensate*, *Nature* **419** (2002) 51–54.
- [24] T. Kinoshita, T. Wenger and D. S. Weiss, *A quantum Newton’s cradle*, *Nature* **440** (2006) 900–903.
- [25] S. Hofferberth, I. Lesanovsky, B. Fischer, T. Schumm and J. Schmiedmayer, *Non-equilibrium coherence dynamics in one-dimensional Bose gases*, *Nature* **449** (2007) 324–327.
- [26] M. Cheneau, P. Barmettler, D. Poletti, M. Endres, P. Schauss, T. Fukuhara, C. Gross, I. Bloch, C. Kollath and S. Kuhr, *Light-cone-like spreading of correlations in a quantum many-body system*, *Nature* **481** (2012) 484–487.
- [27] T. Langen, R. Geiger, M. Kuhnert, B. Rauer and J. Schmiedmayer, *Local emergence of thermal correlations in an isolated quantum many-body system*, *Nature Physics* **9** (2013) 640–643.

- [28] P. Jurcevic, B. P. Lanyon, P. Hauke, C. Hempel, P. Zoller, R. Blatt and C. F. Roos, *Quasiparticle engineering and entanglement propagation in a quantum many-body system*, *Nature* **511** (2014) 202.
- [29] T. Langen, R. Geiger and J. Schmiedmayer, *Ultracold Atoms Out of Equilibrium*, *Annual Review of Condensed Matter Physics* **6** (2015) 201–217.
- [30] J. Bell, *Speakable and Unsayable in Quantum Mechanics: Collected Papers on Quantum Philosophy*. Collected papers on quantum philosophy. Cambridge University Press, 2004.
- [31] W. Myrvold, *Philosophical Issues in Quantum Theory*, in *The Stanford Encyclopedia of Philosophy* (E. N. Zalta, ed.). Metaphysics Research Lab, Stanford University, 2017 ed., 2017.
- [32] A. Aspect, P. Grangier and G. Roger, *Experimental Realization of Einstein-Podolsky-Rosen-Bohm Gedankenexperiment: A New Violation of Bell's Inequalities*, *Physical Review Letters* **49** (1982) 91–94.
- [33] A. Aspect, J. Dalibard and G. Roger, *Experimental Test of Bell's Inequalities Using Time-Varying Analyzers*, *Physical Review Letters* **49** (1982) 1804–1807.
- [34] V. Vedral, *Introduction to Quantum Information Science*. Oxford Graduate Texts. OUP Oxford, 2006.
- [35] R. Horodecki, P. Horodecki, M. Horodecki and K. Horodecki, *Quantum entanglement*, *Reviews of Modern Physics* **81** (2009) 865–942.
- [36] A. E. B. Nielsen, J. I. Cirac and G. Sierra, *Quantum spin Hamiltonians for the $SU(2)_k$ WZW model*, *Journal of Statistical Mechanics: Theory and Experiment* **2011** (2011) P11014.
- [37] M. Ericsson and S. Montangero, eds., *Quantum Information and Many Body Quantum Systems*, vol. 8 of *Publications of the Scuola Normale Superiore*. 2008.
- [38] J. Eisert and M. B. Plenio, *Focus on Quantum Information and Many-Body Theory*, *New Journal of Physics* **12** (2010) 025001.
- [39] R. Augusiak, F. M. Cucchietti and M. Lewenstein, *Many-Body Physics from a Quantum Information Perspective*, in *Modern Theories of Many-Particle Systems in Condensed Matter Physics* (D. C. Cabra, A. Honecker and P. Pujol, eds.), pp. 245–294. Springer Berlin Heidelberg, Berlin, Heidelberg, 2012.
- [40] G. D. Chiara, S. Montangero, P. Calabrese and R. Fazio, *Entanglement entropy dynamics of Heisenberg chains*, *Journal of Statistical Mechanics: Theory and Experiment* **2006** (2006) P03001.
- [41] J. Eisert and T. J. Osborne, *General Entanglement Scaling Laws from Time Evolution*, *Physical Review Letters* **97** (2006) 150404.
- [42] P. Calabrese and J. Cardy, *Entanglement and correlation functions following a local quench: a conformal field theory approach*, *Journal of Statistical Mechanics: Theory and Experiment* **2007** (2007) P10004.

- [43] A. M. Läuchli and C. Kollath, *Spreading of correlations and entanglement after a quench in the one-dimensional Bose–Hubbard model*, *Journal of Statistical Mechanics: Theory and Experiment* **2008** (2008) P05018.
- [44] K. Van Acoleyen, M. Mariën and F. Verstraete, *Entanglement Rates and Area Laws*, *Physical Review Letters* **111** (2013) 170501.
- [45] P. Calabrese and J. Cardy, *Time Dependence of Correlation Functions Following a Quantum Quench*, *Physical Review Letters* **96** (2006) 136801.
- [46] P. Calabrese and J. Cardy, *Quantum quenches in extended systems*, *Journal of Statistical Mechanics: Theory and Experiment* **2007** (2007) P06008.
- [47] M. Rigol, *Quantum Quenches in the Thermodynamic Limit*, *Physical Review Letters* **112** (2014) 170601.
- [48] K. Sengupta, S. Powell and S. Sachdev, *Quench dynamics across quantum critical points*, *Physical Review A* **69** (2004) 053616.
- [49] E. Barouch, B. M. McCoy and M. Dresden, *Statistical Mechanics of the XY Model. I*, *Physical Review A* **2** (1970) 1075–1092.
- [50] E. Barouch and B. M. McCoy, *Statistical Mechanics of the XY Model. II. Spin-Correlation Functions*, *Physical Review A* **3** (1971) 786–804.
- [51] E. Barouch and B. M. McCoy, *Statistical Mechanics of the XY Model. III*, *Physical Review A* **3** (1971) 2137–2140.
- [52] R. Schützhold, M. Uhlmann, Y. Xu and U. R. Fischer, *Sweeping from the Superfluid to the Mott Phase in the Bose-Hubbard Model*, *Physical Review Letters* **97** (2006) 200601.
- [53] A. del Campo and W. H. Zurek, *Universality of phase transition dynamics: Topological defects from symmetry breaking*, *International Journal of Modern Physics A* **29** (2014) 1430018.
- [54] J. Mossel, G. Palacios and J.-S. Caux, *Geometric quenches in quantum integrable systems*, *Journal of Statistical Mechanics: Theory and Experiment* **2010** (2010) L09001.
- [55] V. Alba and F. Heidrich-Meisner, *Entanglement spreading after a geometric quench in quantum spin chains*, *Physical Review B* **90** (2014) 075144.
- [56] P. Bocchieri and A. Loinger, *Quantum Recurrence Theorem*, *Physical Review* **107** (1957) 337–338.
- [57] C. Gogolin, M. P. Müller and J. Eisert, *Absence of Thermalization in Nonintegrable Systems*, *Physical Review Letters* **106** (2011) 040401.
- [58] E. T. Jaynes, *Information Theory and Statistical Mechanics. II*, *Physical Review* **108** (1957) 171–190.
- [59] E. T. Jaynes, *Information Theory and Statistical Mechanics*, *Physical Review* **106** (1957) 620–630.

- [60] M. Srednicki, *Chaos and quantum thermalization*, Physical Review E **50** (1994) 888–901.
- [61] M. Rigol, M. Olshanii and V. Dunjko, *Thermalization and its mechanism for generic isolated quantum systems*, Nature **452** (2008) 854.
- [62] M. Cramer, C. M. Dawson, J. Eisert and T. J. Osborne, *Exact Relaxation in a Class of Nonequilibrium Quantum Lattice Systems*, Physical Review Letters **100** (2008) 030602.
- [63] L. D’Alessio, Y. Kafri, A. Polkovnikov and M. Rigol, *From quantum chaos and eigenstate thermalization to statistical mechanics and thermodynamics*, Advances in Physics **65** (2016) 239–362.
- [64] M. Srednicki, *Thermal fluctuations in quantized chaotic systems*, Journal of Physics A: Mathematical and General **29** (1996) L75.
- [65] M. Srednicki, *The approach to thermal equilibrium in quantized chaotic systems*, Journal of Physics A: Mathematical and General **32** (1999) 1163.
- [66] M. Rigol and M. Srednicki, *Alternatives to Eigenstate Thermalization*, Physical Review Letters **108** (2012) 110601.
- [67] A. Flesch, I. Bloch, I. P. McCulloch, J. Eisert, S. Trotzky, U. Schollwöck and Y.-A. Chen, *Probing the relaxation towards equilibrium in an isolated strongly correlated one-dimensional Bose gas*, Nature Physics **8** (2012) 325.
- [68] M. C. Bañuls, J. I. Cirac and M. B. Hastings, *Strong and Weak Thermalization of Infinite Nonintegrable Quantum Systems*, Physical Review Letters **106** (2011) 050405.
- [69] G. P. Brandino, A. De Luca, R. M. Konik and G. Mussardo, *Quench dynamics in randomly generated extended quantum models*, Physical Review B **85** (2012) 214435.
- [70] M. Rigol, *Quantum quenches and thermalization in one-dimensional fermionic systems*, Physical Review A **80** (2009) 053607.
- [71] A. Faribault, P. Calabrese and J.-S. Caux, *Quantum quenches from integrability: the fermionic pairing model*, Journal of Statistical Mechanics: Theory and Experiment **2009** (2009) P03018.
- [72] A. C. Cassidy, C. W. Clark and M. Rigol, *Generalized Thermalization in an Integrable Lattice System*, Physical Review Letters **106** (2011) 140405.
- [73] P. Calabrese, F. H. L. Essler and M. Fagotti, *Quantum Quench in the Transverse-Field Ising Chain*, Physical Review Letters **106** (2011) 227203.
- [74] P. Calabrese, F. H. L. Essler and M. Fagotti, *Quantum quenches in the transverse field Ising chain: II. Stationary state properties*, Journal of Statistical Mechanics: Theory and Experiment **2012** (2012) P07022.

- [75] P. Calabrese, F. H. L. Essler and M. Fagotti, *Quantum quench in the transverse field Ising chain: I. Time evolution of order parameter correlators*, Journal of Statistical Mechanics: Theory and Experiment **2012** (2012) P07016.
- [76] S. Sotiriadis, D. Fioretto and G. Mussardo, *Zamolodchikov–Faddeev algebra and quantum quenches in integrable field theories*, Journal of Statistical Mechanics: Theory and Experiment **2012** (2012) P02017.
- [77] J.-S. Caux and F. H. L. Essler, *Time Evolution of Local Observables After Quenching to an Integrable Model*, Physical Review Letters **110** (2013) 257203.
- [78] J. Sirker, N. P. Konstantinidis, F. Andraschko and N. Sedlmayr, *Locality and thermalization in closed quantum systems*, Physical Review A **89** (2014) 042104.
- [79] M. Rigol, *Fundamental Asymmetry in Quenches Between Integrable and Nonintegrable Systems*, Physical Review Letters **116** (2016) 100601.
- [80] E. Ilievski, J. De Nardis, B. Wouters, J.-S. Caux, F. Essler and T. Prosen, *Complete Generalized Gibbs Ensembles in an Interacting Theory*, Physical Review Letters **115** (2015) 157201.
- [81] E. Ilievski, M. Medenjak, T. Prosen and L. Zadnik, *Quasilocal charges in integrable lattice systems*, Journal of Statistical Mechanics: Theory and Experiment **2016** (2016) 064008.
- [82] T. Langen, S. Erne, R. Geiger, B. Rauer, T. Schweigler, M. Kuhnert, W. Rohringer, I. E. Mazets, T. Gasenzer and J. Schmiedmayer, *Experimental observation of a generalized Gibbs ensemble*, Science **348** (2015) 207–211.
- [83] L. Vidmar and M. Rigol, *Generalized Gibbs ensemble in integrable lattice models*, Journal of Statistical Mechanics: Theory and Experiment **2016** (2016) 064007.
- [84] M. Rigol, V. Dunjko, V. Yurovsky and M. Olshanii, *Relaxation in a completely integrable many-body Quantum system: An Ab initio study of the dynamics of the highly excited states of 1d lattice hard-core bosons*, Physical Review Letters **98** (2007) 1–4.
- [85] B. Wouters, J. De Nardis, M. Brockmann, D. Fioretto, M. Rigol and J.-S. Caux, *Quenching the Anisotropic Heisenberg Chain: Exact Solution and Generalized Gibbs Ensemble Predictions*, Physical Review Letters **113** (2014) 117202.
- [86] B. Pozsgay, M. Mestyán, M. Werner, M. Kormos, G. Zaránd and G. Takács, *Correlations after Quantum Quenches in the XXZ Spin Chain: Failure of the Generalized Gibbs Ensemble*, Physical Review Letters **113** (2014) 117203.
- [87] E. H. Lieb and D. W. Robinson, *The finite group velocity of quantum spin systems*, Communications in Mathematical Physics **28** (1972) 251–257.
- [88] B. Nachtergaele, H. Raz, B. Schlein and R. Sims, *Lieb-Robinson Bounds for Harmonic and Anharmonic Lattice Systems*, Communications in Mathematical Physics **286** (2009) 1073–1098.

- [89] B. Nachtergaele, B. Schlein, R. Sims, S. Starr and V. a. Zagrebnoy, *On the Existence of the Dynamics for Anharmonic Quantum Oscillator Systems*, *Reviews in Mathematical Physics* **22** (2009) 207–231.
- [90] M. Cramer, A. Serafini and J. Eisert, *Locality of dynamics in general harmonic quantum systems*, in *Quantum Information and Many Body Quantum Systems: Proceedings* (M. Ericsson and S. Montangero, eds.), vol. 8 of *Publications of the Scuola Normale Superiore*, pp. 51–72. 2008.
- [91] S. Bravyi, M. B. Hastings and F. Verstraete, *Lieb-Robinson Bounds and the Generation of Correlations and Topological Quantum Order*, *Physical Review Letters* **97** (2006) 050401.
- [92] P. Calabrese and J. Cardy, *Entanglement entropy and quantum field theory*, *Journal of Statistical Mechanics: Theory and Experiment* **2004** (2004) P06002.
- [93] P. Calabrese, *Entanglement and thermodynamics in non-equilibrium isolated quantum systems*, *Physica A: Statistical Mechanics and its Applications* (2017) .
- [94] P. Calabrese and J. Cardy, *Evolution of entanglement entropy in one-dimensional systems*, *Journal of Statistical Mechanics: Theory and Experiment* **2005** (2005) P04010.
- [95] M. Fagotti and P. Calabrese, *Evolution of entanglement entropy following a quantum quench: Analytic results for the XY chain in a transverse magnetic field*, *Physical Review A* **78** (2008) 010306.
- [96] H. Kim and D. A. Huse, *Ballistic Spreading of Entanglement in a Diffusive Nonintegrable System*, *Physical Review Letters* **111** (2013) 127205.
- [97] L. Bucciattini, M. Kormos and P. Calabrese, *Quantum quenches from excited states in the Ising chain*, *Journal of Physics A: Mathematical and Theoretical* **47** (2014) 175002.
- [98] A. S. Buyskikh, M. Fagotti, J. Schachenmayer, F. Essler and A. J. Daley, *Entanglement growth and correlation spreading with variable-range interactions in spin and fermionic tunneling models*, *Physical Review A* **93** (2016) 053620.
- [99] V. Alba and P. Calabrese, *Entanglement dynamics after quantum quenches in generic integrable systems*, arXiv:1712.07529 [cond-mat, physics:hep-th, physics:quant-ph] (2017) .
- [100] S. Sotiriadis, P. Calabrese and J. Cardy, *Quantum quench from a thermal initial state*, *Europhys. Lett.* **87** (2009) 20002.
- [101] S. Sotiriadis and J. Cardy, *Quantum quench in interacting field theory: A self-consistent approximation*, *Physical Review B* **81** (2010) 134305.
- [102] M. Tegmark and L. Yeh, *Steady states of harmonic oscillator chains and shortcomings of harmonic heat baths*, *Physica A* **202** (1994) 342–362.
- [103] M. Fagotti and F. H. L. Essler, *Reduced density matrix after a quantum quench*, *Physical Review B* **87** (2013) 245107.

- [104] M. Cramer, J. Eisert, M. B. Plenio and J. Dreissig, *Entanglement-area law for general bosonic harmonic lattice systems*, Physical Review A **73** (2006) 12309.
- [105] J. Eisert, M. Cramer and M. B. Plenio, *Colloquium: Area laws for the entanglement entropy*, Reviews of Modern Physics **82** (2010) 277–306.
- [106] T. F. Demarie, *Pedagogical introduction to the entropy of entanglement for Gaussian states*, arXiv:1209.2748 [quant-ph] (2012) .
- [107] A. Coser, E. Tonni and P. Calabrese, *Entanglement negativity after a global quantum quench*, Journal of Statistical Mechanics: Theory and Experiment **2014** (2014) P12017.
- [108] J. Häppölä, G. B. Halász and A. Hamma, *Universality and robustness of revivals in the transverse field XY model*, Physical Review A **85** (2012) 032114.
- [109] S. Montes and A. Hamma, *Phase diagram and quench dynamics of the cluster-XY spin chain*, Physical Review E **86** (2012) 021101.
- [110] O. M. P. Bilaniuk, V. K. Deshpande and E. C. G. Sudarshan, *“Meta” Relativity*, American Journal of Physics **30** (Oct., 1962) 718–723.
- [111] G. Feinberg, *Possibility of Faster-Than-Light Particles*, Physical Review **159** (1967) 1089–1105.
- [112] M. E. Arons and E. C. G. Sudarshan, *Lorentz invariance, local field theory, and faster-than-light particles*, Physical Review **173** (1968) 1622.
- [113] J. Dhar and E. C. G. Sudarshan, *Quantum field theory of interacting tachyons*, Physical Review **174** (1968) 1808–1815.
- [114] Y. Aharonov, A. Komar and L. Susskind, *Superluminal Behavior, Causality, and Instability*, Phys. Rev. **182** (1969) 1400–1403.
- [115] Peskin, M. E and Schroeder, D. V., *An Introduction to Quantum Field Theory*. Addison-Wesley, Reading, USA, 1995.
- [116] A. Sen, *Field theory of tachyon matter*, Modern Physics Letters A **17** (2002) 1797–1804.
- [117] A. Sen, *Rolling Tachyon*, Journal of High Energy Physics **2002** (2002) 048–048.
- [118] L. Bonnes, F. H. L. Essler and A. M. Läuchli, *“Light-Cone” Dynamics After Quantum Quenches in Spin Chains*, Physical Review Letters **113** (2014) 187203.
- [119] F. Englert and R. Brout, *Broken Symmetry and the Masses of the Gauge Vector Mesons*, Physical Review Letters **22** (1964) 321–323.
- [120] P. W. Higgs, *Broken Symmetries and the Masses of Gauge Bosons*, Physical Review Letters **13** (1964) 508–509.
- [121] G. S. Guralnik, C. R. Hagen and T. W. B. Kibble, *Global Conservation Laws and Massless Particles*, Physical Review Letters **13** (1964) 585–587.

- [122] J. J. Sakurai and J. Napolitano, *Modern quantum mechanics*. Addison-Wesley, Reading, MA, 2011.
- [123] H. Murayama, *Lecture notes on quantum mechanics*. <http://hitoshi.berkeley.edu/221a/>, 2006.
- [124] A. Sen, *Tachyon condensation on the brane antibrane system*, Journal of High Energy Physics **1998** (1998) 012.
- [125] J.-P. Bruneton, *Causality and superluminal behavior in classical field theories: Applications to k-essence theories and modified-Newtonian-dynamics-like theories of gravity*, Physical Review D **75** (2007) 085013.
- [126] M. M. Wolf, F. Verstraete, M. B. Hastings and J. I. Cirac, *Area laws in quantum systems: Mutual information and correlations*, Physical Review Letters **100** (2008) 70502.
- [127] I. Affleck, *Field Theory Methods and Quantum Critical Phenomena*, in *Fields, Strings and Critical Phenomena - Les Houches Lecture Notes* (E. Brezin and J. Zinn-Justin, eds.). North-Holland, Amsterdam, 1988.
- [128] S.-J. Chang, *Quantum fluctuations in a ϕ^4 field theory. I. Stability of the vacuum*, Physical Review D **12** (1975) 1071–1088.
- [129] G. I. Sivashinsky, *Weak turbulence in periodic flows*, Physica D: Nonlinear Phenomena **17** (1985) 243–255.
- [130] A. M. Tsvelik, *Quantum Field Theory in Condensed Matter Physics*. Cambridge University Press, Cambridge, UK, 2003.
- [131] C. Gómez, M. Ruiz-Altaba and G. Sierra, *Quantum Groups in Two-Dimensional Physics*. Cambridge Monographs on Mathematical Physics. Cambridge University Press, Cambridge, UK, 1996.
- [132] P. Di Francesco, P. Mathieu and D. Sénéchal, *Conformal field theory*. Graduate texts in contemporary physics. Springer, New York, NY, 1997.
- [133] A. Gogolin, A. Nersisyan and A. Tsvelik, *Bosonization and Strongly Correlated Systems*. Cambridge University Press, Cambridge, UK, 2004.
- [134] G. Mussardo, *Statistical Field Theory: An Introduction to Exactly Solved Models in Statistical Physics*. Oxford Graduate Texts. Oxford University Press, Oxford, New York, 2009.
- [135] T. Hansson, M. Hermanns, S. Simon and S. Viefers, *Quantum Hall physics: Hierarchies and conformal field theory techniques*, Reviews of Modern Physics **89** (2017) 025005.
- [136] C. Nayak, S. H. Simon, A. Stern, M. Freedman and S. Das Sarma, *Non-Abelian anyons and topological quantum computation*, Reviews of Modern Physics **80** (2008) 1083–1159.

- [137] R. B. Laughlin, *Anomalous Quantum Hall Effect: An Incompressible Quantum Fluid with Fractionally Charged Excitations*, *Physical Review Letters* **50** (1983) 1395–1398.
- [138] G. Moore and N. Read, *Nonabelions in the fractional quantum hall effect*, *Nuclear Physics B* **360** (1991) 362–396.
- [139] J. I. Cirac and G. Sierra, *Infinite matrix product states, conformal field theory, and the Haldane-Shastry model*, *Physical Review B* **81** (2010) 104431.
- [140] M. A. Nielsen and I. L. Chuang, *Quantum Computation and Quantum Information: 10th Anniversary Edition*. Cambridge University Press, New York, NY, USA, 10th ed., 2011.
- [141] H.-H. Tu, A. E. B. Nielsen, J. I. Cirac and G. Sierra, *Lattice Laughlin states of bosons and fermions at filling fractions $1/q$* , *New Journal of Physics* **16** (2014) 033025.
- [142] I. Glasser, J. Ignacio Cirac, G. Sierra and A. E. B. Nielsen, *Construction of spin models displaying quantum criticality from quantum field theory*, *Nuclear Physics B* **886** (2014) 63–74.
- [143] H.-H. Tu, A. E. B. Nielsen and G. Sierra, *Quantum spin models for the $SU(n)_1$ Wess–Zumino–Witten model*, *Nuclear Physics B* **886** (2014) 328–363.
- [144] R. Bondesan and T. Quella, *Infinite matrix product states for long-range $SU(N)$ spin models*, *Nuclear Physics B* **886** (2014) 483–523.
- [145] B. Herwerth, G. Sierra, H.-H. Tu and A. E. B. Nielsen, *Excited states in spin chains from conformal blocks*, *Physical Review B* **91** (2015) 235121.
- [146] H.-H. Tu and G. Sierra, *Infinite matrix product states, boundary conformal field theory, and the open Haldane-Shastry model*, *Physical Review B* **92** (2015) 041119.
- [147] I. Glasser, J. I. Cirac, G. Sierra and A. E. B. Nielsen, *Exact parent Hamiltonians of bosonic and fermionic Moore–Read states on lattices and local models*, *New Journal of Physics* **17** (2015) 082001.
- [148] A. E. B. Nielsen, J. I. Cirac and G. Sierra, *Laughlin Spin-Liquid States on Lattices Obtained from Conformal Field Theory*, *Physical Review Letters* **108** (2012) 257206.
- [149] A. E. B. Nielsen, G. Sierra and J. I. Cirac, *Local models of fractional quantum Hall states in lattices and physical implementation*, *Nature Communications* **4** (2013) ncomms3864.
- [150] B. Herwerth, G. Sierra, H.-H. Tu, J. I. Cirac and A. E. B. Nielsen, *Edge states for the Kalmeyer-Laughlin wave function*, *Physical Review B* **92** (2015) 245111.
- [151] I. Glasser, J. I. Cirac, G. Sierra and A. E. B. Nielsen, *Lattice effects on Laughlin wave functions and parent Hamiltonians*, *Physical Review B* **94** (2016) 245104.

- [152] M. P. Zaletel and R. S. K. Mong, *Exact matrix product states for quantum Hall wave functions*, Physical Review B **86** (2012) 245305.
- [153] B. Estienne, Z. Papić, N. Regnault and B. A. Bernevig, *Matrix product states for trial quantum Hall states*, Physical Review B **87** (2013) 161112.
- [154] A. A. Belavin, A. M. Polyakov and A. B. Zamolodchikov, *Infinite conformal symmetry in two-dimensional quantum field theory*, Nuclear Physics B **241** (1984) 333–380.
- [155] G. Moore and N. Seiberg, *Classical and quantum conformal field theory*, Communications in Mathematical Physics **123** (1989) 177–254.
- [156] J. Cardy, *Logarithmic conformal field theories as limits of ordinary CFTs and some physical applications*, Journal of Physics A: Mathematical and Theoretical **46** (2013) 494001.
- [157] P. Ginsparg, *Applied Conformal Field Theory*, arXiv:hep-th/9108028 (1988) .
- [158] D. Simmons-Duffin, *TASI Lectures on the Conformal Bootstrap*, arXiv:1602.07982 [cond-mat, physics:hep-th] (2016) .
- [159] S. Rychkov, *EPFL Lectures on Conformal Field Theory in $D \geq 3$ Dimensions*, arXiv:1601.05000 [cond-mat, physics:hep-ph, physics:hep-th] (2017) .
- [160] D. Gaitsgory, *Notes on 2D conformal field theory and string theory*, in *Quantum fields and strings: a course for mathematicians, Vol. 1, 2*, pp. 1017–1089. American Mathematical Society, Providence, R.I., 1999.
- [161] A. Beilinson and V. G. Drinfeld, *Chiral algebras*. No. 51 in Colloquium Publications. American Mathematical Society, Providence, R.I., 2004.
- [162] G. Moore and N. Seiberg, *Lectures on RCFT*, in *Physics, Geometry and Topology*, NATO ASI Series, pp. 263–361. Springer, Boston, MA, 1990.
- [163] V. Kac, *Vertex Algebras for Beginners*. University lecture series. American Mathematical Society, Providence, R.I., 1998.
- [164] R. Orús, *A practical introduction to tensor networks: Matrix product states and projected entangled pair states*, Annals of Physics **349** (2014) 117–158.
- [165] G. Vidal, *Efficient Classical Simulation of Slightly Entangled Quantum Computations*, Physical Review Letters **91** (2003) 147902.
- [166] I. Affleck, T. Kennedy, E. H. Lieb and H. Tasaki, *Rigorous results on valence-bond ground states in antiferromagnets*, Physical Review Letters **59** (1987) 799–802.
- [167] S. R. White, *Density matrix formulation for quantum renormalization groups*, Physical Review Letters **69** (1992) 2863–2866.
- [168] U. Schollwöck, *The density-matrix renormalization group in the age of matrix product states*, Annals of Physics **326** (2011) 96–192.
- [169] D. Perez-Garcia, F. Verstraete, M. M. Wolf and J. I. Cirac, *Matrix Product State Representations*, Quantum Info. Comput. **7** (2007) 401–430.

- [170] F. Verstraete, V. Murg and J. I. Cirac, *Matrix product states, projected entangled pair states, and variational renormalization group methods for quantum spin systems*, *Advances in Physics* **57** (2008) 143–224.
- [171] G. Sierra and T. Nishino, *The density matrix renormalization group method applied to interaction round a face Hamiltonians*, *Nuclear Physics B* **495** (1997) 505–532.
- [172] F. D. M. Haldane, *Exact Jastrow-Gutzwiller resonating-valence-bond ground state of the spin- $\frac{1}{2}$ antiferromagnetic Heisenberg chain with $1/r^2$ exchange*, *Physical Review Letters* **60** (1988) 635–638.
- [173] B. S. Shastry, *Exact solution of an $S = \frac{1}{2}$ Heisenberg antiferromagnetic chain with long-ranged interactions*, *Physical Review Letters* **60** (1988) 639–642.
- [174] J. C. Talstra and F. D. M. Haldane, *Integrals of motion of the Haldane-Shastry model*, *Journal of Physics A: Mathematical and General* **28** (1995) 2369.
- [175] D. C. Tsui, H. L. Stormer and A. C. Gossard, *Two-Dimensional Magnetotransport in the Extreme Quantum Limit*, *Physical Review Letters* **48** (1982) 1559–1562.
- [176] E. Fradkin, *Field Theories of Condensed Matter Physics*. Cambridge University Press, Cambridge, UK, 2 ed., 2013.
- [177] L. Onsager, *Crystal Statistics. I. A Two-Dimensional Model with an Order-Disorder Transition*, *Physical Review* **65** (1944) 117–149.
- [178] E. Ising, *Beitrag zur Theorie des Ferromagnetismus*, *Zeitschrift für Physik* **31** (1925) 253–258.
- [179] S. G. Brush, *History of the Lenz-Ising Model*, *Reviews of Modern Physics* **39** (1967) 883–893.
- [180] T. Ising, R. Folk, R. Kenna, B. Berche and Y. Holovatch, *The Fate of Ernst Ising and the Fate of his Model*, arXiv:1706.01764 [physics] (2017) .
- [181] R. Peierls, *On Ising's model of ferromagnetism*, *Mathematical Proceedings of the Cambridge Philosophical Society* **32** (1936) 477–481.
- [182] H. A. Kramers and G. H. Wannier, *Statistics of the Two-Dimensional Ferromagnet. Part I*, *Physical Review* **60** (1941) 252–262.
- [183] D. Aasen, R. S. K. Mong and P. Fendley, *Topological defects on the lattice: I. The Ising model*, *Journal of Physics A: Mathematical and Theoretical* **49** (2016) 354001.
- [184] L. P. Kadanoff and H. Ceva, *Determination of an Operator Algebra for the Two-Dimensional Ising Model*, *Physical Review B* **3** (1971) 3918–3939.
- [185] F. J. Wegner, *Duality in Generalized Ising Models and Phase Transitions without Local Order Parameters*, *Journal of Mathematical Physics* **12** (1971) 2259–2272.
- [186] M. Baake, U. Grimm and R. Baxter, *A critical Ising model on the labyrinth*, *International Journal of Modern Physics B* **08** (1994) 3579–3600.

- [187] S.-S. Roan, *Duality and symmetry in chiral Potts model*, Journal of Statistical Mechanics: Theory and Experiment **2009** (2009) P08012.
- [188] T. D. Schultz, D. C. Mattis and E. H. Lieb, *Two-Dimensional Ising Model as a Soluble Problem of Many Fermions*, Reviews of Modern Physics **36** (1964) 856–871.
- [189] S. Sachdev, *Quantum Phase Transitions*. Cambridge University Press, Cambridge, UK, 2 ed., 2011.
- [190] M. Henkel, *Conformal invariance and critical phenomena*. Springer, Berlin, Heidelberg, 2013.
- [191] N. Read and D. Green, *Paired states of fermions in two dimensions with breaking of parity and time-reversal symmetries and the fractional quantum Hall effect*, Physical Review B **61** (2000) 10267–10297.
- [192] P. Fendley, *Modern Statistical Mechanics (book in progress)*. <http://galileo.phys.virginia.edu/~pf7a/book.html>.
- [193] A. Y. Kitaev, *Unpaired Majorana fermions in quantum wires*, Physics-Uspekhi **44** (2001) 131.
- [194] P. Di Francesco, H. Saleur and J. B. Zuber, *Critical Ising correlation functions in the plane and on the torus*, Nuclear Physics B **290** (1987) 527 – 581.
- [195] J. B. Zuber and C. Itzykson, *Quantum field theory and the two-dimensional Ising model*, Physical Review D **15** (1977) 2875–2884.
- [196] P. Fendley, M. P. A. Fisher and C. Nayak, *Dynamical Disentanglement across a Point Contact in a Non-Abelian Quantum Hall State*, Physical Review Letters **97** (2006) 036801.
- [197] P. Fendley, M. P. A. Fisher and C. Nayak, *Edge states and tunneling of non-Abelian quasiparticles in the $\nu = \frac{5}{2}$ quantum Hall state and $p+ip$ superconductors*, Phys. Rev. B **75** (2007) 045317.
- [198] E. Ardonne and G. Sierra, *Chiral correlators of the Ising conformal field theory*, Journal of Physics A: Mathematical and Theoretical **43** (2010) 505402.
- [199] C. Nayak and F. Wilczek, *$2n$ -quasihole states realize $2^n - 1$ -dimensional spinor braiding statistics in paired quantum Hall states*, Nuclear Physics B **479** (1996) 529–553.
- [200] H. Onnes, *The Resistance of Pure Mercury at Helium Temperatures*, Phys. Lab. Univ. Leiden **12** (1911) 120.
- [201] J. Bardeen, L. N. Cooper and J. R. Schrieffer, *Theory of Superconductivity*, Physical Review **108** (1957) 1175–1204.
- [202] M. Ibañez, J. Links, G. Sierra and S.-Y. Zhao, *Exactly solvable pairing model for superconductors with $p_x + ip_y$ -wave symmetry*, Physical Review B **79** (2009) 180501.

- [203] C. Dunning, M. Ibañez, J. Links, G. Sierra and S.-Y. Zhao, *Exact solution of the $p + ip$ pairing Hamiltonian and a hierarchy of integrable models*, Journal of Statistical Mechanics: Theory and Experiment **2010** (2010) P08025.
- [204] H. Li and F. D. M. Haldane, *Entanglement Spectrum as a Generalization of Entanglement Entropy: Identification of Topological Order in Non-Abelian Fractional Quantum Hall Effect States*, Physical Review Letters **101** (2008) 010504.
- [205] D. Levy, *Algebraic structure of translation-invariant spin- $\frac{1}{2}$ XXZ and q -Potts quantum chains*, Physical Review Letters **67** (1991) 1971–1974.
- [206] W. M. Koo and H. Saleur, *Representations of the Virasoro algebra from lattice models*, Nuclear Physics B **426** (1994) 459–504.
- [207] A. Milsted and G. Vidal, *Extraction of conformal data in critical quantum spin chains using the Koo-Saleur formula*, Physical Review B **96** (2017) 245105.
- [208] J. L. Cardy, *Operator content of two-dimensional conformally invariant theories*, Nuclear Physics B **270** (1986) 186–204.
- [209] Y. A. Bashilov and S. V. Pokrovsky, *A conformally invariant limit of the critical lattice Ising model*, Communications in Mathematical Physics **113** (1987) 115–136.
- [210] J. I. Latorre, E. Rico and G. Vidal, *Ground State Entanglement in Quantum Spin Chains*, Quantum Info. Comput. **4** (2004) 48–92.
- [211] I. Peschel, *On the reduced density matrix for a chain of free electrons*, Journal of Statistical Mechanics: Theory and Experiment **2004** (2004) P06004.
- [212] N. Bray-Ali, L. Ding and S. Haas, *Topological order in paired states of fermions in two dimensions with breaking of parity and time-reversal symmetries*, Physical Review B **80** (2009) 180504.
- [213] T. P. Oliveira, P. Ribeiro and P. D. Sacramento, *Entanglement entropy and entanglement spectrum of triplet topological superconductors*, Journal of Physics: Condensed Matter **26** (2014) 425702.
- [214] D. Friedan, Z. Qiu and S. Shenker, *Superconformal invariance in two dimensions and the tricritical Ising model*, Physics Letters B **151** (1985) 37–43.
- [215] E. O’Brien and P. Fendley, *Lattice supersymmetry and order-disorder coexistence in the tricritical Ising model*, arXiv:1712.06662 [cond-mat, physics:hep-th] (2017) .
- [216] E. Fradkin and L. P. Kadanoff, *Disorder variables and para-fermions in two-dimensional statistical mechanics*, Nuclear Physics B **170** (1980) 1–15.
- [217] V. Riva and J. Cardy, *Holomorphic parafermions in the Potts model and stochastic Loewner evolution*, Journal of Statistical Mechanics: Theory and Experiment **2006** (2006) P12001.

- [218] R. S. K. Mong, D. J. Clarke, J. Alicea, N. H. Lindner and P. Fendley, *Parafermionic conformal field theory on the lattice*, Journal of Physics A: Mathematical and Theoretical **47** (2014) 452001.
- [219] A. Feiguin, S. Trebst, A. W. W. Ludwig, M. Troyer, A. Kitaev, Z. Wang and M. H. Freedman, *Interacting Anyons in Topological Quantum Liquids: The Golden Chain*, Physical Review Letters **98** (2007) 160409.
- [220] R. N. C. Pfeifer, P. Corboz, O. Buerschaper, M. Aguado, M. Troyer and G. Vidal, *Simulation of anyons with tensor network algorithms*, Physical Review B **82** (2010) 115126.
- [221] P. Fendley, *Parafermionic edge zero modes in \mathbb{Z}_n -invariant spin chains*, Journal of Statistical Mechanics: Theory and Experiment **2012** (2012) P11020.